Aerosol meteorology of the Maritime Continent for the 2012 7SEAS southwest monsoon intensive study: Part I regional scale phenomena

Jeffrey S. Reid[1], Peng Xian[1] , Brent N. Holben[2], Edward J. Hyer[1], Elizabeth A. Reid[1], Santo V. Salinas[3], Jianglong Zhang[4], James R. Campbell[1], Boon Ning Chew[5], Robert E. Holz[6], Arunas P. Kuciauskas[1], Nofel Lagrosas[7], Derek J. Posselt[8], Charles R. Sampson[1], Annette L. Walker[1], E. Judd Welton[2], Chidong Zhang[9].

[1] {Marine Meteorology Division, Naval Research Laboratory, Monterey CA}
[2] {NASA Goddard Space Flight Center, Greenbelt MD}
[3] {Centre for Remote Imaging Sensing and Processing, National University of Singapore, Singapore}
[4] {Dept. of Atmospheric Science, University of North Dakota, Grand Forks, ND}
[5] {National Environment Agency, Singapore}
[6] {Space Sciences Engineering Center, University of Wisconsin, Madison, WI}
[7] {Manila Observatory, Manila Philippines}
[8] {Jet Propulsion laboratory, Pasadena CA}
[9] {NOAA Pacific Marine Environmental Laboratory Seattle, WA}

Correspondence to: J. S. Reid (jeffrey.reid@nrlmry.navy.mil; 1 831-656-4725)

ABSTRACT:

The largest 7 Southeast Asian Studies (7-SEAS) operations period within the Maritime Continent (MC) occurred in the 2012 August-September biomass burning season. Included were an enhanced deployment of Aerosol Robotic Network (AERONET) sun photometers, multiple lidars, and field measurements to observe transported smoke and pollution as it left the MC and entered the southwest monsoon monsoon trough. Here we describe the nature of the overall 2012 southwest monsoon (SWM) and biomass burning season to give context to the 2012 deployment. The MC in 2012 was in a slightly warm El Nino/Southern Oscillation (ENSO) phase and with spatially typical burning activity. However, overall fire counts for 2012 were 10% lower than the Reid et al., (2012) baseline, with regions of significant departures from this norm, ranging from Southern Sumatra (+30%) to Southern Kalimantan (-42%). Fire activity and monsoonal flows for the dominant burning regions were modulated by a series of Intraseasonal Oscillation events (e.g., Madden-Julian Oscillation or MJO; Boreal Summer IntraSeasonal Oscillation or BSISO). As is typical, fire activity systematically progressed eastward over time, starting with Central Sumatran fire activity in June related to a moderately strong MJO event which brought drier air from the Indian Ocean aloft and enhanced monsoonal flow. Further burning in Sumatra and Kalimantan Borneo occurred in a series of significant events from early-August to a peak in the first week of October, ending when the monsoon started to migrate back to its wintertime northeast flow conditions in mid-October. Significant monsoonal enhancements and flow reversals collinear with tropical cyclone (TC) activity and easterly waves were also observed. Islands of the eastern MC, including Sulawesi, Java and Timor, showed less sensitivity to monsoonal variation, with slowly increasing fire activity that also peaked in early October, but lingered into November. Interestingly, even though fire counts were middling, resultant AERONET 500 nm Aerosol Optical Thickness (AOT's) from fire activity were high, with maximums of 3.6 and 5.6 in the Sumatra and Kalimantan source regions at the end of the burning season, and with an average of ~1. AOTs could also be high at receptor sites, with a mean and maximum of 0.57 and 1.24 in Singapore, and 0.61 and 0.8 in Kuching Sarawak. Ultimately, outside of the extreme 2015 El Nino event, average AERONET AOT values were higher than any other time since sites were established. Thus, while satellite fire data, models and AERONET all qualitatively agree on the nature of smoke production and transport, the MC's complex environment resulted in clear differences in quantitative interpretation of these datasets.

1.0 INTRODUCTION AND BACKROUND

The Maritime Continent (MC) hosts one of the most complicated coupled systems on Earth. The intricate feedbacks between tropical meteorology, land surface, and oceans are complex and a challenge to understand and simulate. Indeed, early findings of the Coordinated Regional Climate Downscaling Experiment (CORDEX; http://www.cordex.org/ ; Giorgi et al. 2012) yielded diverging climate model simulations for the Southeast Asian region. Strong biases in temperature and large uncertainties in precipitation estimates have been diagnosed (Jamandre and Narisma, 2013). Atmospheric models have difficulty representing complex tropical waves in the MC on scales ranging from Kelvin waves through the Madden-Julian Oscillation (MJO) and the regional monsoon (e.g, Misra and Li, 2014; Zhang, 2013). Owing to its dependence on meteorology, the MC's aerosol system is likewise complex, with the added challenge of persistent high clouds obscuring satellite remote sensing observations of aerosol lifecycle (Reid et al., 2013; Campbell et al., 2016). Field measurements in the MC are difficult to obtain in this part of the globe, and likewise quality assure in a complex sampling environment. Ultimately, the high degree of variability in the MC's aerosol environment poses great observational and modeling challenges for determining how aerosol particles, weather, and climate relate.

Given the above research challenges inherent in the MC's environment, the 7 Southeast Asian Studies (7SEAS) program was motivated to improve the ability of the community to observe and analyze aerosol and meteorology interactions in the region (e.g., Reid et al., 2012, 2013; Lin et al., 2013). The role of El Nino Southern Oscillation (ENSO) in regional drought and subsequent feedback into biomass burning have long been a focus of the aerosol community's efforts for the MC's aerosol environment (e.g., Nichol 1998; Field and Shen 2008). However, while ENSO is clearly a strong inter-seasonal modulator of burning activity, biomass burning is important in all years (Reid et al., 2012). Further, if we wish to understand how aerosol particles, weather and climate interact, much finer scale phenomena than ENSO require investigation. The aerosol system is of course dependent on meteorology, and which is defined by the complicated interplay between such phenomena as the MJO and/or Boreal Summer Intra-seasonal Oscillation (BSIO), equatorial waves, tropical cyclones (TCs) and even features as fine as boundary layer dynamics and land-sea breezes (e.g., Reid et al., 2012; 2015; Atwood et al., 2013; Campbell et al., 2013; Gau et al., 2013; Wang et al., 2013; Xian et al., 2013; Ge et al., 2014). At the same time, to infer aerosol impacts on radiation, clouds and climate, meteorological context in relation to these phenomena must be taken into account.

7SEAS has worked to encourage networks and intensive measurements throughout Southeast Asia and integrate these measurements into conceptual and numerical models of the aerosol system. Although all seasons and regions throughout Southeast Asia are of interest to the 7SEAS program, within the MC, 7SEAS field measurements and lifecycle studies have focused on the Southwest Monsoon (SWM) biomass burning season in Indonesia and Malaysia, with Singapore and the Philippines as key receptor sites (e.g., Reid et al., 2012; 2015; Atwood et al., 2013; Chew et al., 2011; 2013; Salinas et al., 2013; Xian et al., 2013; Wang et al., 2013; Yang et al., 2013). The year 2012 was a high water mark for 7SEAS efforts in the MC, with over fifteen Aerosol Robotic Network (AERONET; Holben et al., 1998) sun photometers, and five MicroPulse Lidar Network (MPLNET) lidars on station. Additional intensive measurements were made in Singapore, as well as on a vessel stationed in the Palawan Archipelago as a receptor. Taken together, these sites provided some of the first measurements of natural, industrial and biomass burning-influenced air masses that transited the South China and Sulu Seas on their way into the southwest monsoon monsoon trough (Atwood et al., 2016; Reid et al., 2016).

To support the 2012 7SEAS MC effort, and in particular the Palawan research cruise, this paper is the first of two that presents an analysis of the many scale dependencies of the MC’s aerosol meteorology. The focus of Part I is the regional scale phenomena, such as ENSO, the MJO, monsoon enhancements and TCs, and how they relate to biomass burning activity and transport. Our purpose is to give context to the 2012 effort, examine how 2012 compares to other seasons in regard to overall fire and monsoonal activity, and try to provide an overall narrative to 2012 aerosol meteorology. With the benefit of the research vessel observations from the 2012 deployment, we leave results related to finer scale phenomena such as squall lines and sea breeze fronts to Part II of this pair of papers (Reid et al., 2016).

2.0 ANALYSIS DATA

The SWM burning season generally runs from June through October (Reid et al., 2012), with a peak in September and October. The core 2012 7SEAS study period was August through

September 2012 and is the focus here. Data for these analyses comes from three categories: observations including: surface-based Aerosol Optical Thickness (AOT) from AERONET; thermodynamic structure from radiosondes; satellite-based remote sensing including Moderate resolution Imaging Spectrometer (MODIS) AOT and active fire hotspots, as well as multi sensor precipitation; and modeling based on global US Navy meteorology and aerosol systems. All of the products used are considered operational and thus are only briefly outlined here.

2.1 Observations

The maximum extent of 7SEAS aerosol observations throughout the MC occurred during the 2012 Southwest Monsoon season. Specifically relevant to the analysis of 2012, over fifteen AEROSOL Robotic Network sun photometers were in operation, with start dates from mid to late July through October. Of these, eight were of particular use for evaluating the biomass burning season. Locations are displayed in Figure 1, overlaid on an MTSAT false color image for August 16, 2012, representative of one of the clearer periods during the biomass burning. Identified are AERONET sites (circles) for the following sites (a) Jambi, Sumatra and (b) Palangkaraya, southern Kalimantan in the core biomass burning source regions of Indonesia; (c) Singapore, (d) Tahir, Malay Peninsula, Malaysia, (e) Pontianak, western Kalimantan and (f) Kuching, Sarawak as key coastal exit sites; and (g) Notre Dame of Marbel University, Mindanao and (h) Nha Trang, Vietnam as outer boundaries and receptors. While there are many other sites in the region, they are not used here because of excessive high cloud cover or instrumentation failure (these are marked as dashed circles). Although not analyzed here, for completeness MPLNET sites are marked (stars).

To track overall smoke or pollution transport, we utilize the AERONET operational 500 nm daily averaged fine-mode AOT derived from Level 2.0 Spectral Deconvolution Algorithm (SDA) Version 4.1 (O'Neill et al., 2003). Use of the SDA to separate fine and coarse mode extinction or optical depth has been verified (Kaku et al., 2014). SDA is particularly beneficial as it allows us to track fine-mode particles, such as from biomass burning or anthropogenic sources, while at the same time removing the influence of thin cirrus contamination, which can be large in this region (Chew et al., 2011). Given the wavelength dependencies for biomass burning particles in the region, 500 nm AOT is approximately 10-15% higher than 550 nm AOT used in MODIS.

A second dataset used here is the radiosonde releases at Riau Island north of Borneo (Figure 1-location i) to gauge the strength of the SWM. Data used here was hand evaluated to remove clear reporting errors. Most importantly, we employed the 925 hPa meridional wind to track monsoonal strength and transition. This metric was used in overarching fire meteorology analyses of Reid et al., (2012) as suggested in the monsoonal analysis paper of Lu and Chan (1999). Also from this Riau Island radiosonde site we used the 700 hPa relative humidity field. As discussed in Reid et al., (2015), this metric is indicative of the advection of drier air from the Indian Ocean that has a tendency to cap regional convection. In practice we have found this metric in particular to be a good predictor of convection (moist more convectively active; dry convection is suppressed). To smooth transients, a 3 day boxcar average was applied. Also, for TC fixes and intensities we utilized the Joint Typhoon Warning Center best track and statistics from the Automated Tropical Cyclone Forecast system (ATCF, Sampson and Schrader, 2000).

2.2 Satellite Data

For satellite monitoring of biomass burning, MODIS active fire hotspot analysis was utilized, integrated in the analysis structure of Reid et al. (2012; 2015), with context as laid out in Hyer et al. (2013). In addition to fire we also utilized NASA MODIS Col 6 Level 3 data from monitoring AOT (Levy et al., 2013). As discussed in Reid et al, (2013), all satellite aerosol products suffer from a host of cloud contamination and sampling issues. For evaluating aerosol transport extent, Terra MODIS is preferable due to the generally lower fractions of cloud cover in the AM orbit. This said, the current version of Terra MODIS AOT also suffers from instrument and calibration issues. Hence, we only use the data in a semi-quantitative manner.

Other various data sets are also used, including Geostationary MTSAT satellite products as found on the NEXSAT website, which were examined for the study period to help provide context to day to day variability in meteorology (visible, infrared, cloud heights, scatterometer, etc.; *Miller et al.*, 2006; http://www.nrlmry.navy.mil/nexsat-bin/nexsat.cgi). Daily precipitation was monitored using Climate Prediction Center (CPC) MORPHing product (CMORPH, *Joyce et al.*, 2004).

2.4 Model Data

Model data are used to provide a larger contextual understanding of the regional metrological and aerosol environment. To be consistent with the analyses of Reid et al., (2012; 2013; 2015) Navy Global Atmospheric Prediction System (NOGAPS; Hogan and Rosmond, 1991) is used to provide baseline meteorological data for analyses as well as to drive offline Navy Aerosol Analysis and Prediction System (NAAPS) aerosol simulations. While NOGAPS horizontal resolution is ~0.5^o in this region, spectral files were truncated to 1° x 1° for modeling aerosol transport for this season in a configuration consistent with the NAAPS reanalysis (Lynch et al., 2016). In NAAPS, four species are simulated: dust, biomass burning smoke, anthropogenic/biogenic fine, and sea salt. In the reanalysis configuration, smoke fluxes are driven from the MODIS smoke source function drawn from a MODIS-only version of the Fire Locating and Monitoring of Burning Emissions (FLAMBE; Reid et al., 2009). To improve wet deposition, CMORPH precipitation is used to constrain scavenging (2009). Data assimilation includes MODIS AOT and MISR (Zhang et al., 2008), although there are few data assimilation grade AOT retrievals in this part of the world. Nevertheless, NAAPS capability for smoke characterization in the Maritime Continent region has been demonstrated (e.g., Hyer and Chew, 2010; Reid et al., 2012; 2015; Xian et al, 2013), and has been further improved upon in the reanalysis version used here. For this overview paper, we simply utilize fine NOGAPS winds and AOT analyses to map smoke, transport, and pollution extent.

3.0 RESULTS

For the analysis of the regional meteorology in the 2012 burning season, we break the problem down into a number of sub sections. First, we describe the overall fire and monsoonal activity for 2012 (Section 3.1). Second, we examine the time series of fire activity and monsoonal meteorology for the 2012 monsoon season (Section 3.2). Finally, we examine the variability in AOT throughout the region to assess overall smoke patterns and transport behavior (Section 3.3).

3.1 Overall Fire and Monsoon Characteristics

The SWM in the South China Sea (SCS) typically starts in late April to early May, with flow reversal to northeast monsoon in mid-October (Lu and Chan 1999; Chang et al., 2005; Moron et al., 2009; Reid et al., 2012). Thus, climatologically, the SWM is in full existence from June through September. In regards to precipitation, drier periods in the MC start in Sumatra and propagate eastward over time (Moron et al., 2009). Based on MODIS active fire hotspot data, and as discussed in the time series analysis in Section (3.2), the first significant fire events did not begin until June, with region-wide initiation not beginning until August; typical for the region (Reid et al., 2012). Fire activity largely diminishes with the monsoon reversal in early October, with lingering fire activity in the eastern MC lasting through October. Here we will briefly review these features.

3.1.1 Overall fire activity

Figure 2 presents an overall fire prevalence map constructed from combined Terra and Aqua MODIS active fire hotspot detections for June 1st through October 31st, 2012. Fire counts by island, region or province as defined in the 2003-2009 baseline paper of Reid et al., (2012) are provided in Table 1. Overall fire patterns and activity are highly correlated with the spatial map fire count baseline of Reid et al. (2012). Although there is some fire activity over the entire domain, the most significant areas of activity include Central Sumatra (9135 fires), Southern Sumatra (12241 fires), and Southern Kalimantan (8120 fires). For 2012 the June-November primary burning season accounted for 99% of these fires, although local but significant fire outbreaks occurred all year around. Other significant burning includes Eastern and Western Kalimantan at 1571 and 5721 fires each. Islands such as Java and Timor can also have significant fire prevalence.

From Table 1, overall MC fire counts from MODIS for 2012 were 12% lower than the 2003-2009 baseline. Given the complexities of fire observation and the significant interannual standard deviations of fire prevalence in the region (generally >50%; Reid et al., 2012) we consider this an overall “average” fire season. The most notable enhancements from the norm was in Southern Sumatra and Western Kalimantan with a 30% enhancement. Rates in the fire prone Eastern and Southern Kalimantan were markedly down in 2012, by roughly 40%.

The MODIS fire data suggests that 95% of fire activity was in the June-October burning season, and roughly one cumulative standard deviation of the fire activity on Sumatra and Borneo occurred in August and September in particular (Table 1). This period was at the core of the

SWM period and also corresponded to the peak of the field activity. For the remainder of this section, we therefore focus on these two months.

3.1.2 Overall monsoonal meteorology

Meteorology and MODIS AOT data for August and September 2012 are provided in Figure 3. Included in Figure 3 are (a) overall NOGAPS-derived monsoonal flow at the surface and 700 hPa, overlaid on CMORPH satellite precipitation; (b) likewise monthly anomalies based on the NAAPS-Reanalysis dataset for 2002-2014; (c) MODIS Terra MOD08 average cloud cover; (d) MODIS Terra MOD08 550 nm AOT; and (e) NAAPS fine mode AOT. As is typical, south of the equator, surface winds are southeasterly, wrapping around the islands of Borneo and Sumatra to become southwesterly in the SCS. Over the SCS, winds are also largely typical; southwesterly at the surface and veering to zonal by 700 hPa. Precipitation gradually increases from the south to the north, with a maximum east of the Philippines in association with the summertime monsoonal trough. In August, there were two precipitation maxima, one along the west coast of Luzon, Philippines, the other along the west coast of the northern part of Malay Peninsula, both related to the monsoon flows impinging upon the coastal terrains (e.g., Cruz et al., 2013). Another notable cloud and precipitation enhancement is west of Sumatra, in association with a local vorticity maximum as winds transition from easterly to westerly (Wu et al., 2009; Reid et al., 2012), In September, maximum precipitation became zonally elongated from the Bay of Bengal through the South China Sea to east of the Philippines. This was related partially to the overall summertime monsoonal trough, and partially to an MJO event that pass through the MC (see Section 3.2.1). MODIS cloud cover is spatially correlated with precipitation, ranging from over 50% in southern Borneo to near 100% around Luzon. In general cloud cover is over 70% throughout the monsoon.

There were other clear differences in the meteorology depicted in Figure 3 between August and September. Notably, in August winds were characteristically easterly south of the equator, southerlies across the equator, and ultimately leading to southwesterly in the SCS. However in September winds in the lower free troposphere had stronger zonal components. Cloud cover patterns changed over most of the region from August to September in concert with the precipitation.

Inter-annual anomalies for 2012 were relatively small to moderate compared to the climatological baselines. The most significant driver of inter-annual variability in precipitation (e.g., McBride et al. 2003) and hence biomass burning, is ENSO (e.g., Nichol, 1998; Siegert et al., 2001, Field and Shen 2008; Reid et al. 2012 to name a few). For the 2012 southwest monsoon season, the mean Oceanic Nino Index (ONI) indicated slight warming, at +0.3^{o}C to +0.4^{o}C for July through October coming out of ~0^{o}C in the boreal spring. While in a warmer phase, the burning season is still considered neutral ENSO conditions based on the commonly used 0.5^{o}C threshold, and in line with the climatological average fire counts observed. Reid et al. (2012) noted that there appeared to be a correlation between positive ENSO phase and earlier monsoonal transition from the Southwest to the Northeast phases. As is shown in the next subsection, in 2012 the monsoonal transition appeared to be consistent with this warmer ENSO phase, with northeasterly winds returning by the end of the first week of October.

Metrics for monthly meteorological anomalies were quite mixed for 2012, leading us to believe that 2012 meteorology was overall largely within the “seasonally average” domain. Indeed, given the skill of model and satellite products in the region, and the paucity of rain gauge data, it is difficult to make fine delineations outside of extreme years (Reid et al., 2012; 2013). A full evaluation is out of scope here, but after evaluating a series of gauge networks, satellite and model products (e.g., datasets found in Kalnay et al;, 1996; Chen et al., 2008; Becher et al., 2013; Field et al. 2015). the consensus suggests normal precipitation and neutral drought scores in burning areas. Indeed, CMORPH precipitation was generally neutral in fire prone areas (Figure 3). Near surface wind anomalies in the SCS for June through August were also generally light in the reanalysis products; although stronger monsoonal enhancements in the northern SCS were observed with resulting increases in precipitation. The most significant anomaly was seen in September, where strong but slow moving TCs clearly appear, resulting in significant flow distortions and precipitation enhancements in the SCS. September zonal anomalies maximized at 2-3 m s^{-1} (or 30-40% enhancement) across the SCS region at 700 hPa.

3.1.3 Seasonal Aerosol Fields

By combining fire data with meteorology, we can explain regional AOT fields for the 2012 season (Figure 3). Smoke from biomass burning in Central to Southern Sumatra and Kalimantan, Borneo mixes with pollution emissions and is transported across the South China, Sulu and Celebes Seas by the prevailing monsoonal winds (Reid et al., 2012, 2015; Wang et al., 2013; Xian et al., 2013). There, a clear gradient in AOT forms, from biomass burning in the source regions to cleaner conditions to the northeast where particles are annihilated by ever increasing probability of precipitation.

The veering of winds from southwesterly near the surface to more zonal at 700 hPa results in off-island smoke transport being largely confined to the lowest few kilometers (Reid et al., 2015). This is clearly demonstrated in mean CALIOP extinction profiles derived in the method of Campbell et al., (2012) for a series of $5^o x 5^o$ boxes over the August-October burning period (Figure 4, marked on Figure 3). Included are Sumatra & Malay Peninsula; Borneo; southern SCS, and the Sulu & Celebes Sea. Results are similar to CALIOP analyses found in Campbell et al., (2013); Reid et al., (2013), Wang et al (2013) as well as the Singapore MPLNET climatology by Chew et al., (2013). Significant smoke concentrations are largely confined to or just above the boundary layer.

Consistent with the fire climatology of Reid et al., (2012), there is a shift in the maximum AOT in both MODIS and NAAPS from Central Sumatra/Riau in August towards Southern Sumatra/Sumatera Selatan in September. Advection patterns deduced from the MODIS and NAAPS products are consistent with the wind and precipitation shifts depicted in Figure 3. Smoke is advected predominantly into northern Malay Peninsula and the central SCSs in August. As discussed in the next subsection, September showed significant variability in monsoonal strength. Regardless, overall decreased meridional winds and enhanced precipitation in the SCS from August confines the smoke largely to the Southern SCS. This coincides with a shift in the domain of the Sumatran plume from over Kuala Lumpur and Penang, Malaysia, in August, to centered directly over Singapore in September.

For Borneo, high AOTs are visible in two distinct lobes; in Eastern Kalimantan, and Central/Western Kalimantan. The western half is clearly more dominant in August, with high AOTs spreading throughout the southern half of Borneo by September. Transport of smoke from Borneo is bifurcated by the high mountain ridge running along the border of Malaysian Sarawak and Indonesian Kalimantan (Reid et al., 2013; Wang et al., 2013). Western and some Southern Kalimantan smoke exits over Sarawak into the SCS. Another lobe of smoke from Southern and Eastern Kalimantan exits into the Celebes Sea. Once transported off-island, smoke is advected by the Southwesterly winds. As for smoke from Sumatra, the shift to a stronger zonal wind component in September leads likewise to more eastward zonal transport from Borneo.

While the AOT map gives a good semi-quantitative depiction of the overall aerosol patterns, one must be careful in evaluating AOT maps in this region. NAAPS has lower AOTs than MODIS, both in fire regions and in regard to long range transport. These differences are the result of a number of causes, including likely cirrus contamination in the MODIS products increasing the baseline AOT throughout the region (Reid et al., 2013). At the same time, cloud cover interferes with NAAPS MODIS derived smoke source function. There are also sampling differences inherent in a bulk monthly product to consider. For example, there are very few MODIS retrievals available for compositing (5-10 per month in the above composites shown), and when there is data, it tends to be during periods of reduced convection, enhancing fire. Indeed, there are very few retrievals over land when the cloud fraction is above 30% (Hyer et al., 2011), a true anomaly in a region of such extensive cloud cover. While we expect from the nature of the data that MODIS will have consistently higher AOTs than NAAPS, there are regions where NAAPS has the higher values. These include the mountainous regions of Borneo separating Sarawak and Kalimantan. Such mountain features, up to 3 km high, present a physical barrier to smoke transport, but are difficult to capture in model simulations-particularly at lower resolutions such as in NAAPS (Wang et al., 2013).

3.2 Seasonal time series of fire and monsoon characteristics

While Section 3.1 and Figure 3 provide a good overview of the mean state of the monsoonal and aerosol system during the 2012 7SEAS intensive period, there is considerable high frequency variability in fire detections and emissions. This is demonstrated in Figure 5 for the June 1st through October 31st, 2012 period, which covers nearly all of the burning activity for the 2012 SWM season. First, combined Terra and Aqua MODIS fire detections shown in Figure 2 are broken down by key regions and time in Figure 5(a). Fire activity is demonstrated in five-day box car average time series of combined Terra and Aqua MODIS fire hotspot data for June through October, broken down into the five key regimes defined in Reid et al., (2012; 2015):

Central Sumatra, Southern Sumatra, Indonesian Kalimantan-Borneo (an aggregate of western, southern and eastern Kalimantan), Malay Borneo (Sabah and Sarawak), a combined Sulawesi, Java, and Timor aggregate, and finally far-eastern Maluku, and the entire island of New Guinea. Fire activity in the 2012 Southwest Monsoon was initiated with an event in Central Sumatra in mid-June, followed by a month long hiatus. Fire activity resumed in late July and early August in central Sumatra and Indonesian Kalimantan, subsiding somewhat in late August. The most significant burning activity occurred throughout the MC in a series of events in September through the first week of October.

3.2.1 Time series of ISO, fire and monsoon characteristics for the 2012 burning season

The episodic nature of fire activity in 2012 is related to a desire by inhabitants for burning, coupled with regional meteorological opportunity. Intra-season Oscillations (ISO), such as the MJO, modulate weather on 45-60 day timescales (Zhang, 2005, 2013) and have been shown to modulate aerosol lifecycle across the globes tropical and subtropical domain (Indeed, MJO- (Tian et al., 2011; Reid et al., 2012; Guo et al., 2013). The Boreal Summer Intra-Seasonal Oscillation (BSISO) is similar to the MJO but with distinct northward propagation associated with the SWM (e.g., Kikuchi et al., 2012) in the northern part of the MC (north of 15˚N). Most of the MC is affected by its eastward propagation. As found in Reid et al., (2012) we consider the ~45 day ISO signal as indicted by the Wheeler and Hendon (2004) MJO index a dominant indicator of active convective phases and breaks (Zhang, 2005). Monsoonal strength in turn has a strong influence on fire emissions and aerosol lifecycle (Reid et al. 2012) and likely AOT (Tian et al., 2008).

The Wheeler and Hendon (2004) product of MJO phase and amplitude is provided in Figure 5(b). Conventionally, the MJO exists when the amplitude is greater than 1 (above one standard deviation) and is considered strong when the amplitude is in excess of 1.5. To provide meteorological context for the SCS at shorter time scales, in Figure 5(b) are also the names and categories of TCs entering the area (Tropical Storm-TS; Typhoon-TY; Super Typhoon-STY), timed by their closest approach to the island of Luzon, Philippines. Also, in the Figure 5 time series, meteorological data derived from the Riau Island radiosonde site provides an indication of the state of the SWM. Included are (c) 700 hPa relative humidity (RH), as an indicator of overall convective activity and (d) 925 hPa meridional (v) wind component to monitor the strength and seasonal migration of the monsoon. Correlated with the meteorological parameters presented in Figure 5 are numerous other phenomena, including the onset and length of the monsoon season (Staub et al., 2006; Cook and Buckley, 2009; Tong et al., 2009), TC activity (e.g., Maloney and Hartman, 2001), diurnal cycle of precipitation (e.g., Peatman et al., 2014) and off-island airflow. All of these factors are related to aerosol activity and transport (Reid et al., 2012; 2015; Wang et al., 2013).

If ENSO and the seasonal monsoon migration set the bounds of the burning season, the MJO often regulates the temporal variability and transport within that period. As demonstrated Figure 5(b) for 2012, three ISO events propagated into the MC. Typically in the SWM, the MJO signal is weaker than in boreal winter but clearly present (Zhang 2005; 2013). The burning season was initiated by a moderately strong event from May into early June, with amplitudes well above 1, especially for the drier phases in the MC (Phases 5-8). This MJO was related to the first major burning event that emerged from Central Sumatra/Riau Provence in June and corresponds with dry air in the lower to middle free troposphere with a seasonal low RH of 40% (Figure 5(c)) and a strong monsoonal flow (Figure 5(c)). This dry layer, a common feature of the MJO west of its convective center, is originated from subsiding air and advected subtropical air in the Indian Ocean. It inhibits convection and hence promotes biomass burning. Indeed, Central Sumatra's short pulse of fire activity in June is a recurring feature in the MODIS fire record, and is likely the result of agricultural burning and stacked fuels ready for the first sufficiently dry southwest monsoon period (Reid et al., 2012). While much attention has been paid to the "anomalous" June 2013 burning and smoke event in Sumatra that severely reduced air quality on the Malay Peninsula, this event is actually a recurring feature (Reid et al., 2012), although the impacts to Singapore in 2013 were unprecedented.

The next MJO event, started strong in the Indian Ocean in mid-June (Phase 1 & 2), then stalled on approach to the MC with significant convective activity in the region. This suppressed burning activity. After a brief retreat to the west, it managed to continue move eastward through the MC as a weak event that is barely recognizable in Figure 5. Such weakening of the MJO over the MC is known as a consequence of the "barrier effect" of the MC (Zhang 2014). Further, as discussed in Napitu et al., (2015), a weak MJO event often follows a strong event – particularly in summertime. They hypothesize that this may be a consequence of a more vigorous cooling by the previous strong MJO on sea surface temperature. As this MJO progressed to later phases, a second greater peak in August burning in Central Sumatra and Western Kalimantan (apparent in a peak in the greater Indonesian Kalimantan domain) appeared. As in the previous event, free tropospheric air was likewise drier and the monsoon flow steady if not significantly enhanced. This early to mid-August period typically hosts the first major event to span the MC (Reid et al., 2012) and it too is likely related to burning need and meteorological opportunity around the month of August. From August onward, the burning pattern was eastward propagating through the season, which is consistent with the eastward migration of the monsoon as described by Moron et al. (2009).

The third relevant MJO event, which also coincided with the *Vasco* cruise discussed in Part II of these papers (Reid et al., 2016), formed in the Indian Ocean in mid-August, with its amplitudes as high as 2 through early Phase 3 (its convection center entering the MC). Upon reaching the MC in the last week of August, however, the amplitude weakened to less than 1 (below one standard deviation), propagation was slow from Phase 3 to Phase 6 (the period when the MJO is transiting through the MC), and it subsequently died off in the central Pacific ocean by the end of September. Nevertheless, fire activity tracked this event, reaching a peak at the end of September. Interestingly, for this MJO, free tropospheric air was not as dry as it had been in the previous two events (Figure 5(c)), perhaps related to the weak MJO dying before Phases 7 and 8. Monsoonal flow was also quite unsettled in September with strong enhancements and even flow reversals. As discussed in the next sub section, monsoonal enhancements in the SCS were associated with the propagation of TCs east of the Philippines. Between these enhancements, strong reversals were found, as much as -5 m s^{-1} meridional flow at Riau Island on individual soundings. These impressive reversals are consistent with easterly wave activity between TCs.

Finally, based on the meridional winds in Figure 4(d), the monsoon flow switched to the northeasterly winter phase at the end of the first week of October. This brought enhanced precipitation back to the MC and, effectively, an end to the burning season. Simultaneous with the monsoon switch, another weak and slow moving MJO event started over the Indian Ocean in

October and propagated through in November (not shown). Historically however, the monsoonal shift does not necessarily immediately bring an end to the burning season. As discussed in Reid et al., (2012) in the most significant burning years, the monsoon shift happens in the absence of significant precipitation and can even enhance burning. We speculate that for 2012, more significant smoke generation and transport events advecting westward from Borneo would have been observed had this MJO progressed with more typical speed. Instead, the stalling of the MJO over the MC brought additional rainfall over the ocean (e.g., Chen and Houze 1997; Peatman et al., 2014), further shortening aerosol lifecycles and not bringing late MJO-phase related dry air to the region.

3.2.2 *Tropical cyclone activity*

Throughout the above narrative is the influence of TCs which is, in part, embedded in the overall MJO and monsoonal strength signals. With the ITCZ at its most northern extent, tropical cyclone paths likewise tend to be level with or north of Luzon in early summer, descending southward as the summer progresses (Carmargo et al., 2007; Kim et al, 2008). When TCs are located just east of the Philippines or transiting westward into the SCS or up towards Japan, two significant meteorological impacts on aerosol lifecycle have been hypothesized to occur (Reid et al., 2012; Wang et al., 2013). First, a long area of monsoonal enhancement akin to an inflow “arm” often forms to the south and west of the TC. This monsoon enhancement has been noted to stretch from east of the Philippines to as far west as Sumatra. Such TC induced monsoonal enhancements have been noted by Philippine forecasters to bring heavy rainfall to Luzon (e.g., Cayanan et al., 2011; Cruz et al., 2013). Reid et al., (2012; 2015) and Wang et al., (2013) noted that such enhancements tend to draw out smoke from the MC into the SCS where it is then sometimes annihilated by convection associated with the enhancement. However, as the TC passes, large-scale upper-level subsidence around the TC can inhibit convection and rainfall in the region, thus promoting biomass burning (and enhancing its observation from space). This subsidence can even be cross equatorial and enhance burning activity. The balance of the TCs large scale subsidence and monsoon flow enhancement factors in production, advection and regional changes to precipitation allows TCs to simultaneously modulate multiple aspects of aerosol lifecycle.

According to the Joint Typhoon Warming Center, the 2012 Western Pacific had 25 named storms, compared to 26 in the long term average. Noteworthy is that when TCs were east of the Philippines (closest point within 1000 km of Luzon marked in Figure 5(b)), there were often coincidences with peaks in observed Southwest Monsoon flow (Figure 5(d)), convection (Figure 5(c)) and biomass burning activity (Figure 5(a)). A pair of tropical storms (Mawar and Guchol) passed directly on the eastern edge of the Philippines, just at the initiation of the burning season. A second pair of typhoons (Damrey and Kai-tak), were also associated with monsoon enhancements. The four TCs passing through the region in late August through September were particularly intense: a pair of super-typhoons (Temblin and Bolaven) in late August, and two slower moving and even more intense super-typhoons (Sanba and Jelewat) passing the vicinity in September. The impact of these storms on the mean monthly flow and precipitation of the central SCS in of September is clear in Figure 3. Noteworthy for the September storms was not only their relationship to regional monsoon enhancements, but also with monsoon hiatuses. Indeed, as mentioned in Section 3.2.1 the strongest amplitude shifts in monsoonal strength for the entire 2012 burning season occurred in September when these storms were active. Strong Southwesterly flow was replaced by complete flow reversals in the SCS in a matter of days (Figure 5(d)). These flow reversal features are consistent with the propagation of easterly waves. Also in September, strong tropical storm (Gaemi) formed in the SCS in late September. Aside from winds, the monsoonal enhancements from TCs resulted in the significant precipitation enhancement over the SCS in September. Between winds and precipitation, TC's clearly modulated smoke transport and scavenging.

TCs may also have played a role post monsoon season. The monsoon shift after the first week of October occurred coincident with the arrival of Typhoon Prapiroon in the northeast eastern Philippines, as well as category 3 Son-Tinh as it propagated across the central Philippines. Thus, while the monthly mean wind fields were relatively normal (e.g., Figure 3), significant flow variability existed which as we show affected long range aerosol transport.

3.3 Significant smoke episodes

Moving from burning and monsoonal activity to resultant regional AOT, 2012 showed higher burning-region AOTs in comparison to the 2011 period explored in Reid et al., (2015), and the cold and neutral ENSO phases explored in Xian et al., 2013 . While satellites and models can provide regional AOT patterns, the best indicator for significant smoke events is via AOT from AERONET sites. AERONET, although spatially limited and suffering from its own clear sky bias, has the advantage of more potential samples on any given day, and an ability to quantify AOT for high concentration regions and moderately high cloud fraction. Further, through the SDA method, the fine mode AOT of smoke and pollution can be isolated, minimizing thin cirrus contamination (Chew et al., 2011). While a full analysis of AERONET data is outside of the scope here, in Figure 6 are the time series of fine mode 500 nm AOTs from AERONET sites deployed for the 2012 season to provide an overview of AOT variability. Corresponding statistics for the core burning season, which we take to be August 1st through October 15th, are included in Table 2. Sites include the first AOT measurements made in the heart of the burning areas on Sumatra and Kalimantan, Borneo. To provide spatial context, for some of the most severe events corresponding NAAPS fine mode AOTs are provided in Figure 7.

Comparison of Figure 6 to the temporal time series of Figure 5(a) show that fine-mode AOTs, to a certain degree, were correlated with the fire signal, but not exceedingly so. This is perhaps due to the high coverage of cirrus clouds that can affect satellite fire observations more than it affects AERONET observations with their SDA extraction of fine-mode AOT (*e.g.*, see observability review by Reid et al., (2013)). The weaker MJO periods or TCs may also have perturbed the transport of smoke off-island.

Using Jambi (a) as an indicator of Sumatran source region AOTs, smoke events could be moderately strong in the early to middle month of August, reaching over 1, with a peak 1.5. Late in August, no AOT data were available due to consistent cloud cover and precipitation, as evidenced in Figure 3. However, Jambi AOT grew significantly coincident with Southern Sumatra Burning, with AOTs being mostly over one from September through early October. In comparison to Jambi, (c) Singapore and (d) Tahir, both receptors for Sumatra on the Malay Peninsula, likewise showed peaks in fine AOT. Singapore was the only site operating for the mid-June burning event and showed slightly-elevated fine 500 nm AOTs, on the order of 0.5 above the 25 percentile background level of ~0.3 (not shown).

Beginning in August, Tahir in northern Malaysia appears to be a very strong receptor on August 11-13th which may also correspond with a peak in fine AOT to 0.2 in Nha Trang, Vietnam (h), demonstrating long range transport up the SCS. This is demonstrated in the NAAPS fine AOT fields for Aug. 12th (Figure 7(a)). In fact Tahir, a receptor, had higher August AOTs than Jambi, which was in the source region. As the location of Jambi was south of the Riau burning, the site may be more representative of burning in Southern Sumatra. On the southern tip of the Malay Peninsula, Singapore showed higher AOTs later in the study. As shown in Figure 3 and 5, a southward shift in burning activity on Sumatra and more zonal winds brought the smoke directly over Singapore. The most significant event (Sept. 21st, 2012), had AOTs reaching 1, aided by monsoonal enhancements related to Typhoon Jelewat, with smoke transport being simulated up much of the SCS (Figure 7(c)).

Using Palangkaraya as a source indicator for Southern Kalimantan, the MC's largest single source region, AOT did not depart from background levels of ~0.2 until about September 1st, upon which AOTs increased significantly reaching 1.5 in mid-September, with a second event with AOTs of ~5.6 around October 1st. In comparison, for Pontianak in Western Kalimantan, AOTs had a mean of 0.6 and 25-75% quartiles of 0.35-0.77. These values were more consistent over time with only a slight enhancement in AOTs through the season. As discussed in Reid et al., (2012) and seen in the monthly average AOT plots in Figure 3, the region around Pontianak has its own burning which often follows Sumatra, and thus can be regarded as a local source and a receptor. Kuching Sarawak also had a number of moderate AOT events throughout the season. Mean AOTs were 0.5 with values as high as 1.5-colinear with AOT at Palangkaraya. However, one notable event at Kuching in the middle of September peaked with an AOT of 1. Aided by monsoonal enhancement by TC Sanba exiting the region, this event at Kuching led to a subsequent peak of 0.3 at Marbel University (g) two days later. Smoke from the event was sampled by the mission Vasco cruise (Reid et al., 2016) and was simulated in NAAPS to pass through Mindanao and over the Pacific Ocean (Figure 7(b)).

Burning and AOTs continued to increase through the burning seasons, and dropped precipitously after the first week of October. This is coincident with large scale flow reversal in the SCS signaling the end of the Southwest Monsoon (Figure 5(d)). The monsoon switch, however, is not instantaneous, but migrates in a series of flow reversals from the north. The end result of this situation is low monsoonal winds, and very high AOTs across the region with smoke accumulating in the source regions. Pollution and smoke can also be being transported from Peninsula Southeast Asia and China Southward. This situation is evident with AOTs maximizing at 5 in Palangkaraya on Oct. 1st with a second major pulse on Oct. 6th. Likewise peaks existed in other source and nearfield receptors such as Jambi, Singapore, Kuching, and Pontianak. At the same time, AOTs began to peak at the outer receptors of Nha Trang, Vietnam and Marbel University, Mindanao. This situation, so evident in AERONET, is regionally demonstrated in the NAAPS AOT fields for Oct. 1th (Figure 7(d)). For Nha Trang, the higher AOTs are from advection from the northwest and east, as the site was under the influence of emerging biomass burning in Indochina, and pollution from China. At the same time, flow in the vicinity of Marbel University was slight and devoid of precipitation, and thus high AOTs represent some lingering burning activity from Eastern Kalimantan or Sulawesi transported into the region. In particular, TC Prairoon and Son-Tina provided the last monsoonal enhancements in the Celebes Sea.

Perhaps the final question for a regional overview paper is ultimately, how did smoke events (and thus likely final concentrations and particle emissions) for 2012 compare to other years? Given the complexity of observing the MC aerosol system it is difficult to be quantitative-especially in a region where fire counts alone can vary by an order of magnitude. The most reliable data is certainly AERONET, although the observing network has only recently come into being as part of 7SEAS. But, examination of the three sites with the longest data record is somewhat revealing. Table 3 provides mean and standard deviations of AERONET 500 nm fine mode AOT for Singapore, Kuching Sarawak, and Notre Dame of Marable University Mindanao. Averages are for the entirety of the August through October periods as used in Figure 7. Singapore has the longest data record, being established in 2007. Interestingly, 2012's mean of 0.57 is the second highest of the 8 year period. 2012 was higher than the El Nino year of 2009, but yet only 40% of the 1.5 value for the massive 2015 event. This strong value is consistent with the enhanced burning activity observed in Southern Sumatra in 2012. Kuching, a good receptor for smoke from Borneo, also had 2012 AOTs the second highest of the four available years (2011-2013, 2015). Yet, from a fire detection point of view, both Southern and Eastern Kalimantan were significantly below average. Fire activity in Western Kalimantan, however, was slightly enhanced. This suggests that Kuching may be a better receptor for Western Kalimantan than for the heart of Borneo's burning region. Finally for ND of Marbel Univ., the 2012 season was middling. This suggests it may be a receptor for smoke from Southern and Eastern Kalimantan, wrapping around the Celebes Sea as well as the South Chain Sea. Taken together, AERONET suggests that overall, 2012 was a fairly significant biomass burning year, but still substantially below the massive El Nino events such as 2015, and likely 2006 and 1997.

6.0 DISCUSSION AND CONCLUSIONS

The purpose of this paper is twofold. First, there is a need for a meteorological overview to support the 2012 7SEAS campaign activities. This campaign in particular was a high water mark for observations in the 7SEAS program. Here we provide seasonal plots of fire activity, monsoon characteristics, and AOT coverage to give context to measurements. In particular, we wish to support discussion of finer scale aerosol features in Part II of this series, which focuses on ship observations in the Philippines as an indicator of the characteristics of smoke transported long distances in the South China Sea (Reid et al., 2016) . A second goal of this paper is to provide an opportunity for a narrative of the complex aerosol meteorology of the MC. This narrative, when combined with the 2011 narrative in Reid et al., (2015) and brief seasonal narratives in Reid et al., (2012), allows us to gain an appreciation for the inter-seasonal similarities and differences in MC fire weather and smoke transport.

Fire activity: There are many aspects of the 2012 season that are "typical". Overall fire hotspot detections for the core June-October burning season were only 10% under the 2003-2009 baseline provided by Reid et al., (2012), although notable regional fire perturbations include +30% in Southern Sumatra, and -40% in Southern and Western Kalimantan. In comparison, internal standard deviations for most regions are >50%, %, indicating significant spatial and temporal variation from year to year within regions. Fire activity began early in the west, in June and August, moving to the most significant burning in September and early October. This fire activity was consistent with a slightly warm but technically neutral ENSO phase, which also brought typical if not lightly enhanced precipitation.

Monsoonal flow: While fire and meteorology was well within norms for "means", fire was strongly modulated by the MJO and SWM flow on Sumatra and Borneo, being more systematically increasing in eastern islands as the season progressed. This too is characteristic of regional burning activity (Reid et al., 2012). However, there were periods of strong SWM modulation brought about by a combination of TC passages (enhancing southwest flow) and easterly waves, resulting in sometimes strong meridional flow reversals. When averaged, this activity resulted in anomalously enhanced zonal winds over the central and northern South China Sea-particularly in September when burning was at a maximum. Fire activity largely subsided with the switch of the SWM to the wintertime northeasterly phase in the second week of October.

AOTs: Biomass burning smoke distribution and transport were monitored by a series of AERONET sun photometers, MODIS AOT retrievals, and NAAPS reanalysis model products. For the most part, all products agree on active fire emission areas and transport patterns of smoke off the islands into the South China, Sulu and Celebes Seas by SWM winds. AERONET in particular provided the first region-wide quantitative view of AOTs. Sites within source regions, such as Jambi Sumatra and Palankaraya, Central Kalimantan, had mean and standard deviation 500 nm fine AOTs of 1.3±0.7 and 0.9±0.3, respectively, although, Palankaraya did host the two most significant smoke events, with AOT's one day reaching 5.6. In August, smoke largely travelled up the South China Sea to almost as far north as Luzon, Philippines. During the September peak burning period, anomalous zonal winds kept smoke to the southern South China Sea and south of central Philippines. This so happens to be the key region for the receptor measurement on the *M/Y Vasco* described in Part II of this series (Reid et al., 2016). In comparison to other years in the AERONET data record (going back as far as 2007 for Singapore), 2012 was clearly a substantial year, had heavy smoke over much of the region, exceeding other years with the notable exception of the 2015 El Nino event. This is somewhat at odds with MODIS active fire hotspot data which suggested more average fire activity.

Final commentary: Overall 2012 fire activity and transport patterns were well within "one sigma" for SWM. However, the standard deviations for fire and smoke activity for the region are exceptionally large. Qualitatively, from a fire and smoke closure points of view, there are consistencies in the dataset. Significant fire activity and high AOTs were observed in Southern Sumatra, and at Singapore and Tahir, Malaysia, as a receptor. However, burning on Borneo was generally neutral or slightly enhanced in the west, and 45% lower than average in the core areas of Southern and Western Kalimantan. AOTs at Kuching, an excellent indicator of smoke entering the South China Sea, were high. The complexity of the MC’s meteorology and aerosol system results in non-linear relations between observed fire activity and regional aerosol loading. Previously identified aspects of the system such as monsoonal shifts, the MJO/BSISO, TCs, and the role of orography follow the conceptual modes and examples of Reid et al. (2012) and Wang et al. (2013). But as of yet, observability and predictability of the system are nevertheless still only semi-quantitative. Clearly, the 2012 field measurement dataset, especially in the context of its 2011 preparatory mission, is valuable for further study.

7.0 ACKNOWLEDGEMENTS

We are grateful to all participants in the 2012 7SEAS intensive study, and are in particular grateful to the host institutions for regional AERONET site deployment and the use of derived optical thickness data herein. Authors also benefitted from conversations with Eric Maloney (CSU), Matthew Wheeler (CSIRO), and Chidong Zhang (U of Miami). Funding for US scientist deployment and instrument analysis was provided by the NRL Base Program and ONR 35. Modeling analysis was provided by ONR 32. Remote sensing and model analysis was provided by the NASA Interdisciplinary Science Program. Ground site deployments were supported by the NASA Radiation Science Program through a grant from the Southeast Asia Composition, Cloud, Climate Coupling Regional Study (SEAC^{4}RS) science team. Author JRC acknowledges the support of NASA Interagency Agreement NNG13HH10I on behalf of MPLNET and SEAC^{4}RS science teams.

8.0 REFERENCES:

Atwood, S. A., Reid, J. S., Kreidenweis, S. M., Yu, L. E., Salinas, S. V., Chew, B. N., and Balasubramanian, R.: Analysis of source regions for smoke events in Singapore for the 2009 El Nino burning season, Atmos. Environ.,78, 219-230, doi: 10.1016/j.atmosenv.2013.04.047, 2013.

Atwood, S. A., et. al.: Size resolved aerosol and cloud condensation nuclei (CCN) properties in the remote South China Sea: Measurement and sources. Submitted, Atmos. Chem and Phys., 2016.

Becher, A. et al: A description of the global land-surface precipitation data products of the Global Precipitation Climatology Centre with sample applications including centennial (trend) analysis from 1901–present. Earth Syst. Sci. Data, 5, 71-99 (2013).

Campbell, J. R., Ge, C., Wang, J., Welton, E. J., Bucholtz, A., Hyer, E. J., Reid, E. A., Chew, B. N., Liew, S.-C., Salinas, S. V., Lolli, S., Kaku, K. C., Lynch, P., Mahamud, M., Mohamad, M., and Holben, B. N.: Applying advanced ground-based remote sensing in the Southeast Asian Maritime Continent to characterize regional proficiencies in smoke transport modeling, J. Appl. Meteorol. Clim., 55, 3-22, doi:10.1175/JAMC-D-15-0083.1., 2016.

Campbell, J. R., Reid, J. S., Westphal, D. L., Zhang, J., Tackett, J. L., Chew, B. N., Welton, E. J., Shimizu A., and Sugimoto, N.: Characterizing aerosol particle composition and the vertical profile of extinction and linear depolarization over Southeast Asia and the Maritime Continent:

the 2007-2009 view from CALIOP., Atmos. Res., 122, 520-543, doi:10.1016/j.atmosres.2012.05.007, 2013.

Carmargo, S. J., Robertson, A. W., Gaffnew, S. J., Smyth, P., Ghil, M.: Cluster analysis of typhoon tracks. Part 1. General properties, *J. of Clim., 20*, 3635-3653, 2007.

Cayanan, E. O., Chen, T.-C, Argete, J. C., Yen, M.-C., and Nilo, P. D., 2011, The effect of tropical cyclones on southwest monsoon rainfall in the Philippines, J. Meteor. Soc. of Japan, 89A, 123-139, 2011.

Chang, C.-P., Wang, Z., Mcbride, J., and Liu, C.-H.: Annual cycle of Southeast Asia-Maritime Continent rainfall and asymmetric monsoon transition, J. Climate, 18, 287-301, 2005.

Chen, M. Y., Shi, W., Xie, P. P., Silva, V. B. S., Kousky, V. E., Higgins, R. W., and Janowiak, J. E.: Assessing objective techniques for gauge-based analyses of global daily precipitation, J. Geophys. Res., 113, D04110, doi:10.1029/2007JD009132, 2008.

Chen SS, Houze RA. 1997. Diurnal variation and life-cycle of deep convective systems over the tropical Pacific warm pool. Q. J. R. Meteorol. Soc. 123: 357–388.

Chen, S. S. and Houze, R. A.: Diurnal variation and life-cycle of deep convective systems over the tropical Pacific warm pool, Q. J. Roy. Meteor. Soc., 123, 357–388, 1997.

Chew, B. N., Campbell, J. R., Reid, J. S., Giles, D. M., Welton, E. J., Salinas, S. V., and Liew, S. C.: Tropical cirrus cloud contamination in sun photometer data, Atmos. Environ., 45, 6724-6731, doi:10.1016/j.atmosenv.2011.08.017, 2011.

Chew, B. N., Campbell, J. R., Salinas, S. V., Chang, C. W., Reid, J. S., Welton, E. J., Holben, B. N., and Liew, S. C.: Aerosol particle vertical distributions and optical properties over Singapore, Atmos. Environ., 79, 599-613, doi:10.1016/j.atmosenv.2013.06.026, 2013.

Cruz, F. T., Narisma, G. T., Villafuerte, M. Q., Cheng Chua, K. U., and Olaguera, L. M.: A climatological analysis of the southwest monsoon rainfall in the Philippines, Atmos. Res., 122, 609-616, doi:10.1016/j.atmosres.2012.06.010, 2013.

Field, R.D. and Shen, S.S.P.: Predictability of carbon emissions from biomass burning in Indonesia, J. Geophys. Res., 113, G04024, doi:10.1029/2008JG000694, 2008.

Field, R. D., Spessa, A. C., Aziz, N. A., Camia, A., Cantin, A., Carr, R., de Groot, W. J., Dowdy, A. J., Flannigan, M. D., Manomaiphiboon, K., Pappenberger, F., Tanpipat, V., and Wang, X.: Development of a global fire weather database, Nat. Hazards Earth Syst. Sci., 15, 1407-1423, doi:10.5194/nhess-15-1407-2015, 2015.

Ge, C., Wang, J., and Reid J. S.: Mesoscale modeling of smoke transport over the Southeast Asian Maritime Continent: coupling of smoke direct radiative feedbacks below and above the low-level clouds, Atmos. Chem. Phys., 14, 159-174, doi:10.5194/acp-14-159-2014, 2014.

Giorgi, F., Coppola, E., Solomon, F., Mariotti, L., Sylla, M. B., Bi, X., Elguindi, N., Diro, G. T., Nair, V., Giuliani, G., Turuncoglu, U. U., Cozzini,S., Guttler, I., O'Brien, T. A., Tawfik, A. B., Shalaby, A., Zakey, A. S., Steiner, A. L., Stordal, F., Sloan, L. C., Brankovic, C.: RegCM4: model description and preliminary tests over multiple CORDEX domains, Climate Research, 52, 7-29, 2012.

Guo, Y. J., Tian, B., Kahn, R. A., Kalashnikova, O., Wong, S., Waliser, D. E.: Tropical Atlantic dust and smoke aerosol variations related to the Madden-Julian Oscillation in MODIS and MISR observations, J. Geophys. Res., 118, 4947-4963, doi:10.1002/jgrd.50409, 2013

Holben, B. N., Eck, T. F., Slutsker, I., Tanre, D., Buis, J. P., Setzer, A., Vermote, E., Reagan, J. A., Kaufman, Y. J., Nakajima, T., Lavenu, F., Jankowiak, I., and Smirnov, A.: AERONET - A federated instrument network and data archive for aerosol characterization, Remote Sens. Environ., 66, 1-16, 1998.

Hogan , T.F. and Rosmond, T.E., The description of the U.S. Navy Operational Global Atmospheric Prediction System’s spectral forecast model, Mon. Wea. Rev., 119, 1786-1815, 1991.

Hyer, E. J. and Chew, B. N.: Aerosol transport model evaluation of an extreme smoke episode in Southeast Asia, Atmos. Environ., 44, 1422-1427, doi:10.1016/j.atmosenv.2010.01.043, 2010.

Hyer, E. J., Reid, J. S., and Zhang, J: (2011), An over-land aerosol optical depth data set for data assimilation by filtering, correction, and aggregation of MODIS Collection 5 optical depth retrievals, *Atmos. Meas. Tech.*. 4, 379-408, doi:10.5194/amt-4-379-2011, 2011.

Hyer, E. J., Reid, J. S., Prins, E. M., Hoffman, J. P., Schmidt, C. C., Miettinen, J. I., and Giglio, L.: Patterns of fire activity over Indonesia and Malaysia from polar and geostationary satellite observations, Atmos. Res., 122, 504-519, doi:10.1016/j.atmosres.2012.06.011, 2013.

Jamandre, C. A. and Narisma, G. T.: Spatio-temporal validation of satellite-based rainfall estimates in the Philippines, Atmos. Res., 122, 599-608. doi: 10.1016/j.atmosres.2012.06.024., 2013.

Joyce, R. J., Janowiak, J. E., Arkin, P. A., and Xie, P.: CMORPH: A method that produces global precipitation estimates from passive microwave and infrared data at high spatial and temporal resolution, J. Hydrometeorol., 5, 487-503, 2004.

Kaku, K. C., Reid, J. S., O'Neill, N. T., Quinn, P. K., Coffman, D. J., and Eck, T. F., Verification and application of the extended spectral deconvolution algorithm (SDA+) methodology to estimate aerosol fine and coarse mode extinction coefficients in the marine boundary layer, Atmos. Meas. Tech., 7, 3399-3412, doi:10.5194/amt-7-3399-2014, 2014.

Kalnay et al.: The NCEP/NCAR 40-year reanalysis project, Bull. Amer. Meteor. Soc., 77, 437-470, 1996.

Kikuchi, K., Wang, B., and Kajikawa, Y., 2012., Bimodal representation of the tropical intraseasonal oscillation, Clim. Dyn., 38, 1989-2000, doi: 10.1007/s00382-011-1159-1

Kim, J. H., Chang, C. H., Kim, H. S., Sui, C.-H., and Park, S. K., 2008. Systematic variation of summertime tropical cyclone activity in the Western North Pacific in relation to the Madden–Julian Oscillation. *J. Climate*, 21, 1171–1191 doi: http://dx.doi.org/10.1175/2007JCLI1493.1

Levy, R. C., Mattoo, S., Munchak, L. A., Remer, L. A., Sayer, A. M., Patadia, F., and Hsu, N. C.: The Collection 6 MODIS aerosol products over land and ocean, Atmos. Meas. Tech., 6, 2989-3034, doi:10.5194/amt-6-2989-2013, 2013.

Lin, N.-H., et al., An overview of regional experiments on biomass burning aerosols and related pollutants in Southeast Asia: From BASE-ASIA and the Dongsha Experiment to 7-SEAS, Atmospheric Environment, 78, 1-19. 2013, doi.org/10.1016/j.atmosenv.2013.04.066

Lu, E. and Chan, J. C. L.: A unified monsoonal index for South China, J. Clim., 12, 2375-2385, 1999.

Lynch, P., Reid, J. S., Westphal, D. L., Zhang, J., Hogan, T. F., Hyer, E. J., Curtis, C. A., Hegg, D. A., Shi, Y., Campbell, J. R., Rubin, J. I., Sessions, W. R., Turk, F. J., Walker, A. L.: Development studies towards an 11-year global gridded aerosol optical thickness reanalysis for climate and applied applications, Geosci. Model Dev., 9, 1489-1522, doi:10.5194/gmd-9-1489-2016, 2016.

Maloney, E. D. and Hartman, D. L.: The Madden Julian oscillation, barotropic dynamics, and the North Pacific tropical cyclone formation, part 1: Observations, J. Atmos. Sci., 58, 2545-2558, 2001.

McBride, J. L., Malcolm, R. Haylock, N. N.: Relationships between the Maritime Continent heat source and the El Niño–Southern Oscillation phenomenon. J. Climate, 16, 2905-2914, 2003.

Miller, S. D., Hawkins, J. D., Kent, J., Turk, F. J., Lee, T. F., Kuchiauskas, A. P., Richardson, K., Wade, R. and Hoffman, C.: NexSat: Previewing NPOESS/VIIRS imagery capabilities, Bull. Amer. Meteor. Soc., 87, 433–446, doi: 10.1175/BAMS-87-4-433, 2006.

Misra, V. and Li, H.: The seasonal predictability of the Asian summer monsoon in a two tiered forecast system, Clim. Dynam., 42, 2491-2507, doi:10.1007/s00382-013-1838-1, 2014.

Moron, V., Robertson, A.W., and Beer, R.: Spatial coherence and seasonal predictability of monsoon onset over Indonesia, J. Climate, 22, 840-850, 2009.

Napitu, A. M., Gordon, A.L., Pujiana K., Intraseasonal sea surface temperature Variability across the Indonesian Sea, *Jour of Climate*., Vol. 28, No. 22: 8710-8727, 2015. Nichol, J.: Smoke haze in Southeast Asia: A predictable recurrence, Atmos. Environ., 32, 2715-2716, 1998.

O'Neill, N. T., Eck, T. F., Smirnov, A., Holben, B. N., and Thulasiraman, S.: Spectral discrimination of coarse and fine mode optical depth, J. Geophys. Res., 108, 4559, doi: 10.1029/2002JD002975, 2003.

Peatman, S. C., Mathews, A. J., and Stevens, D. P.: Propagation of the Madden-Julian Oscillation through the Maritime Continent and scale interaction with the diurnal cycle of precipitation, Q. J. Roy. Meteor. Soc., 140, 814-825, doi:10.1002/qj.2161, 2014.

Reid, J. S., Hyer, E. J., Prins, E. M., Westphal, D. L., Zhang, J. L., Wang, J., Christopher, S. A., Curtis, C. A., Schmidt, C. C., Eleuterio, D. P., Richardson, K. A., and Hoffman, J. P.: Global Monitoring and Forecasting of Biomass-Burning Smoke: Description of and Lessons From the Fire Locating and Modeling of Burning Emissions (FLAMBE) Program, IEEE J. Sel. Top. Appl., 2, 144-162, doi: 10.1109/JSTARS.2009.2027443, 2009.

Reid., J. S., Xian, P., Hyer, E. J., Flatau, M. K., Ramirez, E. M., Turk, F. J., Sampson, C. R., Zhang, C., Fukada, E. M., and Maloney, E. D.: Multi-scale meteorological conceptual analysis of observed active fire hotspot activity and smoke optical depth in the Maritime Continent, Atmos. Chem. Phys., 12, 1–31, doi:10.5194/acp-12-1-2012, 2012.

Reid, J. S., Hyer, E. J., Johnson, R. S., Holben, B. N., Yokelson, R. J., Zhang, J., Campbell, J. R., Christopher, S. A., Di Girolamo, L., Giglio, L., Holz, R. E., Kearney, C., Miettinen, J., Reid, E. A., Turk, F. J., Wang, J., Xian, P., Zhao, G., Balasubramanian, R., Chew, B. N., Janjai, S., Lagrosas, N., Lestari, P., Lin, N. H., Mahmud, M., Nguyen, A. X., Norris, B., Oanh, N. T. K., Oo, M., Salinas, S. V., Welton, E. J., and Liew, S. C.: Observing and understanding the Southeast Asian aerosol system by remote sensing: An initial review and analysis for the Seven Southeast Asian Studies (7SEAS) program, Atmos. Res., 122, 403-468, doi:10.1016/j.atmosres.2012.06.005, 2013.

Reid, J. S., Lagrosas, N. D., Jonsson, H. H., Reid, E. A., Sessions, W. R., Simpas, J. B., Uy, S. N., Boyd, T. J., Atwood, S. A., Blake, D. R., Campbell, J. R., Cliff, S. S., Holben, B. N., Holz, R. E., Hyer, E. J., Lynch, P., Meinardi, S., Posselt, D. J., Richardson, K. A., Salinas, S. V., Smirnov, A., Wang, Q., Yu, L., and Zhang, J.: Observations of the temporal variability in aerosol properties and their relationships to meteorology in the summer monsoonal South China Sea/East Sea: the scale-dependent role of monsoonal flows, the Madden–Julian Oscillation, tropical cyclones, squall lines and cold pools, Atmos. Chem. Phys., 15, 1745-1768, doi:10.5194/acp-15-1745-2015, 2015.

Reid, J. S., Lagrosas, N. D., Jonsson, H. H., Reid, E. A., Atwood, S. A., Boyd, T. J., Ghate, V. P., Lynch, P., Posselt, D. J., Simpas, J. B., Uy, S. N., Zaiger, K., Blake, D. R., Bucholtz, A., Campbell, J. R., Chew, B. N., Cliff, S. S., Holben, B. N., Holz, R. E., Hyer, E. J., Kreidenweis, S. M., Kuciaskas, A. P., Lolli, S., Oo, M., Perry, K. D., Salinas, S. V., Sessions, W. R., Smirnov, A., Walker, A. L., Wang, Q., Yu, L., Zhang, J., and Zhao, Y.: Aerosol meteorology of the

Maritime Continent for the 2012 7SEAS southwest monsoon intensive study: Part II regional scale phenomena, Atmos. Chem. Phys. Discuss., doi:10.5194/acp-2016-214, in review, 2016.

Rose, D., Nowak, A., Achtert, P., Wiedensohler, A., Hu, M., Shao, M., Zhang, Y., Andreae, M.O., and Pöschl, U.: Cloud condensation nuclei in polluted air and biomass burning smoke near the mega-city Guangzhou, China – Part 1: Size-resolved measurements and implications for the modeling of aerosol particle hygroscopicity and CCN activity, Atmos. Chem. Phys., 10, 3365–3383, 2010.

Salinas, S. V., Chew, B. N., Mohamad, M., Mahmud, M., and Liew, S. C.: First measurements of aerosol optical depth and Angstrom exponent number from AERONET's Kuching site, Atmos. Environ., 78, 231-241, doi:10.1016/j.atmosenv.2013.02.016, 2013.

Sampson, C. R. and Schrader A. J.: The Automated Tropical Cyclone Forecasting System (Version 3.2), Bull. Amer. Meteor. Soc., 81, 1231-1240, 2000.

Siegert, F., Ruecker, G., Hinrichs A., and Hoffmann A. A.:. Increased damage from fires in logged forests during droughts caused by El Nino. Nature, 414, 437-440, 2001.Sessions, W., Reid, J. S., Benedetti, A., Colarco, P., da Silva, A., Lu, S, Sekiyama, T., Tanaka, T., Baldasano, J., Basart, S., Brooks, M., Eck, T., Iredell, M., Hansen, J., Jorba, O., Juang, H., Lynch, P., Morcrette, J., Moorthi, S., Mulcahy, J., Pradhan, Y., Razinger, M., Sampson, C., Wang, J., Westphal, D.: Development towards a global operational aerosol consensus: basic climatological characteristics of the International Cooperative for Aerosol Prediction Multi-Model Ensemble (ICAP-MME) Atmos. Chem. Phys., 15, 2533-2534, doi: 10.5194/acp-15-2533-2015, 2015.

Staub, K. H., Kilandis, G. N., and Ciesielski, P. E.: The role of equatorial waves in the onset of the South China Sea summer monsoon and the demise of the El Nino during, 1998, Dynam. Atmos. Oceans, 42, 216-238, doi: 10.1016/j.dynatmoce.2006.02005, 2006.

Tian, B., Waliser, D. E., Kahn, R. A., Li, Q., Yung, Y. L., Tyranowski, T., Geogdzhayev, I. V., Mishchenko, M. I., Torres, O., Smirnov, A.: Does the Madden-Julian Oscillation influence aerosol variability?, J. Geophys. Res., 113, D12215, doi: 10.1029/2007JD009372, 2008.

Tian, B., Waliser, D. E., Kahn, R. A.,Wong, S.: Modulation of Atlantic aerosols by the Madden-Julian Oscillation, J. Geophys. Res., 116, 12, doi:10.1029/2010jd015201, 2011.

Tong, H. W., Chan, J. C. L., Zhou, W: The role of the MJO and mid-latitude fronts in the South China Sea Summer monsoon onset, Clim. Dynam., 33, 827-841, doi: 10.1007/s00382-008-0490-7, 2009.

Wang, J., Gei, C., Yang, Z., Hyer, E., Reid, J. S., Chew, B. N., and Mahmud, M.: Mesoscale modeling of smoke transport over the South Asian maritime continent: vertical distributions and topographic effect, Atmos. Res., 122, 486-503, 2013.

Wiedinmyer, C., Greenberg, J., Guenther, A., Hopkins, B., Baker, K., Geron, C., Palmer, P. I., Long, B. P., Turner, J. R., Pétron, G., Harley, P., Pierce, T. E., Lamb, B., Westberg, H., Baugh, W., Koerber, M., and Janssen, M.: Ozarks Isoprene Experiment (OZIE): Measurements and modeling of the ''isoprene volcano,'' J. Geophys. Res., 110, D18307, doi: 10.1029/2005JD005800, 2005.

Wheeler, M. C. and Hendon, H. H.: An all-season real-time multivariate MJO index: Development of an index for monitoring and prediction, Mon. Wea. Rev., 132, 1917–1932, 2004.

Wu, P., Hara, M., Hamada, J.-I., Yamanaka, M.D., and Kimura, F.:Why a large amount of rain falls over the sea in the vicinity 0f western Sumatra island during nighttime. Appl. Meteorol. 48, 1345–1361, doi: 10.1175/2009JAMC2052.1, 2009.

Xian, P., Reid, J. S., Turk, J. F., Hyer, E. J., and Westphal D. L.: Impact of modeled versus satellite measured tropical precipitation on regional smoke optical thickness in an aerosol transport model, Geophys. Res. Lett., 36, L16805, doi: 10.1029/2009GL038823, 2009.

Xian, P., Reid, J. S., Atwood, S. A., Johnson, R., Hyer, E. J., Westphal, D. L., and Sessions, W.: Smoke transport patterns over the Maritime Continent, Atmos. Res., 122, 469-485, doi:10.1016/j.atmosres.2012.05.006, 2013.

Yang, L., Nguyen, D. M., Jia, S. H., Reid, J. S., and Yu L. E.: Impacts of biomass burning smoke on the distributions and concentrations of C_2–C_5 dicarboxylic acids and dicarboxylates in a tropical urban environment, Atmos. Environ., 78, 211-218, doi:10.1016/j.atmosenv.2012.03.049, 2013.

Zhang, C.: Madden-Julian Oscillation, Rev. Geophys., 43, RG2003, doi:10.1029/2004RG000158, 2005.

Zhang, C.: Madden-Julian Oscillation: Bridging Weather and Climate, Bull. Amer. Meteor. Soc., 94, 1849-1870, doi: 10.1175/BAMS-D-12-00026.1, 2014.

Zhang, J. L., Reid, J. S., Westphal, D. L., Baker, N. L., and Hyer, E. J.: A system for operational aerosol optical depth data assimilation over global oceans, J. Geophys.Res. Atmos., 113, D10208, doi: 10.1029/2007JD009065, 2008.

Table 1. 2012 Active fire hot spot prevalence from combined Terra and Aqua MODIS for key areas of the Maritime Continent. Included is the 2003-2009 average from Reid et al., (2012), the sum off all fire detections in 2012, the number in the June-October study period here, and the fraction of the 2012 total thereof.

Location	*Average Annual Prevalence (# yr^{-1}) ±fractional StDev Reid et al., (2012)*	*Annual Prevalence (# yr^{-1}),2012*	2012:Climo (%)		*June-Oct Fire Count 2012*	*June-Oct (%)*
Brunei	55±50%	60	109		55	92
Indonesia						
Java and Bali	2120±21%	2157	102		2049	95
Kalimantan, Eastern	3085±52%	1571	51		1400	89
Kalimantan, Southern	13892±91%	8120	58		8021	99
Kalimantan, Western	5370±59%	5742	107		5720	100
Maluku Islands	890±58%	775	87		638	82
Papua	2460±80%	2139	87		1146	54
S. Islands & Timor	3985±21%	4088	103		3516	86
Sumatra, Central	10990±68%	9135	83		9082	99
Sumatra, Northern	210±32%	221	105		219	99
Sumatra, Southern	9400±78%	12241	130		12166	99
Sumatra, Westward	1760±35%	1943	110		1928	99
Sulawesi	3430±53%	2113	62		1718	81
Subtotal	57592±75%	50245	87		47603	95
Malaysia						
Malay Peninsula	1550±55%	1206	78		1163	96
Sabah, Borneo	640±43%	326	51		318	98
Sarawak, Borneo	1982±64%	2557	129		2496	98
Subtotal	4172±59%	4089	98		3977	97
Papua New Guinea	5170±52%	4487	87		2935	59
Timor Leste	1120±21%	856	76		787	92

Table 2. Descriptive statistics of daily averaged 500 nm fine mode AOT from active AERONET for August-October 15, 2012 core burning season.

Site	Jambi	Palangkaraya	Singapore	Tahir	Pontianak	Kuching	ND of Marbel Univ.	Nha Trang
Map locator	(a)	(b)	(c)	(d)	(e)	(f)	(g)	(h)
Region	Central Sumatra	Central Kalimantan	Malay Peninsula	Malay Peninsula	Western Kalimantan	Southern Sarawak	Mindanao	Vietnam
Type	Source	Source	Near-field Receptor	Near-field Receptor	Near-field Receptor	Near-field Receptor	Far-field Receptor	Far-field Receptor
Online (2012)	Jul 24th	Jul 21st	Feb 9st	Jul 10th	Jul 24th	Aug 8th	Jun 30th	Jul 7th
N Days	52	49	46	41	56	45	37	25
Mean/Median	1.27/1.01	0.92/0.45	0.57/0.52	0.34-0.21	0.79/0.67	0.61/0.50	0.13/0.11	0.14/0.12
Stdev	0.74	1.03	0.29	0.36	0.58	0.43	0.06	0.08
Min-Max	0.39-3.6	0.11-5.6	0.11-1.24	0.05-1.46	0.10-2.6	0.27-0.80	0.06-0.33	0.05-0.44
Quartiles (25-75%)	0.67-1.8	0.31-1.20	0.37-0.68	0.10-0.43	0.44-0.91	0.27-0.70	0.07-0.15	0.08-0.18

Table 3. August through October means and standard deviations of AERONET 500 nm Fine Mode AOT for three sites with the longest data record in the Maritime Continent.

Year	Singapore	Kuching	ND of Marble U.
2007	0.26±0.15	N/A	N/A
2008	0.21±0.12	N/A	N/A
2009	0.39±0.29	N/A	N/A
2010	0.27±0.29	N/A	0.09±0.04
2011	0.33±0.17	0.30±0.25	0.16±0.09
2012	0.57±0.29	0.58±0.43	0.14±0.08
2013	0.21±0.10	0.29±0.19	0.10±0.05
2014	0.56±0.36	N/A	0.23±0.19
2015	1.5±1.2	1.3±1.2	0.35±0.25

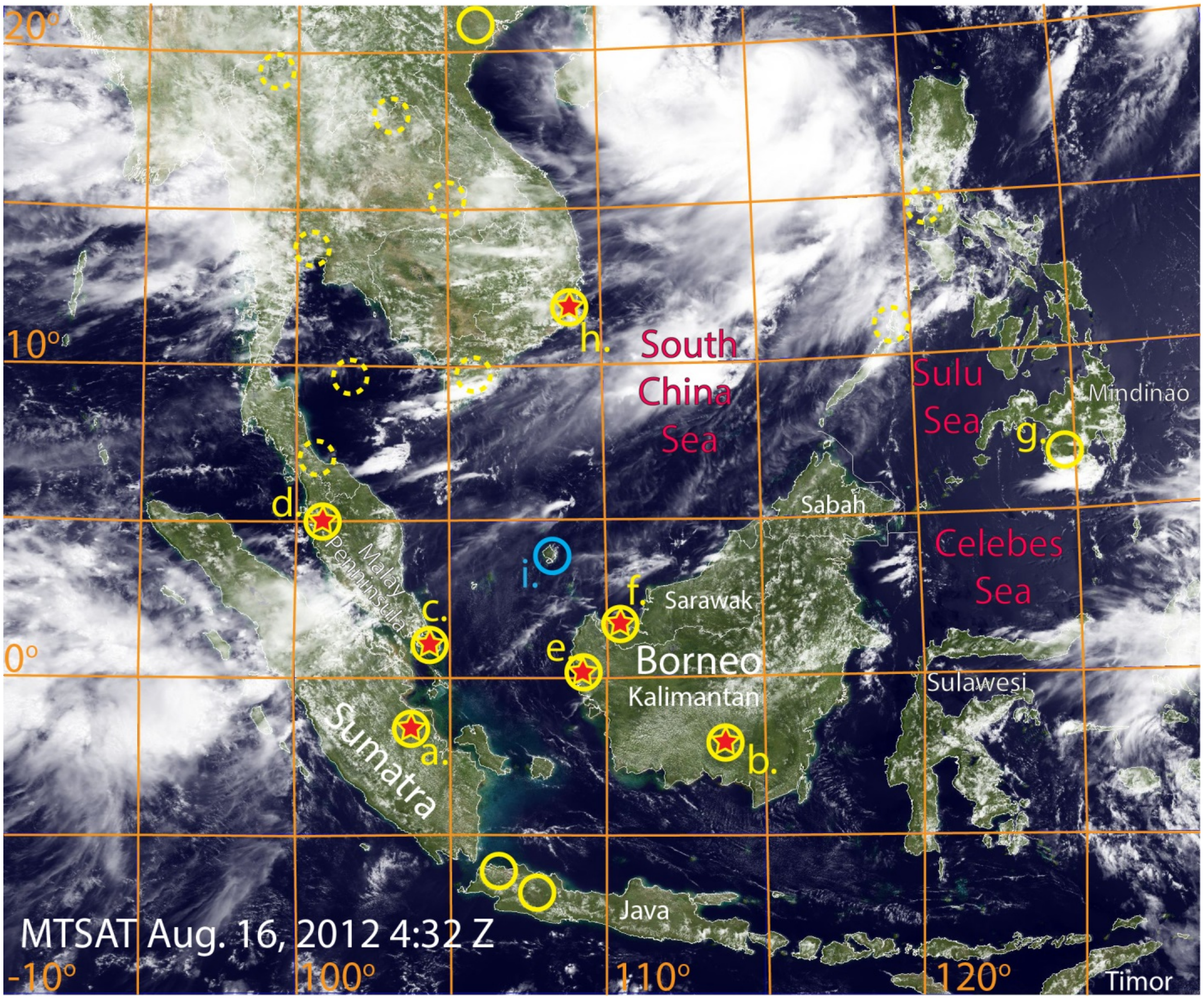

Figure 1. Map of network sites for the 2012 7SEAS southwest monsoon intensive. Included are AERONET sites used in this analysis (yellow circles), other AERONET sites (dashed yellow circles), and MPLNET sites (red stars). Site are: a.-Jambi; b.-Palangkaraya; c.-Singapore; d.-Tahir; e.-Pontianak; f.- Kuching; g.- Notre Dame of Marbel University, Mindanao; h.- Nha Trang. Also marked is the Riau Island radiosonde site (blue circle, i.)

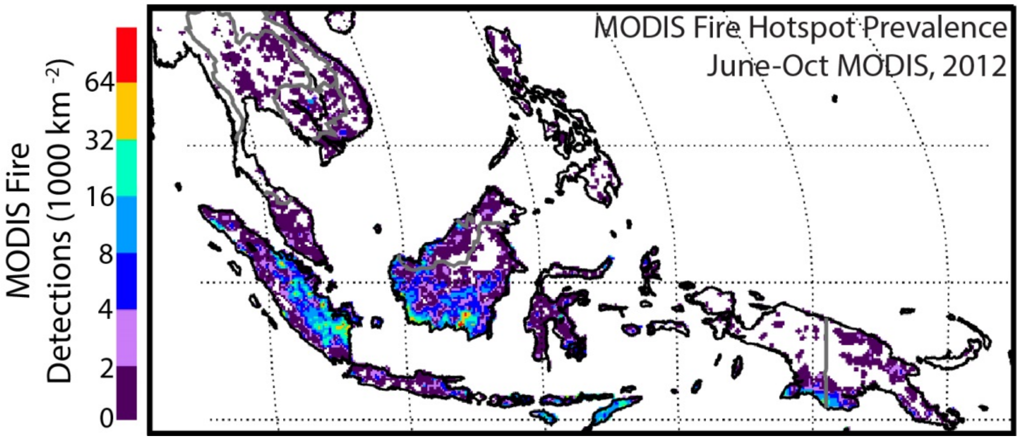

Figure 2. Overall Terra and Aqua MODIS detected fire prevalence for June through October 2012;

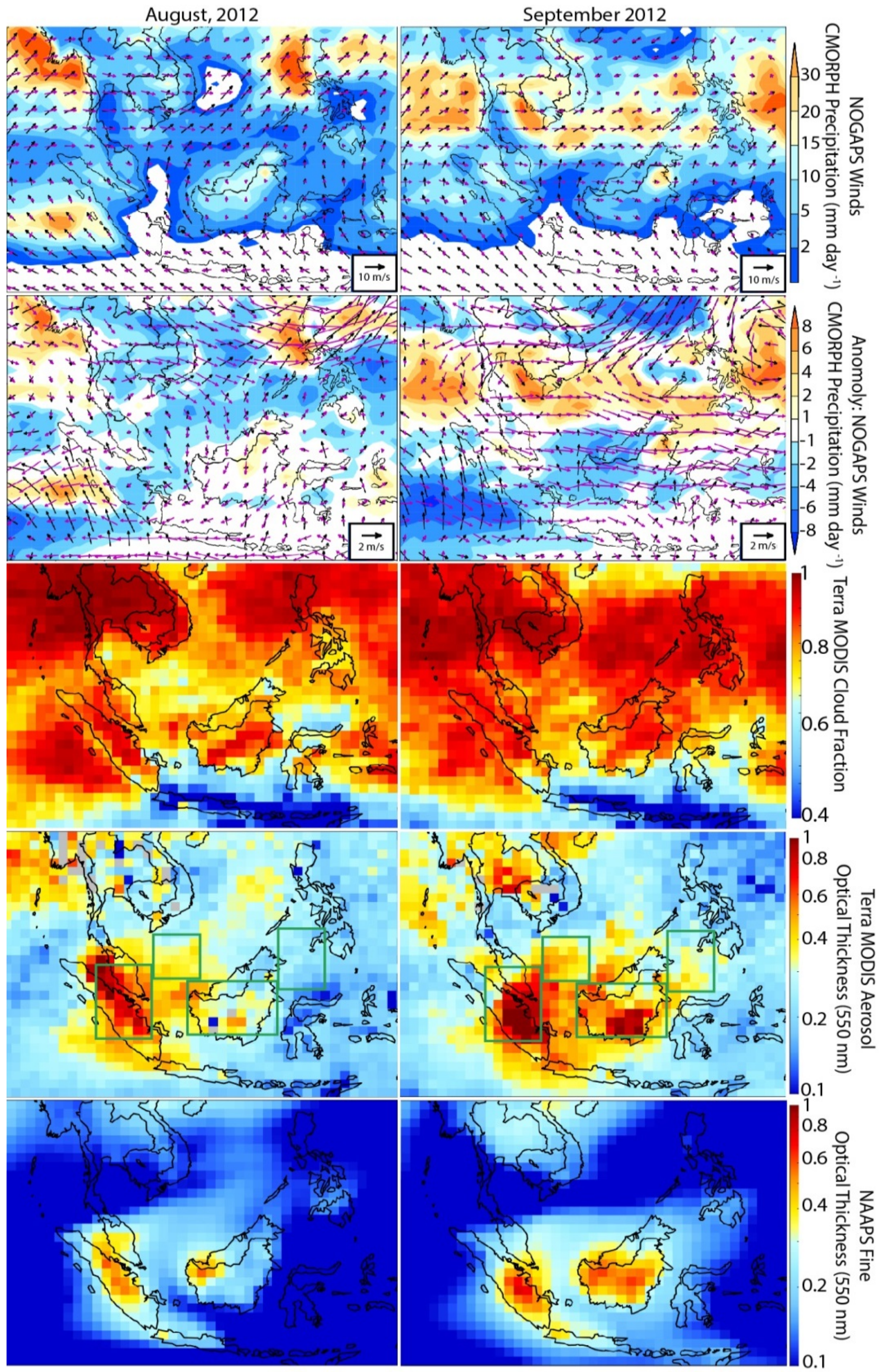

Figure 3. Average August & September 2012 of key fields to represent the overall nature of the southwest monsoon during the 7SEAS intensive. Included are: NOGAPS Surface (Black) and 700 hPa (Magenta) winds overlaid on average CMORPH derived rain rate; monthly anomalies of likewise data; Terra MODIS mean day and night cloud cover; Terra MODIS C6 average 550 NM Aerosol Optical Thickness (AOT); and NAAPS Reanalysis 500 nm fine mode AOT.

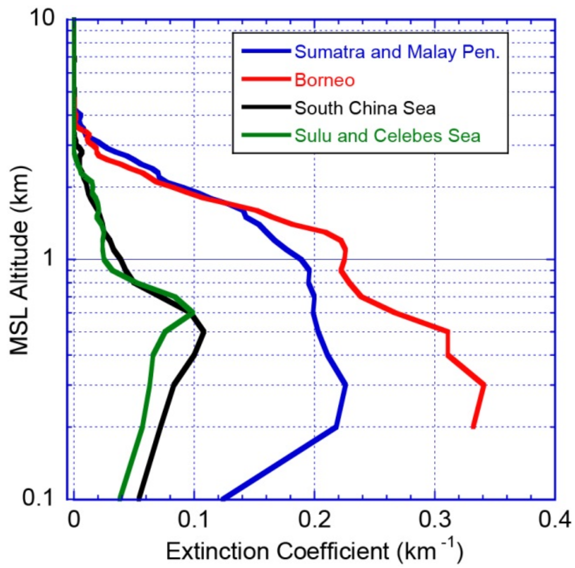

Figure 4. August-October mean CALIOP extinction coefficients for 5x5 degree boxes over Southern/Central Sumatra and the Malay Peninsula; South-Central Borneo, the southern South China Sea, and the Sulu and Celebes Sea.

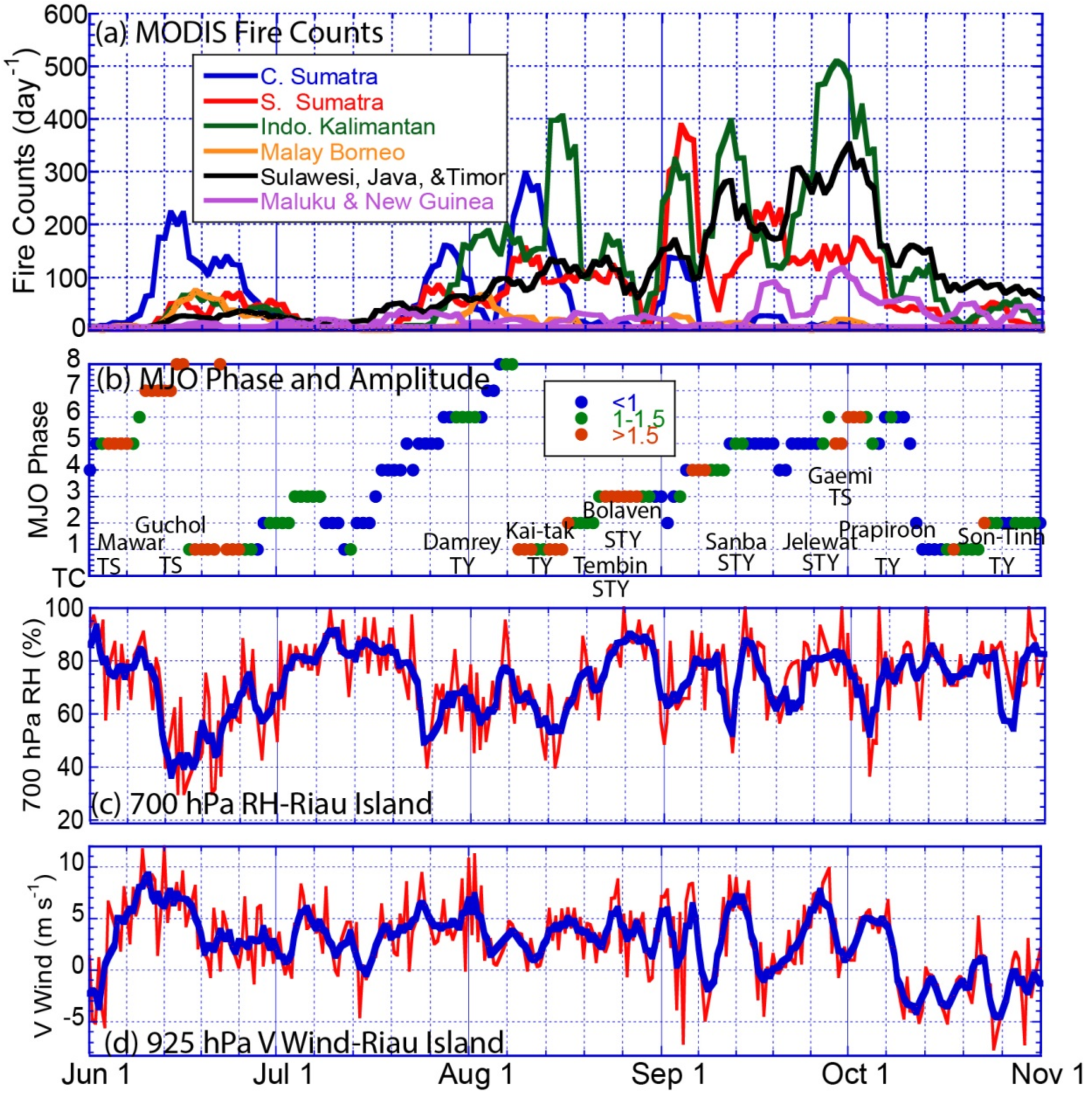

Figure 5. Time series data for the 2012 MC burning season. (a) A 5-day box car average of observed Terra and Aqua combined active fire hotspot detections for the 2012 Maritime Continent burning season by region as defined in Reid et al., (2012; 2015); (b) Wheeler index of MJO phase and color coded amplitude, where amplitudes above one are considered statistically significant, and above 1.5 as strong. Regional tropical cyclones and categories passing near Luzon are also listed (Tropical Storm-TS; Typhoon-TY; Supertyphoon-STY); (c) 700 hPa RH from radiosondes released at Riau Island, in the South China Sea as an indicator of convective activity and/or inhibition. Shown are instantaneous (red) and 3-day boxcar values (blue). (d) Likewise meridional wind at 925 hPa at Riau Island as an indicator of monsoonal strength.

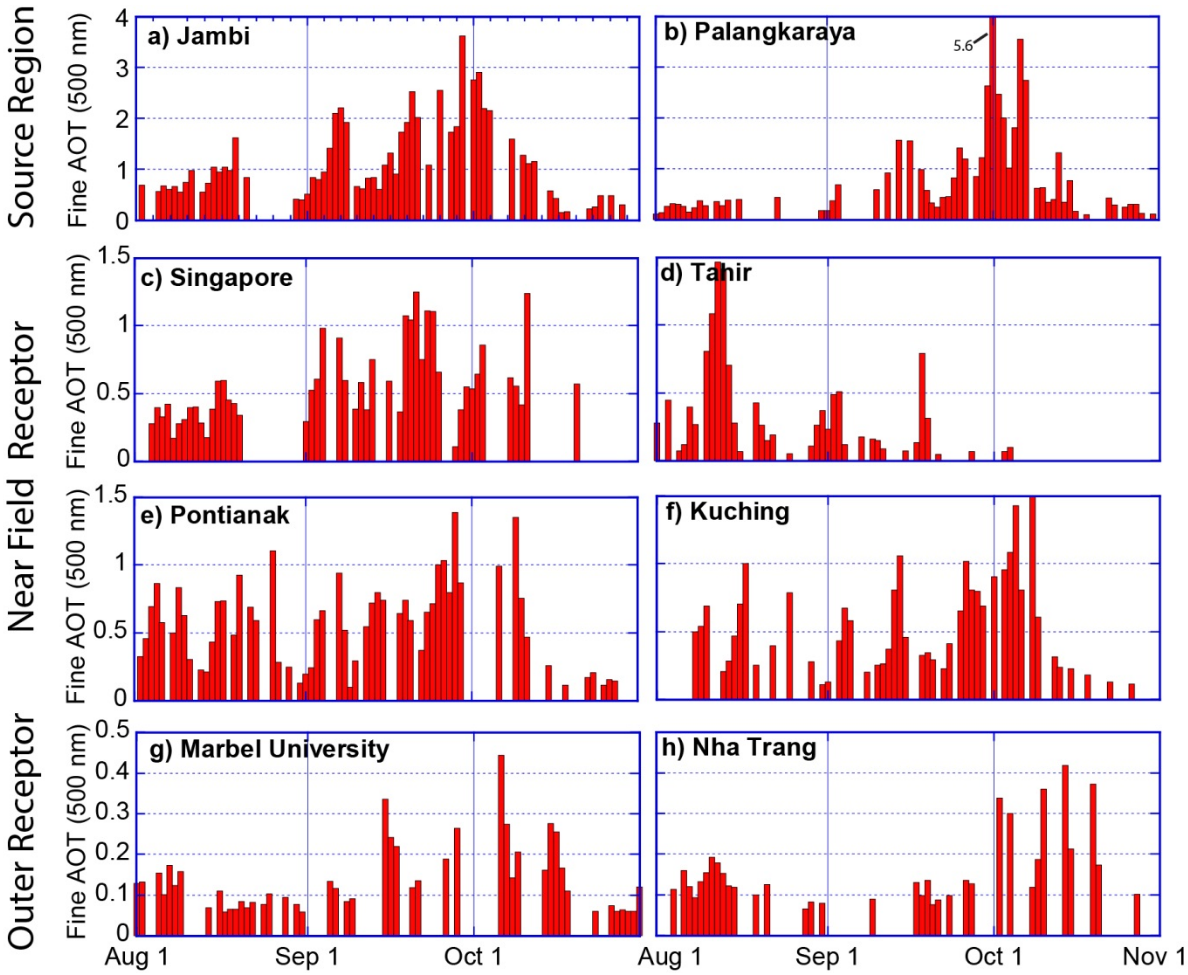

Figure 6. Daily SDA extracted fine mode AOT from AERONET from August-October, 2012.Site locations are labeled with Figure 1. Zero values indicate data non-availability. For these sites nearly all non-available data is due to cloud cover.

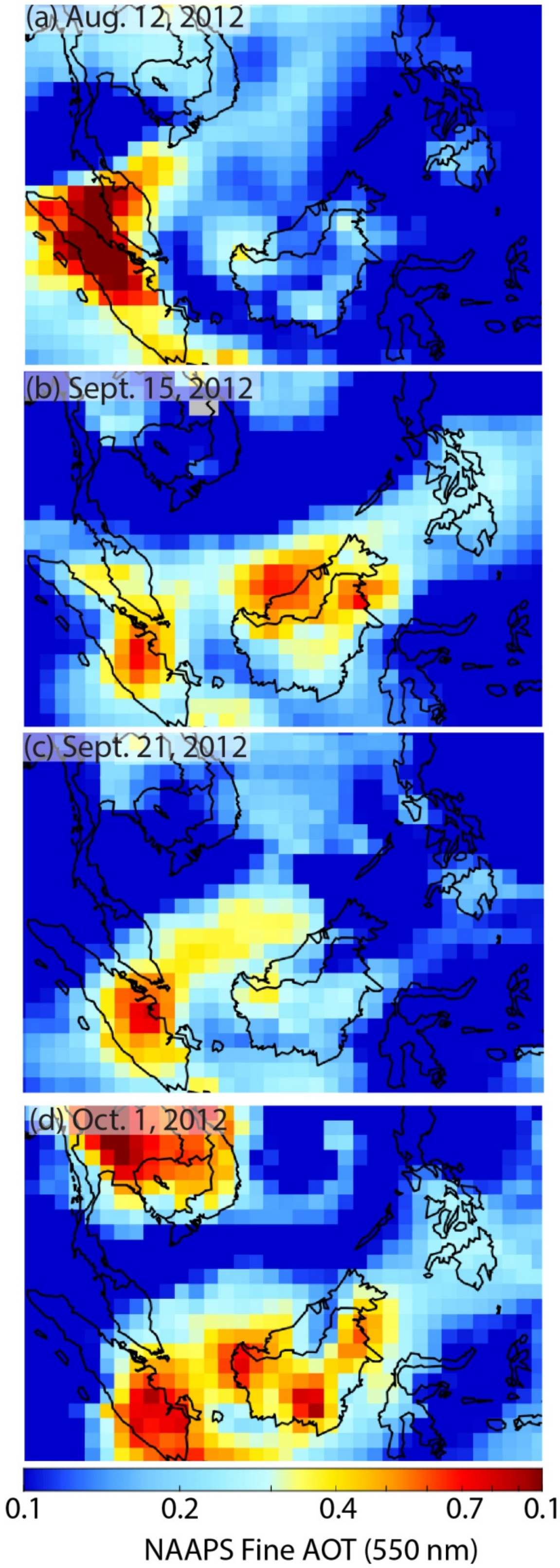

Figure 7. NAAPS fine mode 550 nm AOTs for midday (~6Z) for four significant smoke transport events.

Aerosol meteorology of Maritime Continent for the 2012 7SEAS southwest monsoon intensive study: Part II Philippine receptor observations of fine scale aerosol behavior

Jeffrey S. Reid[1], Nofel D. Lagrosas[2], Haflidi H. Jonsson[3], Elizabeth A. Reid[1], Samuel A. Atwood[4], Thomas J. Boyd[5], Virendra P. Ghate[6], Peng Xian[1], Derek J. Posselt[7], James B. Simpas[2]; Sherdon N. Uy[2], Kimo Zaiger[8], Donald R. Blake[9], Anthony Bucholtz[1], James R. Campbell[1], Boon Ning Chew[10], Steven S. Cliff[11], Brent N. Holben[12], Robert E. Holz[13], Edward J. Hyer[1], Sonia M. Kreidenweis[4], Arunas P. Kuciauskas[1], Simone Lolli[14], Min Oo[13], Kevin D. Perry[15], Santo V. Salinas[16], Walter R. Sessions[13], Alexander Smirnov[17], Annette L Walker[1], Qing Wang[3], Liya Yu[18], Jianglong Zhang[19], Yongjing Zhao[11]

[1] {Marine Meteorology Division, Naval Research Laboratory, Monterey CA}
[2] {Manila Observatory, Manila Philippines}
[3] {Department of Meteorology, Naval Postgraduate School, Monterey CA}
[4] {Dept. of Atmospheric Science, Colorado State University, Ft. Collins, CO}
[5] {Biogeochemistry Section, Naval Research Laboratory, Washington DC}
[6] {Argonne National Laboratory, Argonne, IL, USA}
[7] {Dept. of Atmospheric, Oceanic, and Space Sciences, University of Michigan, Ann Arbor, MI}
[8] {NAVFAC Engineering and Expeditionary Warfare Center Port Hueneme, CA}
[9] {Dept. of Chemistry, University of California, Irvine, CA}
[10] {National Environment Agency, Singapore}
[11] {Department of Applied Science, University of California Davis, CA}
[12] {NASA Goddard Space Flight Center, Greenbelt MD}
[13] {Space Sciences Engineering Center, University of Wisconsin, Madison, WI}
[14] {University of Maryland Baltimore County-JCET, Baltimore, MD}
[15] {University of Utah, Salt Lake City, UT}
[16] {Centre for Remote Imaging Sensing and Processing, National University of Singapore, Singapore}
[17] {Science Systems and Applications, Inc., Lanham, MD 20706}
[18] {Dept. of Environmental Engineering, National University of Singapore, Singapore}
[19] {Dept. of Atmospheric Science, University of North Dakota, Grand Forks, ND}

Correspondence to: J. S. Reid (jeffrey.reid@nrlmry.navy.mil; 1 831-656-4725)

ABSTRACT:

The largest 7 Southeast Asian Studies (7-SEAS) operations period within the Maritime Continent (MC) occurred in the 2012 August-September biomass burning season. Data included were observations aboard the M/Y *Vasco*, dispatched to the Palawan Archipelago and Sulu Sea of the Philippines for September 2012. At these locations, the *Vasco* observed MC smoke and pollution entering the southwest monsoon (SWM) monsoonal trough. Here we describe the research cruise findings and the finer scale aerosol meteorology of this convectively active region. This 2012 cruise complimented a 2 week cruise in 2011, and was generally consistent previous findings in terms of how smoke emission and transport related to monsoonal flows, tropical cyclones (TC) and the covariance between smoke transport events and the atmosphere's thermodynamic structure. Biomass burning plumes were usually mixed with significant amounts of anthropogenic pollution. Also key to aerosol behavior were squall lines and cold pools propagating across the South China Sea (SCS) and scavenging aerosol particles in their path. However, the 2012 cruise showed much higher modulation in aerosol frequency than its 2011 counterpart Whereas in 2011 large synoptic scale aerosol events transported high concentrations of smoke into the Philippines over days, in 2012, measured aerosol events exhibited a much shorter term variation, sometimes only 3-12 hours. Strong monsoonal flow reversals were also experienced in 2012. Nucleation events in cleaner and polluted conditions, as well as in urban plumes were observed. Perhaps most interestingly, several cases of squall lines heralding major aerosol events were observed, as opposed to 2011 observations where these lines largely scavenged aerosol particles from the marine boundary layer. Combined, these observations indicate pockets of high and low particle counts are not uncommon in the region. These perturbations are difficult to observe by satellite, and very difficult to model. Indeed, the Navy Aerosol Analysis and Prediction System (NAAPS) simulations captured longer period aerosol events quite well, but largely failed to capture the timing of high frequency phenomena. Ultimately, the research findings of these cruises demonstrate the real world challenges of satellite based missions, significant aerosol lifecycle questions such as those the future Aerosol-Cloud-Ecosystem (ACE) will investigate, and point to the importance of small scale phenomena such as sea breezes, squall lines and nucleation events embedded within SWM patterns in dominating aerosol lifecycle and potential relationships to clouds.

1.0 INTRODUCTION AND BACKROUND

The 7 Southeast Asian Studies (7SEAS) program has motivated observations of the Maritime Continent (MC) aerosol environment that have led to significant advances in understanding the region's aerosol life cycle and climate impacts (Reid et al., 2012; 2013; Lin et al., 2013). While linkages between biomass burning and the El Niño Southern Oscillation (ENSO) have long been identified for this region (e.g., Nichol 1998; Field and Shen 2008), the relative importance of the Madden-Julian Oscillation (MJO), equatorial waves, tropical cyclones and even features as fine-scale as boundary layer dynamics and squall lines have been recently connected to aerosol lifecycle (e.g., Reid et al., 2012; 2015; Atwood et al., 2013; Campbell et al., 2013; Wang et al., 2013; Xian et al., 2013; Ge et al., 2014). Yet the complexity of MC meteorology continues to pose great challenges to quantitative characterization and prediction of MC atmospheric composition. Indeed, the region's high cloud cover prevents contiguous monitoring of aerosol particles (Reid et al., 2013). Yet, we have long known the response of clouds and precipitation to smoke particle loading to be strongly non-linear (e.g., Reid et al., 1999; Feingold et al., 2001; Andreae et al., 2004; Lohman and Feichter 2005).

The largest intensive operations period in the MC for 7SEAS occurred in 2012. Included was the deployment was a research cruise by the M/Y *Vasco* to study aerosol properties on the edge of the southwest monsoon (SWM) trough. Studied were "natural" particles, as well as biomass burning and industrial emissions being transported from Indonesia, Malaysia and Singapore into the eastern South China and Sulu Seas. The *Vasco* previously supported 7SEAS in late Sept. 2011 by performing a research cruise in the northern Palawan Archipelago (~11^{o} N; 119^{o} E) and sampling two major aerosol events originating from Borneo and Sumatra (*Reid et al.*, 2015). This 2011 cruise was a trial for the more substantial 2012 effort described here, and provided the means to conduct a detailed seasonal examination of how biomass burning emissions and lifecycle related to Southeast Asian meteorology. Together, these two cruises provide the first ever, to our knowledge, measurements of aerosol properties in the remote SWM regions, increasing our understanding of their relation to regional meteorology and transport patterns.

Findings of the 2011 cruise were consistent with the conceptual analysis of MC aerosol lifecycle in the monsoonal flow, as put forth by Reid et al. (2012), with supporting mesoscale simulations by Wang et al., (2013). In particular, the 2011 cruise highlighted the role of intraseasonal oscillations such as the Madden Julian Oscillation (MJO) or Boreal Summer Interseasonal Oscillation (BSISO) in regulating aerosol emissions and transport. While relationships between the MJO and aerosol loadings have long been hypothesized (e.g., Tian et al., 2008; Beegum et al., 2009; Reid et al., 2012), these research cruises provided direct verification of conceptual and numerical model simulations of what was occurring in environments under the clouds. The 2011 cruise showed that incorporated into the MJO signal was the associated tropical cyclone (TC) cyclogenesis relationship put forth by Maloney and Hartman (2001). Reid et al. (2012) and Wang et al. (2013) suggested that this relationship strongly influences the development of aerosol events advecting into the South China and Sulu Seas by way of monsoonal enhancements followed by large scale subsidence associated with TC passage. Further, the 2011 *Vasco* cruise highlighted the importance of finer-scale features such as squall lines in regulating over-ocean wet deposition. Ultimately, a key finding of the 2011 cruise was that while monsoonal scale flow patterns and convection are important, short-lived phenomena can strongly modulate cloud condensation nuclei (CCN) concentrations, resulting in significant perturbations to large scale aerosol transport events that are difficult to account for in both observational and modeling studies. Demonstrated covariance of thermodynamic structure and aerosol properties in convective environments highlighted the need for any study of aerosol, cloud, and precipitation interaction to control for meteorological confounding with aerosol properties to potential cloud and precipitation impacts.

This paper is the second of two examining the scale dependencies of regional aerosol meteorology for the 2012 SWM season. We rely on Part I (Reid et al., 2016) to provide an overview of the MC's 2012 biomass burning season. Here, focus is on the observations of the Sept. 2012 research cruise as an indication of the aerosol behavior in the largely unobserved South China and Sulu Sea region. The description of the 2012 cruise contained in his paper continues the narrative set forth from 2011. Cruise track, instrumentation and other data is given. Results begin with a review of cruise relevant meteorology and aerosol transport. Observation results focus on the time series of *Vasco* measurements and their relation to the regional meteorology. Details on aerosol microphysics and chemistry will be provided in related papers-notably Atwood et al. (2016, submitted). In the final results section, we examine the nature of individual aerosol events, including from biomass burning and homogenous nucleation. We close with a discussion of the nature of aerosol meteorology found in the 2011 and 2012 cruises.

2.0 CRUISE INSTRUMENTATION, TRACK, AND SUPPORTING DATA

The Sept. 4th -29th 2012 research cruise was conducted on the same vessel with largely the same instrumentation and measurement configuration as the 2011 cruise (Reid et al., 2015). The vessel used was the Cosmix Underwater Research Ltd M/Y *Vasco*, a 186 ton/35 m ship used for regional diving applications, including salvage, tourism and research. However, the cruise was 12 days longer in duration and ventured further south, as far as Balabac Island on the southern tip of the Palawan Archipelago (7.6 N; 117.0 E), less than 100 km from the northern tip of Borneo (Figure 1). Details on the *Vasco* and its instrumentation can be found in Reid et al., (2015), although a brief overview and notable changes from 2011 are described below. This is followed by descriptions of the cruise track and finally of the ancillary data used in this analysis.

2.1 Vasco Instrumentation

Instrumentation for 2012 was largely similar to 2011. A bow mast provided high-rate sampling at 50 Hz for turbulent fluxes using a Campbell CSAT3 3-D sonic anemometer and LI-COR H_2O/CO_2 gas analyzer. An Inertial Measurement Units (IMU) consisting of a GPS, a gyro stabilized electronic compass, and accelerometers was used to characterize the ship position and orientation for ship motion removal from the turbulence measurements. Mean meteorological measurements were made by an RM Young propeller anemometer, a Campbell ventilated temperature and humidity probe and a barometer for static pressure. Duplicate measurements for mean meteorology and precipitation were made by a Vaisala Weather Transmitter WXT520 for quality assurance purposes. Differences between all sensors for temperature were within 0.3^{o}C, RH within 5%, pressure within 0.5 hPa, and winds within 0.5 m s^{-1}. Downwelling short and longwave radiation was measured by Kipp and Zonen CMP 22 and CGR4 instruments, respectively. Cloud cover was monitored with a Vaisala C31 ceilometer. InterMet 1-AB radiosondes were released two to three times a day when the ship was at a moorage. New to the 2012 cruise was an OTT Parsivel disdrometer to monitor rain rate and droplet size distribution.

Atmospheric composition measurements made on the bow also largely mimicked the 2011 cruise. $PM_{2.5}$ filters were collected by 5 lpm Minivol Tactical Air Samplers (TAS), and analyzed by gravimetric, XRF and ion chromatography at the Desert Research Institute. A second set of filters was analyzed for organic and black carbon by the thermal-optical method of Chow et al. (1993). The period of filter sampling ranged from one to two-and-a-half days, depending on estimated aerosol concentration. Size-resolved elemental data from Na through Pb was provided by XRF analysis at the Lawrence Berkeley Lab Advanced Light Source (ALS) on samples collected by an 8 stage Davis Rotating-drum Uniform size-cut Monitor (DRUM) sampler (unheated PM10 inlet and cut points at 5 µm, 2.5 µm, 1.15 µm, 0.75 µm, 0.56 µm, 0.34 µm, 0.26 µm, and 0.07 µm; Cahill et al., 1985). Due to an electronics failure during ship installation, this instrument was manually rotated to provide data during specific periods. While total mass concentrations are still in analysis, we have high confidence in PM_1 elemental ratios presented in this paper. As in Reid et al. (2015), sulfur, potassium, and vanadium ratios are used as markers to help separate industrial anthropogenic from biomass burning particles. For trace-gas analysis, 95 whole-air gas samples were collected for gas chromatography analysis by the University of California Irvine (See Colman et al., 2001 for a list of 60+ compounds provided, details on analysis methods and relative uncertainties). Of these, 85 passed internal quality assurance tests.

Aerosol microphysics instrumentation was located in a forward locker fed by a 3 cm diameter/4 m long inlet. Wind directional data were used to ensure that only periods with air moving over the bow were used, in order to remove periods of contamination and self-sampling. Periods of residual self-sampling were also abundantly clear from CN and total particle counts. Like the previous cruise, a base set of aerosol scattering, absorption number and size was made and processed by two TSI three wavelength (450, 550, 700 nm) nephelometers (Anderson et al., 1996)-one ambient and one hearted dry (50% RH), a Radiance Research three wavelength (440 nm, 523 nm, 660 nm) Particle Soot Aerosol Photometer (PSAP; Bond et al. 1999), TSI Condensation Nuclei Counter (CPC), a combined DMT bench top Passive Cavity Aerosol Sizing Spectrometer (PCASP) and a TSI Aerodynamic Particle Sizer (APS; Reid et al., 2006) for fine and coarse model particle sizing, respectively. A Maritime Aerosol Network Microtops hand-held sun photometer (MAN; Smirnov et al., 2011) was brought on board for measuring Aerosol Optical Thickness (AOT) on those rare cloud free occasions that permitted solar observation.

Significant additions were made to 2012 cruise relative to 2011 in regard to aerosol microphysics. First, data from previous campaigns showed that the lab-bench PCASP instrument was prone to calibration drift, and so a second PCASP configured in an aviation pod and heated inlet was placed on the *Vasco* top mast in a manner as described in Reid et al. (2006). This instrument proved to be much more reliable and steadfast in calibration, and hence is used in this paper's analysis. Also supplementing particle size in 2012 was a combined electrostatic classifier-cloud condensation nucleation counter (CCNc) package to measure the size-resolved CCN characteristics. This system and its analysis are described in detail in Atwood et al. (2016; submitted), but are summarized here. This system provided aerosol particle size distributions and hygroscopicities across a size range of 17-500 nm using a size-resolved CCN system similar to Petters et al. (2009). Coarse-mode particles were first removed using a URG cyclone with an approximate 1 um and 50% size cut before being dried using a Permapure poly-tube Nafion column. Air was drawn through a TSI 3080 Electrostatic Classifier and Model 3081 long DMA column, measuring particles between 17 and 500 nm in diameter. Sampled air was then split between a TSI 3782 Water Condensation Particle Counter (CPC) with a flow rate of 0.6 lpm, and a DMT CCN Counter (CCNc). Hygroscopicity was assessed with the kappa parameter (Petters and Kreidenweis, 2007) using three-parameter activated fraction fits similar to Rose et al. (2010).

Finally, in parallel with the PSAP, multi-spectral absorption was measured with the newly-developed NOAA Continuous Light Absorption Aerosol Photometer (CLAP). The CLAP is a filter-based system of similar configuration to the PSAP, although loaded with seven sequential filters, eliminating the need for frequent filter changes. Its design requirements were driven by the high sensitivity necessary to monitor aerosol absorption in more pristine conditions at Global Atmospheric Watch stations. Both laboratory and field comparisons between the CLAP and PSAP show that they agree to within 10% (John Ogren, NOAA *manuscript in preparation*). For the 2012 cruise, the CLAP was integrated with the dry nephelometer.

2.2 Vasco Cruise Track and Sampling Schedule

The *Vasco* cruise track is superimposed on a MODIS Terra image in Figure 1 (a). Like the previous cruise, the *Vasco* home ported from Navotas, Manila Bay, Philippines. Aerosol sampling was also performed in a manner similar to the 2011 cruise, conducted at a series of anchorages that were protected from the swell yet provided unobstructed sampling of the ocean. Typically these anchorages were behind reef zones or small islands that had little breaker activity or swell. Aerosol sampling was also conducted when the air was flowing within +/-50^o of the bow both while in transit and at moorage. Given the consistent nature of winds while at moorage, the *Vasco* naturally weather-vaned with the bow pointed into the wind.

The *Vasco* took on provisions once at Liminangcong (11.0^o N, 119.3 ^{o} E) near the El Nido anchorage on Sept. 10th, and twice at Puerto Princesa, Palawan Island (9.7^o N, 118.8^o E) overnight on Sept. 13th and 19th, 2012. The Puerto Princesa port calls divided the cruise into thirds, which were distinct in geographic region and the sampled environment. In the first phase of the cruise (Sept. 4th -13th), the *Vasco* sampled the same locations as the 2011 cruise. From Manila Bay, the *Vasco* transited to Apo Reef for a day of sampling (12.7^o N, 120.5^o E; Sept 6th), followed by a day at Coron Island (11.9^o N, 120.3^o E, Sept 7th and finally four days on station at El Nido behind the Guntao Islands reef (11.1^o N, 199.2^o E; Sept. 8th-12th). On the 12th, the *Vasco* transited the east side of Palawan Island to provision in Puerto Princesa overnight on the 13th. The *Vasco* headed south the morning of the 14th, starting the second phase of the cruise that brought the *Vasco* to the southern tip of the Palawan Archipelago on the western side of Balabac Island in the Balabac Great Reefs (7.9^o N, 116.9^o E; Sept. 15th-19th), 100 km off of the northern tip of Borneo. This site provided excellent shelter, while enabling unobstructed sampling of air from the southern South China Sea (SCS). Returning to Puerto Princesa on Sept. 19th and departing on Sept. 20th, the *Vasco* then entered its third phase of sampling; the middle of the Sulu Sea at Tubbataha Reef (8.8^o N, 199.9^o E). The *Vasco* then returned to Navotas Manila Bay Sept. 26th -29th, but following winds prevented sampling.

2.3 Ancillary Model and Satellite Data

Ancillary model and satellite data were utilized to provide a larger contextual understanding of the regional meteorological and aerosol environment. As described in Part 1 (Reid et al., 2016), for global scale meteorology and aerosol monitoring we utilize the Navy Global Atmospheric Prediction System (NOGAPS; Hogan and Rosmond, 1991) and the offline Navy Aerosol Analysis and Prediction System (NAAPS) reanalysis (Lynch et al., 2015), respectively. In

NAAPS four species are simulated: dust, biomass burning smoke, anthropogenic/biogenic fine, and sea salt. Here we focus entirely on fine mode biomass burning and ABF species.

The *Vasco* data analysis was enhanced by using geostationary MTSAT satellite products (visible, IR, cloud heights, scatterometer, etc.) as found on the NEXSAT website (*Miller et al.,* 2006; http://www.nrlmry.navy.mil/nexsat-bin/nexsat.cgi). To map regional precipitation, the Climate Prediction Center (CPC) MORPHing precipitation product is used (CMORPH, *Joyce et al.*, 2004). NASA MODIS Col 6 level 3 data were also used (Levy et al., 2013). We also rely on key AErosol RObotic NETwork (AERONET) sites, located to monitor smoke exiting the MC (Holben et al., 1998; Reid et al., 2016). These included Singapore, indicative of smoke exiting Sumatra into the SCS; Kuching, Sarawak, indicating smoke departing western Borneo into the SCS; and Notre Dame of Marbel University (ND Marbel) on Mindanao, as an indicator of smoke transported into the Philippines via the Sulu and Celebes Sea (Figure 1). To monitor fine AOT, the Spectral Deconvolution Algorithm (SDA) product is used (O'Neill et al., 2003)

3.0 RESULTS I: RELEVANT METEOROLOGICAL AND AEROSOL ENVIRONMENT

An overview of the aerosol meteorology during the 2012 7SEAS campaign is provided in Part I (Reid et al., 2016), and thus not repeated in detail here. From a seasonal point of view, 2012 was a nominally "typical" biomass burning year for a slightly-warm ENSO phase. There were low overall wind anomalies, and precipitation and fire activity were well within one standard deviation. However, regional AOTs were the second highest of the past several years, surpassed by the mammoth 2015 El Nino induced fire season. While the averages are close to normal, the daily meteorology during the 2012 study period was quite variable, particularly during the research cruise. In context to *Vasco* observations, here we discuss these relevant phenomena.

The most notable aspect of the 2012 cruise relative to its 2011 counterpart, and indeed all other 7SEAS regional studies, was the extreme variability in the monsoonal flows. This may in part be due to the MJO only weakly propagating across the MC during September in a fairly active convective phase (Reid et al., 2016). While at the seasonal mean level, wind patterns were near normal, with typical southwesterly winds and slight zonal enhancements aloft; during the entire month of September, daily flow patterns over the SCS changed measurably (Reid et al., 2016).

These periods were largely defined by the migration of two tropical cyclones (TC 17 W Sanba and TC 18 W Jelawat), separated by easterly waves with significant flow reversals. The winds, precipitation, and boundary layer smoke patterns for the mission are exemplified in Figure 2. Provided every four to five days through the cruise were NOGAPS winds at the surface (10 m; black) and 700 hPa (Magenta) overlaid on daily average CMORPH precipitation. Also shown are the midday MTSAT false color visible image, and the corresponding NAAPS surface concentration of fine mode particles (taken as a sum of biomass burning smoke and anthropogenic and biogenic fine species). For comparison, daily averaged AERONET 500 nm fine mode AOTs for three sites surrounding the study region are presented in Figure 3. These include Singapore, Kuching-Sarawak, ND of Marbel-Mindanao.

During the very first week at sea, monsoonal flow across the SCS was weak, associated with a westward propagating wave consistent with the features of a tropical depression/easterly wave. On the day of *Vasco*'s departure from Manila (Sept. 4th, 2012), the Sulu Sea was already exhibiting anomalous southeasterly winds at the surface and nearly calm winds through the mid troposphere. Winds shifted with the propagation of the wave, moving from southeasterly, to westerly and northwesterly into the eastern part of the SCS, followed by full westerly and even northerly winds by the 7th (Figure 2). Northeasterly winds at 700 hPa reached 10 m s^{-1}. Thus for the first five days of the cruise at Apo Reef, Coron, and the first several days at El Nido, sampled air was largely not from the SCS, but rather from the islands of Luzon, Mindoro, and Iloilo. NAAPS predicted likewise, with slightly above background fine mode particle concentrations in the *Vasco* area dominated by the ABF specie, originating locally. The reversal in monsoonal winds clearly kept smoke transport to the southern SCS. AOTs were nevertheless moderate at Singapore and Kuching early in the mission (above 0.5) as smoke advection was weak (Figure 3). However, consequently AOTs at ND Marbel were at background levels, ~0.1.

Monsoonal flow returned and precipitation began developing on Sept. 10th 2012 while the *Vasco* was stationed in El Nido. This reestablishment of more characteristic flows occurred in association with the formation of what would become super-typhoon (STY) Sanba (TC 17 W) at Palau. By the 12th (Figure 2), Sanba grew to typhoon strength, followed by rapid intensification to *a* supertyphoon the very next day. The slow northward migration of STY Sanba resulted in enhanced westerly components of the marine boundary layer and mid-tropospheric winds, as well as enhanced precipitation in a well-defined zonally-aligned monsoonal enhancement/inflow arm. When the *Vasco* transited to Puerto Princesa on Sept. 12th and 13th, the region was still under significant influence of TC Sanba. NAAPS predicted smoke remaining to the south due to enhanced zonal flow in the SCS and indeed, significant ejection from eastern Borneo into the Celebes Sea south of the *Vasco* operating area occurred as was predicted by NAAPS. Due to cloud cover, this ejection event was not visible in AERONET or MODIS data.

Upon departure from port on Sept. 14th, heading for Balabac Island at the southern tip of the Palawan Archipelago, the slow moving super-typhoon Sanba was still west of Luzon, with a well-defined monsoonal enhancement associated with the storm across the SCS. A massive smoke ejection event was modeled and observed coming out of Kuching into the SCS and being detected at ND Marbel a day later (Figure 3). Likewise, smoke from eastern Borneo was exiting into the Celebes Sea. Even through Sept. 16th, the influence of TC Sanba lingered as monsoonal enhancement extended from the Malay Peninsula through Luzon, with NAAPS suggesting smoke passing through the central Philippines.

For Sept. 17th through 21st, 2012, monsoonal winds slackened yet again, with westerly winds in the northern SCS, and even some northerly components in the lower free troposphere. This is consistent with the propagation of a second easterly wave across the region, and like before, smoke and pollution were largely confined to the southern SCS. During this period, the *Vasco* transited back to Puerto Princesa (Sept 19th), finally departing the morning of Sept. 21st for its last station at Tubbataha Reef in the middle of the Sulu Sea. While on station there, monsoonal flow returned, with the formation of another super-typhoon, Jelawat (TC 18 W). Jelawat had a similar lifecycle to STY Sanba, forming over Palau and slowly migrating up the eastern side of the Philippines with a well-defined inflow enhancement across the SCS (e.g., Sept. 26th). Also like STY Sanba, Jelawat intensified rapidly, becoming an intense super-typhoon; the strongest of the season. While surface winds had a typical southwesterly direction, winds in the free troposphere had significant northerly components across the SCS; unusual relative to the more typical westerly to southwesterly winds. Significant peaks in AOT were observed at Kuching and ND Marbel (Figure 3). NAAPS suggested the *Vasco* at Tubbataha was influenced by two smoke plumes, a northern plume ejected from Kuching, and a southern plume exiting eastern Borneo. The *Vasco* then returned back to home port in Navotas, Manila (Sept. 27th-29th) on the southern edge of the northward propagating inflow of STY Jelawat.

4.0 RESULTS II: THE TIMESERIES OF MEASURMEENT ON THE VASCO

Given the meteorological overview provided in Section 3, we can begin to interpret the aerosol and meteorological data from the cruise. Figure 4 provides the *Vasco* data time-series of key meteorology, including one minute (a) ventilated temperature, (b) & (c) RM Young wind, and (d) disdrometer-derived precipitation. Also shown are key aerosol and gas data during appropriate sampling conditions, the (e) CN concentrations, and (f) PCASP derived aerosol volume and whole-air gas can-sampled carbon monoxide (CO). Finally, the derived NAAPS fine-mode surface aerosol concentrations of biomass burning (gold) and anthropogenic fine (red) are also provided in (g). Also overlaid was NAAPS 550 nm fine AOT.

Overall, there was significant variability in weather and aerosol parameters across the cruise. Winds ranged from becalmed in monsoonal breaks, to sustained 12 m s^{-1} during monsoon enhancements, with peaks to 16-18 m s^{-1}. Temperature, with a typical baseline of 28 ^{o}C, saw frequent drops to of 2-4^{o}C with corresponding spikes in wind speed-a telltale sign of cold pool passage (Reid et al., 2015). Roughly ~25 cold pool passages were observed. Peaks in temperature above 28^{o}C baseline were rare, associated with cases of offshore flow from a nearby island while in transit. Precipitation occurred on all but three days, in short lived but moderately intense rain showers (~ 1 cm hr^{-1}). Particle concentrations also showed significant variability, with a baseline of ~ 400-600 cm^{-1} in number, and 1-2 μm^{-3} cm^{-3} in volume (to get μg m^{-3} estimated mass, multiply by assumed density, such as 1.4 g cm^{-3} as deemed appropriate with this dataset; e.g., 1 μm^{-3} cm^{-3} is ~1.4 μg m^{-3}). CO, a key tracer for biomass burning, also showed significant variability, with a baseline of ~70-80 ppbv, with multiple samples above 200 ppbv.

Variability in measured parameters is in line with the meteorology and aerosol environment discussed in Section 3. Early in the cruise, while under the influence of the strong monsoonal break (e.g., Sept. 4th-9th), winds were generally light and variable, precipitation infrequent, and particle mass concentrations low. NAAPS suggests the particles were largely anthropogenic and biogenic in origin with little biomass burning influence. CO observations support this. We attribute one prolonged spike in CN on Sept. 6th and another peak in number but not mass on Sept. 13th, 2012 to a nucleation events. These nucleation events are discussed in the next section.

When the SWM winds returned (as is evident in the ship time series, notably ~Sept. 10th to 19th, 2012), particle concentrations increased, peaking in mass around the 14th-16th, in agreement with the smoke event modeled in NAAPS (Figure 2), although not necessarily in relative magnitude. Relaxation of the monsoon on the 19th and 20th showed an associated decrease in particle concentration. After the second monsoon break when the *Vasco* left for Tubbataha Reef on the 21st, the monsoon flow returned, bringing pockets of polluted air with particle counts to 2000 cm^{-3} and CO to 200 ppbv. NAAPS simulated these pockets of air as a low frequency signal, and was largely unable to resolve fine scale features.

With the overall time series of ship measured meteorology and particle concentrations in agreement with the overall regional analysis, we can delve more deeply into particle and gas characteristics, presented in Figure 5. Shown is (a) non sea-salt $PM_{2.5}$ gravimetry from filters, with corresponding quartz filter analyses of organic and black carbon. For comparison, an inferred 30 minute PCASP-derived dry mass concentration using an assumed density of 1.4 g cm^{-3} is presented. This value of density provided good closure (unity slope; r^2=0.8) between the temporally-integrated PCASP and gravimetric values, and is close to the density for dry biomass burning of 1.35 g cm^{-3} as measured by Reid et al. (1998). Zero values of filter mass are associated with no-sampling periods due to the relative wind direction over the bow. Shown in Figure 5(b) are the Teflon filter-derived K and SO_4 values, followed by (c) elemental ratios of vanadium and potassium to sulfur from the DRUM sampler, used as an indicator to separate aerosol with industrial from biomass burning origins. Also provided in Figure 5 are key whole-air gas sample species. While there are no unique chemical identifiers to isolate natural, biomass burning and other anthropogenic sources, several species warrant attention. Included are: (d) CO and CH_4; (e) benzene and methyl-iodide as commonly used key indicators for biomass burning (Ferek et al., 1998; Akagi et al., 2011); (f) i- and n-pentane as well as their ratios , with enhanced ratios suggesting more industrial rather than biomass burning sources (McGaughey et al., 2004; Simpson et al., 2014); and finally, (g) isoprene and 2-BuONO, a photo-oxidation product of butane and indicator of photochemistry. Based on these data, we provide sample data for background and particularly interesting events in Table 1. These are discussed in Section 5.

"Baseline" particle characteristics in Table 1 are taken as the lowest quarter of measured concentrations. Particle number baseline concentrations in the marine boundary layer was ~500 cm^{-3}, with concentration rarely dropping much below that. Similarly, baseline fine mode aerosol mass concentrations from filters and inferred from the PCASP were on the order of 1-2 $\mu g\ m^{-3}$. Baseline CO was ~77 ppbv. These values are somewhat larger than what was found in 2011, which had baseline particle number and mass concentrations of 150-350 $cm^{-3}$and 1 $\mu g\ m^{-3}$. Part of this difference is 2012's closer proximity to Borneo source regions along the cruise track. Further, for periods when the *Vasco* was in the northern region, winds were anomalous and precipitation reduced due to the presence of easterly waves. Thus, there was more sampling of Philippines islands, and regionally reduced wet scavenging. Interestingly, CO baseline values of 75ppbv were lower than the 2011 cruise of ~90 ppbv. This may be representative of wet scavenging of particles in 2011, with slight CO enhancements remaining.

Perturbing the aerosol baseline were many significant events with particle number and mass concentrations to +2500 cm^{-3} and 20-30 $\mu g\ m^{-3}$, respectively. Of particular note were aforementioned spikes in CN measured when the *Vasco* was moored at Apo Reef and Coron, in air masses moving offshore of the islands of Mindoro and Luzon. Also, spikes were observed entering port or in the vicinity of island cities, such as Sept. 13th and 20th while the *Vasco* was downwind of Puerto Princesa. In one event (Sept. 13th, 2012), high number (>10,000 cm^{-3}) but low mass concentration periods was observed consistent with a particle nucleation event. CO and VOCs also showed significant variability and enhancements (Figure 5 and Table 1).

Observations of AOT from the Vasco were rare due to the high cloud cover associated with the SWM. Nevertheless, several observations of 500 nm AOT from the MAN provided MicroTops hand held sun photometer were made throughout the cruise (labeled on Figure 5 (a)). Background conditions were just that, ranging from 0.05 to 0.11- typical of remote oceans (Smirnov et al., 2011). Only two observations were available during significant aerosol events transported from the MC however. These included a value of 0.18 in the second half of the first event on Sept. 16, and a high of 0.37 for the peak of the second event on Sept. 25th, 2012.

In comparison to observations, the NAAPS model simulations of aerosol loadings near the *Vasco* exhibited mixed performance relative to the outstanding comparisons for 2011. For example, NAAPS did simulate some aspects of aerosol transport, such as the broader aspects of the Sept. 13th -18th, 2012 period. However, the model had difficulty capturing the most significant pulses, such as observed spikes on Sept. 14th and 25th. NAAPS also included other moderate events that did not materialize, such as Sept. 10th -11th, and Sept. 24th and 29th. The use of satellite precipitation to constrain scavenging processes in NAAPS improves representation of variability in aerosol loadings in high emission and high convection environments, although finer scale features, unresolvable in a 1x1 degree transport model, are clearly important.

In regards to AOT, the NAAPS analysis performed exceedingly well. This is despite the fact that NAAPS had little data to assimilate in the *Vasco* region. Background NAAPS AOTs were on the order of 0.05-0.1, equivalent to 0.07 to 1.2 if one predicts an AOT at 500 nm. NAAPS also predicted the two MicroTops AOT observations well; predicting 0.2 at 550 nm or 0.22 at 500 nm for the Sept. 16th case measured at 0.18, and 0.37 at 550 nm or 0.40 at 500 nm, for Sept 26th measured at 0.38.

Finally, from a photochemistry point of view, there were notable observations throughout the cruise track. For example, spikes in isoprene were frequently found in the vicinity of islands (Figure 5(g)), but also occasionally a day’s distance from shore. At concentrations near 100 pptv, these levels are rather low compare to terrestrial source regions, where values on the order of 1-5 ppbv are expected and measured (e.g., Wiedenmyer et al., 2005; Hu et al., 2015). However, spot cans on the interior of islands taken as part of the 2011 Vasco cruise did reach 1 ppbv (Reid et al., 2015). Similarly, 2-$BuONO_2$, an indicator of photochemistry, also showed sporadic behavior, in this case associated with both smoke events and urban plumes alike. Finally we observed sporadic cases of strongly enhanced methane (to 1.95 ppmv from a 1.77 ppmv baseline), which in general did not correlate with CO or any other species. This very easily could be indicative of gas hydrate derived methane production in under-ocean cold seeps in the SCS (*Suess*, 2014). While these observations are interesting, we leave their analysis to another paper.

5.0 RESULTS: AEROSOL METEOROLOGY OF SIGNIFICANT AEROSOL EVENTS

From Sections 3 and 4, the measured aerosol and meteorological environment during the 2012 cruise was found to be much more complex than the 2011 counterpart. The meteorology was more variable, and additional aerosol phenomena, including from urban plumes and nucleation events, were sampled. Ultimately, the aerosol events were relatively short lived compared to 2011. Indeed, more prevalent high frequency phenomena, such as particle concentration drops due to cold pool or the occasional spike in CN were observed (Figure 4). In this section, we delve into more detail on the aerosol meteorology of key aerosol events. To help inter-compare aerosol events, particle concentrations and key whole-air can samples with associated aerosol particle concentrations are provided in Table 1. Thermodynamic data for soundings collected in three key events are given in Figure 6. Atwood et al., (2016; ACPD in review) go into much greater detail on the implications of these events to aerosol microphysics.

5.1 Significant Events Transported from the Maritime Continent

One can interpret the NAAPS data coupled with PCASP-inferred mass, CO versus CH4, elemental ratios, and gas ratios (notably the ratio of *i*-to-*n*-pentane) as indicative of two very clear biomass burning-dominated event periods sampled on the *Vasco*: Sept. 14th -17th and 25th-27th, 2012. There are also multiple small aerosol and CO enhancements visible, especially late in the cruise. While we say these are biomass burning events, we must emphasize that it is likely that other species were transported with the open burning emissions, including urban and shipping fossil fuel emissions and biofuel. Regardless, the two major event periods have every indication of being dominated by open burning (including the smoke we could smell on the ship) and warrant special attention. Extracted from Figure 3 and 4 are major gas species and ratios in Table 1. These include the peak values for biomass burning on Sept. 16th and 26th, as well as a mixed biomass burning/anthropogenic pollution period on Sept. 16th. The *Vasco* time series, radiosondes releases in Figure 6, and particular samples in Table 1 are discussed in detail below.

5.1.1 Puerto Princesa to Balabac Sampling: The Sept 14th-17th 2012, event

Details of the Sept. 14th - 17th event are provided in time series fashion in Figure 7 for the *Vasco* departing Puerto Princesa through its Balabac anchorage and the start of its return home. To describe the lead up to the event, included in Figure 7 are MTSAT visible satellite images for (a) Sept. 13th and (b) 14th at 0432Z with the combined Terra and Aqua 550 nm AOT for that day. Also recall that wind, precipitation, and satellite imagery for the middle of the event are presented in Figure 5(c). Included in Figure 7 is the *Vasco* time series of several key parameters, including (c) PCASP volume distributions, (d) temperature, (e) wind speed, and (f) precipitation. In terms of duration and of fine particle and (based on Figure 7) CO concentrations, the Sept. 14-16th event was the most significant burning event sampled during the 2012 cruise (Table 1). Peak values for particle number and CO concentration reached as high as 2000 cm^{-3} and 250 ppbv respectively, just as the *Vasco* moved south from Puerto Princesa and into the SWM flow. Whole-air sample data taken at this point give all of the key VOC markers of biomass burning dominated aerosol loading, including very high ethene and benzene. The ratio of i-to-n-pentane was ~1.3, also suggesting biomass burning over other anthropogenic emissions.

Based on the spike in AERONET AOT at Kuching and ND of Marbel University, Mindanao (Figure 3) coupled with the satellite images of Figure 7, this smoke event was part of a mass smoke ejection from Borneo starting on Sept. 12th -13th, 2012 associated with the SWM enhancement from TC Sanba. Smoke extended through the Philippines into the Pacific Ocean (Figure 2) with a fine-mode 500 nm AOT of 0.34 reported at ND of Marbel University, Mindanao on Sept. 14th. As discussed in detail in Atwood et al., (2016, ACP submitted) particle size distributions were fairly constant, with a dry volume median diameter of ~0.3 μm.

The transported smoke into the region was immediately noticed upon departure from Puerto Princesa ~00Z on Sept. 14th 2012, from both the data and a strong biomass burning smell. For the transit south to Balabac, weather was somewhat stormy, with moderate winds and periods of rain. However, the particle and CO concentrations continued to increase as the *Vasco* transited southward toward Balabac Island. At 12Z on the 14th, a very rapid drop in particle concentrations occurred while the *Vasco* was approaching the southern tip of Palawan Island (down to 500 cm^{-3}), with partial particle and CO recovery when the *Vasco* made anchor at Balabac Island. There, higher particle concentrations remained for another two days with a slow decay to cleaner conditions of 500 cm^{-3}, bringing the event to a close. On anchorage, isolated cells of precipitation were frequently observed in the vicinity. A final peak was observed and modeled in NAAPS as the *Vasco* departed for a return to Puerto Princesa near 23Z on the 19th.

The first radiosonde release occurred upon arrival at Balabac Anchorage on Sept. 15th, 2012 and showed generally moist conditions in the lower free troposphere (Figure 6). However, air was dry in the upper troposphere and, based on our assessment, showed large scale subsidence in association with TC Sanba. This dry air aloft may have inhibited some of the deep convection, thus allowing the transport event to persist.

The Sept. 14th -17th, 2012 event has several interesting characteristics. First, while the NAAPS model generally predicted this event, the initial peak particle mass concentration was significantly underestimated. Second, the dramatic drop in particle concentration ~ 12 hours into the event would normally imply a cold pool. However, the particle decline occurred over a period of 45 minutes, as opposed to the minute or two which one would expect from a cold pool event. While there was a temperature drop associated with the particle reduction, it was not as dramatic or rapid as other events. Indeed, there are several significant temperature drops in the hours during the high concentration period with only moderate perturbations to particle count. The NAAPS model did, however, have some reaction to the event and particle recovery. Clearly, this was not a typical cold pool as observed in the 2011 cruise (Reid et. al., 2015).

We hypothesize that the dynamics of this particular event were based on two meteorological components coupled with an orography effect from Palawan Island. The first is related to coastal and orographic flows in western Borneo. The Sept. 14-17th 2012 event was initiated with the aforementioned outflow event on Sept. 12th -13th. Fine-mode AOTs at Kuching peaked at 1 on this date, while AOTs at Pontianak, further south were constant at ~1. Throughout the mission however, as seen in the model data in Figure 5, the NOGAPS model had very low surface wind speeds right offshore of Kuching. In the lower free troposphere where winds are higher, they tended to be westerly, thus preventing smoke above the boundary layer from being advected offshore into the SCS. Thus in the model, the smoke does not get advected offshore very far, and clings to the coast. However based on MODIS AOT in Figure 7(a), we see that in fact the smoke was transported hundreds of kilometers offshore. This plume feature may also have had contributions from Sumatra. As hypothesized in Reid (2012), and then demonstrated in mesoscale simulations by Wang et al., (2013), the sea/land breeze and orography play a significant role in modulating smoke transport on and off the islands of the MC. We hypothesize that orography and land breezes coupled with additional enhancement in monsoonal flows due to TC Sanba resulted in this significant ejection event. This phenomenology resulted in the significant smoke loadings at the *Vasco* as it left Puerto Princesa and was simultaneously underrepresented in the model. As the *Vasco* moved south, the model was able to account for the smoke that was transported closer to the Borneo coast.

The second significant feature of the Sept 14th-17th, 2012 event, the precipitous drop in smoke particle concentrations on Sept. 14th at 1230Z, was due to the remnant of a massive squall line, clearly visible in the Figure 7(b) satellite image. Based on inspection of the MTSAT data, this was formed from a series of isolated cells aligned from south of the southern tip of Vietnam to the Malay Peninsula the night before. Cold pools from these cells were advected to the east as part of accelerated winds over the SCS in association with TC Sanba, eventually resulting in a squall line that was nearly 700 km long before daybreak on the 14th. MTSAT imagery suggests the arrival of this squall line at Palawan Island at ~12Z on the 14th, coincident with the drop in particle concentration. Palawan Island likely broke up this particular squall line and its associated cold pool, thus slowing the more typical rapid temperature and particle drop. We also suspect that the orography of Palawan Island had a role in the lack of particle perturbations in the cold pool events observed just after departure from Puerto Princesa around 08Z on Sept. 14th.

In addition to modulation in particle concentration from the meteorology, aerosol and gas phase chemistry also showed significant variation during the event. To compare and contrast, within Table 1 are data from the peak of the event, sampled on Sept. 14th, and another case two days later (labeled mixed). From the initial biomass burning onset through Sept. 16th, all indications were that anthropogenic pollution could account for significant amounts of fine mode aerosol mass. Noteworthy in Table 1, is that the ratio of excess PM_1 to CO (based on the subtraction of the background level baseline) doubled between the early and late event periods. At the same time the V to S ratio, an indicator of industrial emissions, also doubled. Meanwhile the ratio of

K to S, an indicator of biomass burning, had clear and continuous variations starting at 0.1, rising to 0.2 and then falling back to 0.1 (Figure 5). Also from Figure 5, there was a remarkable decrease in OC mass fractions, dropping from 50% at the peak burning period (very typical of burning, Reid et al., 2005), to 25%. The ratio of i- to n- pentane increased from 1.3 to 1.75 for the two cases as well. All of these indicators are consistent with the hypothesis that significant amounts of anthropogenic pollution were also being advected with biomass burning compounds in ever-increasing quantities through the event. Indeed, based on filter data, sulfate alone could account for 3/8ths of $PM_{2.5}$ mass in the second half of the event.

5.1.2 Puerto Princesa to Tubbataha Sampling and the Sept 25th-26th, 2012 event

The second biomass burning event occurred while the *Vasco* was moored at Tubbataha Reef. The *Vasco* departed from Puerto Princesa to Tubbataha Reef in the Sulu Sea on Sept. 21st, and ended its sampling with the return voyage back to Manila on Sept. 27th. While there were sporadic peaks in particle and CO concentration on Sept 23rd and 24th, the event was sampled for a 12 hour period over Sept 25th-26th. This event had peak particle concentrations and CO values nearly as high as the Sept. 14th event, but was considerably shorter in duration-nominally only eight hours long. There were also a number of minor events flanking either side of the primary event. NAAPS suggested a peak in smoke concentrations, although 12-18 hours earlier than observed. NAAPS over predicted smoke and pollution thereafter.

More detailed data from the Sept 25th-26th, 2012 period is presented in Figure 8 in a manner similar to Figure 7. Some aspects of the Sept 25th-26th event mimic the earlier Sept 14-16th event. Particle size distributions, with a volume median diameter of ~0.3 μm, were similar. Key VOC markers, as listed in Table 1, looked similar to the Sept 14th event. A TC (here Jelawat) was just east of the Philippines, with an extensive inflow arm reaching to Southern Vietnam (e.g., Sept 24th meteorology and imagery in Figure 5(d)). A day later, as TC Jelawat migrated northward, a large aerosol ejection event occurred along northwestern Borneo into the SCS, again visible in the AERONET time series (Figure 3). Large scale convection was suppressed from upper tropospheric subsidence on the backside of the TC (Figure 6). At the same time, NAAPS and MODIS AOT data suggest that for this case, a large event also departed Sumatra, which we speculate may have been part of the sampled airmass of the principal event, or perhaps of the secondary event that appeared 12Z on the 26th. Regardless, neither the modeling nor the remote sensing data provide enough information to make this attribution. As in the previous Sept 14th-16th event, the TC's continued northward migration ended the event. Soundings were similar between the two events: relatively moist in the lower troposphere, with some drying aloft.

The comparison of the weather and PCASP time series for this event does show some interesting features. The most significant increase in particle concentration at 18Z on the 25th was heralded by a cold pool, with near instantaneous temperature drop and increased wind speeds. Generally, we think of cold pools being associated with convectively washed-out air or, as in the early period case (Sept 14th), as having little effect on particle concentrations. But in this case, particle concentrations increased, though the magnitudes of the temperature, wind and precipitation perturbations were quite small. Thus, the event may have been associated with some minor convection along the leading edge of the airmass.

5.2 Local aerosol events

While the primary focus of the 2012 *Vasco* cruise was to observe the nature of long-range biomass burning and anthropogenic aerosol transport from Borneo and Sumatra to the Philippines, we were mindful of the potential impact of local aerosol sources and nucleation. Indeed, there is significant diversity in model nucleation rates in the region (Yu et al., 2010), and virtually no observations. During the cruise, two significant types of local sources were observed; a nucleation event at Apo Reef on Sept. 5th -6th, and a series of urban plumes as the *Vasco* neared the vicinity of port towns such as Coron and Puerto Princesa. These events are discussed in more detail below.

5.2.1 Apo Reef Nucleation Event

The first anchorage reached after departing Manila was at Apo Reef in the middle of the Mindoro Strait, on Sept. 5th and 6th, 2012. As noted in Sections 3 and 4, during this period the SCS was experiencing a strong break in the SWM. The atmosphere was relatively dry above 700 hPa (Figure 6), with only scattered cumulus and congestus in the region. Boundary layer and lower free-tropospheric winds were generally northwesterly to easterly in the northern Philippines on these days, instead of the much more typical SWM flow. Consequently, sampled air masses on the *Vasco* were downwind from Luzon and/or Mindoro. On Sept. 6^{th} at ~01Z (~9:00 LST) the *Vasco* sampled a significant spike in CN, in excess of 1500 cm^{-3}. At the same time, filter and PCASP-inferred particle mass concentrations were low, only perhaps 1-3 μg m^{-3}, and CO was only slightly above background at ~100-110 ppbv. During this early period in the cruise, the electrostatic classifier was still operational and resolved the aerosol particle size dynamics from 0.02-0.5 μm (Figure 7). Three whole-air samples were also collected during the event, including 2220Z Sept. 5^{th} as a pre-event can, 2:45Z Sept 6^{th} in the middle of the event, and 730Z Sept. 6 as a post-event sample (Table 1).

The aerosol dynamics for Apo Reef show the characteristics of a classic nucleation event (e.g., see review by Kulmala et al., 2004). Leading up to the event, particle concentrations were at ~500 cm^{-3}, with an estimated mass concentration ~1 μg m^{-3}. The fine-mode particle number distribution was fixed to a count median diameter (CMD) of 0.1 μm, but with significant enhancements throughout the event. Clearly, an airmass change occurred at ~ 23Z Sept 5^{th}, with an increase in particle concentration to 1000 cm^{-3}, and a slight fine-mode particle volume increase to ~1.5 μg m^{-3}. Nucleation was indicated 9:00 local time, as solar radiation was increasing throughout the morning. Total concentration peaked at 1800 cm^{-3}. The CMD of the ultrafine mode initialized at 0.02 μm, growing to 0.05 μm in five hours. By 06Z (14:00 LST), the bimodal nature of the fine-mode aerosol population ended, with a strong 0.1 μm number mode in place. The fine mass concentration was estimated to be ~ 3-5 μg m^{-3} throughout the core of the event. While the ultrafine mode may have grown into this fine mode, there were additional modal shifts to 0.08 μm over the next two hours, which may actually be more representative of the airmass. Also noteworthy is that at ~03Z a simultaneous enhancement in both the fine and ultrafine mode occurred, suggesting a covariance in both the fine mode particles and the nucleation event precursor gases. Indeed, this is consistent as the nucleation event occurred along with a strong increase in fine particle concentration.

While a separate paper will be devoted to the whole-air samples from the 2011 and 2012 cruises, it is noteworthy here that the VOC profile during the event is consistent with the nucleation event, coinciding with reactive anthropogenic gas emissions (Table 1). There were enhancements in reactive alkenes; roughly a factor of two enhancements in ethene and propene.

There was also a factor of 2.5 increases in dimethyl sulfide over background, and a slight increase in CH_4, *i*-pentane and *i*-$PrONO_2$. All other species were relatively constant. Interesting, isoprene was near detectable limits, as were pinenes, suggesting that terrestrial biogenic influences had been photochemically removed upwind. Also missing are enhancements in biomass burning markers. CO was fairly constant at 95-100 ppbv, as was benzene. Further the ratio of i- to n-pentane increased from 1.3 to 1.7. All of this data points to the likelihood that the nucleation precursors were anthropogenic in origin from Luzon and/or Mindanao.

5.2.2 Puerto Princesa Plumes

A second class of observed local aerosol phenomena occured in association with urban plumes. While the *Vasco* cruise track was designed away from population centers, there were times during transit that their influence were considerable. These ranged from small boat emissions around coastal villages, to observation of the urban plume of Puerto Princesa as the *Vasco* entered and exited the port to take on supplies. Focusing on Puerto Princesa, the *Vasco* visited on Sept. 13th and 20th 2012, leading to four sets of observations. On three occasions, significant enhancement in particles due to the Puerto Princesa plume were clearly observed (for the exit on Sept. 14th, the aerosol environment was dominated by the smoke event).

As the *Vasco* was nearing Puerto Princesa on Sept. 13th, 2:00Z UTC (~10:00 LST) at approximately 30 km out, CN concentrations rapidly increased to instrument saturation at 10,000 cm^{-3}. At this point, the crew immediately suspected self-sampling, and quickly shut instrumentation down. However, it was then realized that the wind was in fact traveling directly over the bow. Some of the instrumentation was then restarted, and a whole-air sample was collected. While the boundary layer was clearly biomass burning-dominated upon departure the following day, the crew prepared to sample the plume on the next visit, Sept. 19th -20th, for which cases concentrations peaked at only ~2200 cm^{-3}.

The pair of visits, while relatively isolated samples, nevertheless provide some insight into the nature of particle populations within the Philippines Islands. Key particle and gas measurements are included in Table 1, and can be compared to the Apo Reef and biomass burning events. Most importantly, the very high particle concentrations for arrival on Sept. 13th have every indication of being a nucleation event. Unfortunately, as the electrostatic classifier was inoperative for this portion of the cruise, we cannot directly compare size distributions with the Apo reef case. But comparison of PCASP and CN count showed a substantial aerosol population with diameters less than 0.1 μm. Winds were clearly in an outflow region for the city, and solar radiation was fairly intense in the late morning under only moderately cloud free skies. On the visit on Sept. 19th, a sample was taken just before arrival, and a subsequent sample was collected as the *Vasco* entered the harbor. Clear enhancements in CN were observed. Although, as reported by Atwood et al. (2016; submitted), there was no nucleation mode in this case, suggesting these particles were primary; this is not unexpected given the earlier time of arrival (~8:00 AM LST) and full cloud cover. Similarly, upon departure in the 21st, at 6:00 AM LST, particle concentrations were low (<400 cm^{-3}), possibly partly as this was even before the morning commute.

Whole-air sample data for these cases provide us with other useful information. First and most notably, the use of the ratio of *i*- to *n*-Pentane in previous studies seemed to be justified, with values above 2 being clearly associated with the urban plume, and also slightly enhanced in the Apo Reef plume. Also hexane, a gasoline derivative, also appears to be a strong signature for Puerto Princesa. But in general for most species, the differentiation between “urban” and “biomass burning” in older plumes is not so straightforward.

6.0 DISCUSSION: COMPARISON OF THE 2011 AND 2012 STUDIES

This paper had two primary objectives. First, to provide a broad overview of the 2012 *Vasco* cruise, including instruments carried, cruise track, and the general characteristics of the regional environment sampled. Second we wished to utilize the 2012 *Vasco* as a vehicle for continuing the narrative put forth in the 2011 effort on the nature of aerosol populations associated with the SWM. To our knowledge, these cruises provide the first published aerosol field measurements in the boreal summertime South China and Sulu Sea regions.

The similarities and contrasts between the 2011 and 2012 cruise observations portray key aspects of the SWM aerosol system, pointing to a number of observational and prediction challenges. Certainly from an inter-seasonal, seasonal, and even monthly time period, the conceptual models of aerosol lifecycle in the SWM by Reid et al. (2012) largely hold. Within the season, the MJO, in part, regulates large-scale precipitation patterns, which then affect aerosol event timing. Tropical cyclones develop well-defined areas of monsoonal enhancement/inflow arms with accelerated surface winds that help draw smoke further into the monsoonal flow, and but may also lead to enhanced scavenging. Subsidence after TC passage, however, reduces convection, allowing for the smoke to be transported great distances in the monsoonal enhancements. At the same time, major land/sea breeze events can lead to significant aerosol ejections off-island. Ultimately, multi-day events are possible, such as the two events for 2011, and the Sept 14th -17th event for 2012. Finally, while near "pure" biomass burning events are possible, there is more typically a mixture of biomass burning and other anthropogenic emissions. Both the comparison of the seasonal behavior and the measurements on the cruises bear these similarities out.

Several key differences between long-range transport characteristics in 2011 and 2012 are highly noteworthy. First, while the monsoon frequently has weak and strong phases, the 2012 case clearly showed how strong the effect of tropical waves moving through the region can be on low-level flow patterns. Indeed, the first week of the 2012 cruise coincided with uncommonly clear skies and even northerly winds. Such clear periods provide some of the rare opportunities for satellite observations. Yet from a climatological point of view, this clear sky bias fundamentally represents a skewed portrait of the aerosol system (Reid et al., 2013).

A second significant difference between 2011 and 2012 is that in 2012 biomass bringing events showed higher frequency characteristics. This is likely in part due to the closer proximity of the *Vasco* to Borneo, where we speculate that a more significant role of convection along the coast of Borneo led to more pockets of smoke. Further, in 2012, the *Vasco* did not experience a regional clear day, as was caused by a TC propagating across Luzon and into the SCS at the end of the 2011 cruise. This leads to suspicion that many pockets of polluted air may be migrating through the region on a regular basis, obscured from satellite detection. Given the remote expanse of the region, such phenomenon can probably only be surveyed by aircraft.

High-frequency events in 2012 also included observation of two nucleation events and urban plumes. While it is often thought that these types of nucleation events only occur in the presence of gas precursors when there are few aerosol particles (e.g., Mäkelä et al., 1997; Kulmala et al., 2004; Boy et al., 2008), for the tropics and subtropics, nucleation events have also been noted in polluted urban environments (e.g., Cheung et al., 2011; Betha et al., 2013; Kanawade et al., 2014, Brines et al., 2015), and even in dense tropical smoke plumes (Reid et al., 2005). The *Vasco* observed both kinds. The Apo Reef nucleation event seemed to follow the more traditional relationship, starting with precursor gases in the presence of low aerosol particle surface area. Indeed, while in clean mid-latitude marine conditions, Covert et al., (1992) observed explosive nucleation events and discounted local or transported sources. Instead, they suggested such an event being a natural outcome for a marine boundary layer having low particle surface area. It was later argued that nucleation in some remote sub-tropical to mid latitude areas is assisted by ion-mediated nucleation events (IMEs) formed by the ionization of molecules by cosmic rays (Yu et al., 2008). While Yu et al., (2008) considers such nucleation generally unfavorable in tropical regimes, they did predict significant nucleation on the periphery-notably west of the northern Philippines, south of Java and east of New Guinea. Indeed, Yu et al., (2008) placed a nucleation hotspot right at our point of observation. Aided by anomalously clear skies, and thus high photolysis rates, we see this nucleation mechanism as being a reasonable contributor to the event. Indeed, it was the only such observed event in the two *Vasco* cruises.

The second type of nucleation event, in the outflow of a polluted urban plume, was observed by the *Vasco* outside of Puerto Princesa. Nucleation events with concentrations this high have been reported in urban tropical air in late morning (e.g., Cheung et al., 2011; Betha et al., 2013; Kanawade et al., 2014, Brines et al., 2015). Ultimately, whether in clean or more polluted conditions, aerosol nucleation events are probably not uncommon in the MC.

In addition to nucleation events, the *Vasco* in 2012 intersected many small plumes, as well as the strong urban plume of Puerto Princesa (population =~250,000). These observations remind us that while many of the islands of the MC are thought of as “remote” and outside of the megacities, they can nevertheless harbor reasonably sized populations. Given the significant use of biofuel or highly polluted engines, these islands can clearly emit significant amounts of CCN.

Finally, and perhaps most interestingly, the 2012 cruise demonstrated a new relationship between aerosol events, convective cells and more organized squall lines. In 2011, drops in particle concentration were coincident with temperature; consistent with the notion that cold pool air was advecting into the region with aerosol particles already deposited out. From the wind shear and variable wind speeds shown in the profiles, the steering winds of the squall lines roll over polluted airmasses underneath. Thus, these squall lines may be likened to "lawn mowers", ingesting or scavenging aerosol particles as they propagate.

Based on the work of Seigel and van den Heever (2012), which showed that dust generated ahead of cold pools on the leading edge of thunderstorms is lifted to mid-levels where the potential impact of aerosol particles as CCN was minimal, the 2011 cruise suggested that the nature of convection in the region often insulated itself from potential aerosol impacts. Certainly, the *Vasco* observed some of this behavior in 2012, but also observed the opposite; cases where the telltale cold pool signs of rapid temperature drop and spikes in wind heralded the coming of a polluted airmass. Indeed, during the Sept. 14th-18th period in Figure 7, both clear air and polluted air followed cold pools. While the wiring diagram for larger scale features is largely well known, and to some extent can be qualitatively captured by a coarse-grid model such as NAAPS, run with additional constraint from satellite precipitation products, there remains much to understand about aerosol lifecycle in the vicinity of convective cells and squall lines. We suspect that a clue to the behavior when air pollution follows a cold pool event lies in the rather shallow temperature drops (1-2^{o}C versus 5-6^{o}C). This may be an indicator that the convection is not so strong, or that it may in part be a remnant. Such events may also be related to the nature of the initial formation of convection or a squall line relative to a polluted airmass. The origin of the convection, whether from a coastal ejection event or a large convective system, may play a role. Or, steering winds and wind shear may be such that some moisture convergence occurs on the leading edge of an ejection event, leading to weak convection along the boundary. However, this situation thus far has not been observable from satellite.

To speculate, these events of thick aerosol plumes behind convection seem to be consistent with a land breeze origin, propagated much further than normal by the monsoonal flows. Certainly the temperature change and high aerosol loading behind a cloud top front matches aircraft observations of large land breeze ejection events in the Arabian Gulf (e.g., Reid et al., 2008). In the MC case, cloud development along land breeze fronts is much larger, leading to significant convection offshore of islands (e.g., Liberti et al., 2001; Qian 2008; Virts et al., 2013).

Ultimately, 7SEAS and the *Vasco* cruises demonstrate that the arsenal of tools, in situ measurements, remote sensing and models clearly have difficulty mapping contiguous aerosol fields and properties. Indeed, core aerosol science goals for the NASA Aerosol-Cloud-

Ecosystem (ACE) mission focus on the use of remote sensing to constrain aerosol lifecycle and cloud impacts. The transition of polluted to pristine aerosol environments is a significant science question. The Vasco cruises point to the real world challenges posed to scientists studying aerosol-cloud interaction and challenge us to understand the many scale dependences inherent in the system ranging from ENSO to the micro meteorology and physics around clouds.

6.0 CONCLUSIONS

This paper provides an overview of the meteorological and aerosol environment measured by the *M/Y Vasco*, which sampled Maritime Continent (MC) air in September 2012 along the entire length of the Palawan Archipelago, Philippines. This cruise was a longer follow-on to a similar research cruise the previous year (Reid et al., 2015) and was a significant component of the 2012 7 Southeast Asian Studies (7SEAS) southwest monsoon (SWM) intensive period-a high water mark for observations throughout the MC. The Palawan region for this research cruise was selected for being a receptor of smoke and anthropogenic emissions from Borneo, Sumatra and the Malay Peninsula as emissions were advected by SWM flow into the seasonal monsoonal trough east of the Philippines. The key conclusions of this study are:

1) The 2012 cruise home ported at Manila, Philippines, and sampled three major regions: (a) the upper Palawan chain and El Nido for Sept. 4th -13th, 2012; (b) the southern Palawan chain and Balabac Island on the southern tip of the Palawan chain, ~100 km north of the northern tip of Borneo, Sept. 14th-19th; and (c) the Sulu Sea and Tubbataha Reef Sept. 21st-29th, 2012. In the northern locations, the atmosphere was under the influence of an easterly wave, bringing unseasonable north-to-northeasterly winds and air from the northern Philippine islands of Luzon and Mindoro. Observations included a pronounced particle nucleation event in relatively clean conditions in a region where ion mediated nucleation was predicted by Yu et al., (2008). In the southern and Sulu Sea locations, biomass burning and anthropogenically-polluted air masses were sampled, largely modulated by enhancement in monsoonal flows associated with two *Category 5* tropical cyclones (TCs). Fine particle concentrations reached ~35 μg m^{-3}, and CO was as high as 250 ppbv. Finally, while transiting through Puerto Princesa for supplies, the city plume was also sampled, including a nucleation event in more polluted conditions with CN concentrations of 10,000 cm^{-3}. In comparison, "background" values of aerosol particle

concentrations were on the order of 500 cm^{-3}, roughly 50-100% higher than the cleaner background conditions sampled by the 2011 cruise.

2) The large-scale relationships between aerosol emissions, aerosol transport and regional meteorology during the cruise broadly matched the conceptual models of Reid et al. (2012) regarding relationships to the MJO and tropical cyclones. However, easterly waves resulted in significant weakening of the monsoonal flow, and two slow moving TCs located southeast of the Philippines resulted in monsoonal winds with enhanced northerly and westerly components

3) While a multi-day biomass burning event was observed, in comparison to 2011, aerosol events showed much higher frequency behavior. Even in the middle of the Sulu Sea, pulses of aerosol particles on the order of 3-6 hours were observed. This behavior is likely in part due to influence of scattered convection, leaving pockets of polluted and clean air masses. In addition, the aforementioned nucleation events and urban plumes added additional high-frequency signals. This high frequency behavior further complicates an already complex aerosol and cloud system, and specifically hinders interpretation of temporally discrete measurements.

4) The 2011 cruise pointed to the important role of organized squall lines and cold pools in scavenging aerosol particles from the marine boundary layer. While very clean air was observed behind the squall lines, there were many cases in the 2012 cruise where the opposite relationship was observed. That is, a rapid temperature drop and spike in wind heralded not clean air behind a squall line, but highly polluted air. This difference may be a result of squall line origin, meteorology, and/or lifecycle. Some of the effects may be a result of remnant cold pools. Alternatively, the steering winds and wind shear may have been such that some moisture convergence occurred on the leading edge of an ejection event leading to weaker convection along the boundary. However, our prevailing hypothesis is that these events are a result of convection forming from a coastal land breeze ejection event that is caught in enhanced monsoonal flows. Clearly, understanding the dynamics of aerosol particles around such organized convective features is a high priority for future work.

5) Finally, taken together, the 2011 and 2012 cruises cast doubt on our ability to deterministically predict or characterize the complex aerosol and cloud environment in tropical regions, particularly around the MC. While the dynamics that set the large scale context are generally well characterized (e.g., TCs, the SWM, and convectively coupled waves in general), the specifics of aerosol burden, chemistry, and microphysics are in no small part determined by

high frequency events that are challenging to observe and to model. Indeed, outstanding science questions exist on how polluted air masses transform into cleaner ones. And, aerosol flows around individual cloud features are a key priority for measurements in the future. Such questions need to be considered at the heart of future mission requirements such as for ACE.

7.0 ACKNOWLEDGEMENTS

Organization of this research cruise and the overall 2012 IOP required the assistance of a number of organizations, including the staff of the Office of Naval Research-Global program office and reservist unit (esp. Joseph Johnson, Blake McBride, Paul Marshall), the Manila Observatory (esp. Antonia Loyzaga and Fr. Daniel McNamara), US State Department/ Embassy in Manila (esp. Maria Theresa Villa and Dovas Saulys), and the Naval Postgraduate School (esp. Richard Lind). We are most grateful to the *Vasco* ship management and crew, operated by Cosmix Underwater Research Ltd, (esp. Luc Heymans and Annabelle du Parc). We are also grateful to the host institutions for regional AERONET site deployment and the use of derived optical thickness data herein. Authors also benefitted from conversations with Eric Maloney (CSU) and Matthew Wheeler (CSIRO). Funding for this research cruise and analysis was provided numerous sources. *Vasco* ship time procurement was provided by the NRL 6.1 Base Program via an ONR Global grant to the Manila Observatory. Funding for US scientist deployment and instrument analysis was provided by the NRL Base Program and ONR 35. Modeling analysis was provided by ONR 32. Remote sensing and model analysis was provided by the NASA Interdisciplinary Science Program. Reservist support was provided by ONR Program 38. Ground site deployments were supported by the NASA Radiation Science Program through a grant from the Southeast Asia Composition, Cloud, Climate Coupling Regional Study (SEAC^{4}RS) science team. Gas chemistry was provided by the NASA Tropospheric Chemistry Program. Author JRC acknowledges the support of NASA Interagency Agreement NNG13HH10I on behalf of MPLNET and SEAC^{4}RS science teams.

8.0 REFERENCES:

Akagi, S. K., Yokelson, R. J., Weidinmyer, C., Alvarado, M. J., Reid, J. S., Karl, T., Crounse, J. D., and Wennberg, P. O.: Emission factors for open and domestic biomass burning for use in atmospheric models, Atmos. Chem. Phys., 11, 4039–4072, doi:10.5194/acp-11-4039-2011, 2011.

Anderson, T. L., Covert, D. S., Marshall, S. F., Laucks, M. L., Charlson, R. J., Waggoner, A. P., Ogren, J. A., Caldow, R., Holm, R. L., Quant, F. R., Sem, G. J., Wiedensohler, A., Ahlquist, N. A., and Bates, T. S.: Performance characteristics of a high-sensitivity three wavelength, total, backscatter nephelometer, J. Atm. Ocean Tech., 13, 967-986, 1996.

Andreae, M. O., Rosenfeld, D., Artaxo, P., Costa, A. A., Frank, G. P., Longo, K. M., Silva-Dias, MAF, Smoking rain clouds over the Amazon, Science, 303, 1337-1342. 10.1126/science.1092779, 2004.

Atwood, S. A., Reid, J. S., Kreidenweis, S. M., Yu, L. E., Salinas, S. V., Chew, B. N., and Balasubramanian, R.: Analysis of source regions for smoke events in Singapore for the 2009 El Nino burning season, Atmos. Environ.,78, 219-230, doi: 10.1016/j.atmosenv.2013.04.047, 2013.

Atwood, S. A., et. al.: Size resolved aerosol and cloud condensation nuclei (CCN) properties in the remote South China Sea: Measurement and sources. To be submitted, Atymos. Chem and Phys. 2016.

Beegum, S. N., Krishna Moorthy, K., Babu, S.S., Reddy, R. R., and Gopal, K. R.: Large scale modulations of spectral aerosol optical depths by atmospheric planetary waves, Geophys. Res. Lett., 36, L03810, doi: 10.1029/2008GL036509, 2009.

Betha, R., Spracklen, D. V., and Balasubramanian, R.: Observations of new aerosol particle formation in a tropical urban atmosphere, Atmos. Environ., 71, 340-351, doi:10.1016/j.atmosenv.2013.01.049, 2013.

Brines, M., Dall'Osto, M., Beddows, D. C. S., Harrison, R. M., Gómez-Moreno, F., Núñez, L., Artíñano, B., Costabile, F., Gobbi, G. P., Salimi, F., Morawska, L., Sioutas, C., and Querol, X.: Traffic and nucleation events as main sources of ultrafine particles in high-insolation developed world cities, Atmos. Chem. Phys., 15, 5929-5945, doi:10.5194/acp-15-5929-2015, 2015.

Bond, T. C, Anderson, T. L., and Campbell, D.: Calibration and intercomparison of filter based measurements of visible light absorption by aerosols, Aerosol Sci. Tech., 30, 582-600, doi:10.1080/027868299304435, 1999.

Boy, M., Karl, T., Turnipseed, A., Mauldin, R. L., Kosciuch, E., Greenberg, J., Rathbone, J., Smith, J., Held, A., Barsanti, K., Wehner, B., Bauer, S., Wiedensohler, A., Bonn, B., Kulmala, M., and Guenther, A.: New particle formation in the Front Range of the Colorado Rocky Mountains, Atmos. Chem. Phys., 8, 1577-1590, doi:10.5194/acp-8-1577-2008, 2008.

Cahill, T. A., Goodart, C., Nelson, J. W., Eldred, R. A., Nasstrom, J. S., and Feeny, P. J.: Design and evaluation of the DRUM impactor, in: Proceedings of the International Symposium on Particulate and Multiphase Processes, Ariman, T. and Veziroglu, T. N. (Eds.), Hemisphere Publishing Corporation, Washington, D. C., 319-325, 1985

Campbell, J. R., Reid, J. S., Westphal, D. L., Zhang, J., Tackett, J. L., Chew, B. N., Welton, E. J., Shimizu A., and Sugimoto, N.: Characterizing aerosol particle composition and the vertical profile of extinction and linear depolarization over Southeast Asia and the Maritime Continent: the 2007-2009 view from CALIOP., Atmos. Res., 122, 520-543, doi:10.1016/j.atmosres.2012.05.007, 2013.

Chow, J. C., Watson, J. G., Pritchett, L. C., Pierson, W. R., Frazier, C. A., and Purcell, R. G.: The DRI thermal/optical analysis system: Description, evaluation and applications in U.S. air quality studies, Atmos. Environ., 27A, 1185–1201, 1993.

Cheung, H. C., Morawska, L., and Ristovski, Z. D.: Observation of new particle formation in subtropical urban environment, Atmos. Chem. Phys., 11, 3823-3833, doi:10.5194/acp-11-3823-2011, 2011.

Colman, J. J., Swanson, A. L., Meinardi, S., Sive, B. B., Blake, D. R., and Rowland, F. S.: Description of the analysis of a wide range of volatile compounds in whole air samples collected during PEM-Tropics A and B, Anal. Chem., 73, 3723-3731, 2001.

Covert, D. S., Kapustin, V. N., Quinn, P. K., Bates, T. S.: New particle formation in the marine boundary layer, J. Geophys. Res., 97, 20581-20589, 1992.

Feingold, G., Remer, L. A., Ramaprasad, J., and Kaufman, Y. J.: Analysis of smoke impact on clouds in Brazilian biomass burning regions: An extension of Twomey's approach, J. Geophys. Res., 106, 22907-22922, doi: 10.1029/2001JD000732 , 2001.

Ferek, R.J., Reid, J. S., Hobbs, P.V., Blake, D.R and Liousse, C. (1998), Emission factors of hydrocarbons, halocarbons, trace gases, and particles from biomass burning in Brazil, *J. Geophys. Res., 103*, 32,107-32,118, 1998.

Field, R.D. and Shen, S.S.P.: Predictability of carbon emissions from biomass burning in Indonesia, J. Geophys. Res., 113, G04024, doi:10.1029/2008JG000694, 2008.

Ge, C., Wang, J., and Reid J. S.: Mesoscale modeling of smoke transport over the Southeast Asian Maritime Continent: coupling of smoke direct radiative feedbacks below and above the low-level clouds, Atmos. Chem. Phys., 14, 159-174, doi:10.5194/acp-14-159-2014, 2014.

Holben, B. N., Eck, T. F., Slutsker, I., Tanre, D., Buis, J. P., Setzer, A., Vermote, E., Reagan, J. A., Kaufman, Y. J., Nakajima, T., Lavenu, F., Jankowiak, I., and Smirnov, A.: AERONET - A federated instrument network and data archive for aerosol characterization, Remote Sens. Environ., 66, 1-16, 1998.

Hogan , T.F. and Rosmond, T.E.: The description of the U.S. Navy Operational Global Atmospheric Prediction System's spectral forecast model, Mon. Wea. Rev., 119, 1786-1815, 1991.

Hu, L, Millet, D. B., Baasandorj, M., Griffis, T. J., Turner, P., Helmig, D., Curtis, A. J., and Hueber, J.: Isoprene emissions and impacts over an ecological transition region in the U.S. Upper Midwest inferred from tall tower measurements, J. Geophys. Res. Atmos., 120, 3553–3571, doi: 10.1002/2014JD022732, 2015.

Joyce, R. J., Janowiak, J. E., Arkin, P. A., and Xie, P.: CMORPH: A method that produces global precipitation estimates from passive microwave and infrared data at high spatial and temporal resolution, J. Hydrometeorol., 5, 487-503, 2004.

Kanawade, V. P., Tripathi, S. N., Siingh, D., Gautam, A. S., Srivastava, A. K., Kamra, A. K., Soni, V. K., Sethi, V.: Observations of new particle formation at two distinct Indian subcontinental urban locations, Atmos. Environ., 96, 370-379, doi:10.1016/j.atmosenv.2014.08.001, 2014.

Kulmala, M., Vehkamaki, H., Petaja, T., Dal Maso, M., Lauri, A., Kerminen, V.-M., Birmili, W., and McMurry, P. H.: Formation and growth rates of ultrafine atmospheric particles: a review of observations, J. Aerosol Sci., 35, 143-176, 2004.

Levy, R. C., Mattoo, S., Munchak, L. A., Remer, L. A., Sayer, A. M., Patadia, F., and Hsu, N. C.: The Collection 6 MODIS aerosol products over land and ocean, Atmos. Meas. Tech., 6, 2989-3034, doi:10.5194/amt-6-2989-2013, 2013.

Liberti, G. L., Chéruy, F., and Desbois, M.: Land effect on the diurnal cycle of clouds over the TOGA COARE area, as Observed from GMS IR Data. *Mon. Wea. Rev.*, **129**, 1500–1517, 2001.

Lin, N.-H. et al., (2013), An overview of regional experiments on biomass burning aerosols and related pollutants in Southeast Asia: From BASE-ASIA and the Dongsha Experiment to 7-SEAS, Atmospheric Environment, 78, 1-19.

Lohmann, U. and Feichter, J.: Global indirect aerosol effects: a review, Atmos. Chem. Phys., 5, 715-737, doi:10.5194/acp-5-715-2005, 2005.

Lynch, P., Reid, J. S., Westphal, D. L., Zhang, J., Hogan, T. F., Hyer, E. J., Curtis, C. A., Hegg, D. A., Shi, Y., Campbell, J. R., Rubin, J. I., Sessions, W. R., Turk, F. J., Walker, A. L.: Development studies towards an 11-year global gridded aerosol optical thickness reanalysis for climate and applied applications, Geosci. Model Dev. Discuss., 8, 10455-10538, doi:10.5194/gmdd-8-10455-2015, 2015

Mäkelä, J. M., Aalto, P., Jokinen, V., Pohja, T., Nissinen, A., Palmroth, S., Markkanen, T., Seitsonen, K., Lihavainen, H., Kulmala, M.: Observations of ultrafine aerosol particle formation and growth in boreal forest, Geophys. Res. Let, 24, 1219-1222, 1997.

Maloney, E. D. and Hartman, D. L.: The Madden Julian oscillation, barotropic dynamics, and the North Pacific tropical cyclone formation, part 1: Observations, J. Atmos. Sci., 58, 2545-2558, 2001.

McGaughey, G. R., Desai, N. R., Allen, D. T., Seila, R. L., Lonneman, W. A., Fraser, M. P., Harley, R. A., Pollack, A. K., Ivy, J. M., Price, J. H.: Analysis of motor vehicle emissions in a Houston tunnel during the Texas Air Quality Study 2000, Atmos. Environ., 38, 3363-3372, doi:10.1016/jatmosenv.2004.03.006, 2004.

Miller, S. D., Hawkins, J. D., Kent, J., Turk, F. J., Lee, T. F., Kuchiauskas, A. P., Richardson, K., Wade, R. and Hoffman, C.: NexSat: Previewing NPOESS/VIIRS imagery capabilities, Bull. Amer. Meteor. Soc., 87, 433–446, doi: 10.1175/BAMS-87-4-433, 2006.

Nichol, J.: Smoke haze in Southeast Asia: A predictable recurrence, Atmos. Environ., 32, 2715-2716, 1998.

O'Neill, N. T., Eck, T. F., Smirnov, A., Holben, B. N., and Thulasiraman, S.: Spectral discrimination of coarse and fine mode optical depth, J. Geophys. Res., 108, 4559, doi: 10.1029/2002JD002975, 2003.

Petters, M. D. and Kreidenweis, S. M.: A single parameter representation of hygroscopic growth and cloud condensation nucleus activity, Atmos. Chem. Phys. 7, 1961–1971, 2007.

Petters, M. D., Carrico, C. M., Kreidenweis, S. M., Prenni, A. J., DeMott, P. J., Collett, J. L., and Moosmüller, H.: Cloud condensation nucleation activity of biomass burning aerosol, J. Geophys. Res. Atmos., 114, D22205, doi:10.1029/2009JD012353, 2009.

Qian, J.-H.: Why precipitation is mostly concentrated over islands in the Maritime Continent. *J. Atmos. Sci.*, **65**, 1428–1441, doi: http://dx.doi.org/10.1175/2007JAS2422.1, 2008

Reid, J. S., Brooks, B., Crahan, K. K., Hegg, D. A., Eck, T. F., O'Neill, N., de Leeuw, G., Reid, E. A., and Anderson K. D.: Reconciliation of coarse mode sea-salt aerosol particle size measurements and parameterizations at a subtropical ocean receptor site, J. Geophys. Res., 111, D02202, doi:10.1029/2005JD006200, 2006.

Reid J.S., Hobbs, P.V. , Rangno, A.L., and Hegg D.A.: Relationships between cloud droplet effective radius, liquid water content and droplet concentration for warm clouds in Brazil embedded in biomass smoke, *J. Geophys. Res.*, *104*, 6145-6153, 1999.

Reid, J. S., Hobbs, P. V., Ferek, R. J., Martins, J. V., Blake, D., Dunlap, M. R., and Liousse, C.: Physical, chemical and optical properties of regional hazes dominated by smoke in Brazil, J. Geophys. Res., 103, 1998.

Reid, J. S., Hyer, E. J., Johnson, R. S., Holben, B. N., Yokelson, R. J., Zhang, J., Campbell, J. R., Christopher, S. A., Di Girolamo, L., Giglio, L., Holz, R. E., Kearney, C., Miettinen, J., Reid, E. A., Turk, F. J., Wang, J., Xian, P., Zhao, G., Balasubramanian, R., Chew, B. N., Janjai, S., Lagrosas, N., Lestari, P., Lin, N. H., Mahmud, M., Nguyen, A. X., Norris, B., Oanh, N. T. K., Oo, M., Salinas, S. V., Welton, E. J., and Liew, S. C.: Observing and understanding the Southeast Asian aerosol system by remote sensing: An initial review and analysis for the Seven Southeast Asian Studies (7SEAS) program, Atmos. Res., 122, 403-468, doi:10.1016/j.atmosres.2012.06.005, 2013.

Reid, J. S., Koppmann, R., Eck, T. F., and Eleuterio, D. P.: A review of biomass burning emissions part II: intensive physical properties of biomass burning particles, Atmos. Chem.

Phys., 5, 799–825, 2005.Reid, J. S., Lagrosas, N. D., Jonsson, H. H., Reid, E. A., Sessions, W. R., Simpas, J. B., Uy, S. N., Boyd, T. J., Atwood, S. A., Blake, D. R., Campbell, J. R., Cliff, S. S., Holben, B. N., Holz, R. E., Hyer, E. J., Lynch, P., Meinardi, S., Posselt, D. J., Richardson, K. A., Salinas, S. V., Smirnov, A., Wang, Q., Yu, L., and Zhang, J.: Observations of the temporal variability in aerosol properties and their relationships to meteorology in the summer monsoonal South China Sea/East Sea: the scale-dependent role of monsoonal flows, the Madden–Julian Oscillation, tropical cyclones, squall lines and cold pools, Atmos. Chem. Phys., 15, 1745-1768, doi:10.5194/acp-15-1745-2015, 2015.

Reid, J. S., Lynch, P., Holben, B. N., Hyer, E. J., Reid, E. A., Salinas, S. V., Zhang, J., Campbell, J. R., Chew, B. N., Holz, R. E., Kuciauskas, A. P., Lagrosas, N., Posselt, D. J., Samposon, C., Walker, A. L., Welton, E. J., Zhan, C.: Aerosol meteorology of the Maritime Continent for the 2012 7SEAS southwest monsoon intensive study: Part I regional scale phenomena, Atmos. Chem and Phys. Discussions, 2016.

Reid, J. S., S. Piketh, S., Burger, R., Ross, K., Jensen, T., R. Bruintjes, Walker, A., Al Mandoos, A., Miller, S., Hsu, C., Kuciauskas, A., and D. L. Westphal., D. L.:An overview of UAE2 flight operations: Observations of summertime atmospheric thermodynamic and aerosol profiles of the southern Arabian Gulf, *J. Geophys. Res.*, *113*, D14213, doi:10.1029/2007JD009435, 2008.

Reid., J. S., Xian, P., Hyer, E. J., Flatau, M. K., Ramirez, E. M., Turk, F. J., Sampson, C. R., Zhang, C., Fukada, E. M., and Maloney, E. D.: Multi-scale meteorological conceptual analysis of observed active fire hotspot activity and smoke optical depth in the Maritime Continent, Atmos. Chem. Phys., 12, 1–31, doi:10.5194/acp-12-1-2012, 2012.

Rose, D., Nowak, A., Achtert, P., Wiedensohler, A., Hu, M., Shao, M., Zhang, Y., Andreae, M.O., and Pöschl, U.: Cloud condensation nuclei in polluted air and biomass burning smoke near the mega-city Guangzhou, China – Part 1: Size-resolved measurements and implications for the modeling of aerosol particle hygroscopicity and CCN activity, Atmos. Chem. Phys., 10, 3365–3383, 2010.

Seigel, R. B. and van den Heever, S. C.: Dust lofting and ingestion by supercell storms, J. Atmos. Sci., 69, 1453–1473, doi:10.1175/JAS-D-11-0222.1, 2012.

Simpson, I. J., Aburizaiza, O. S., Siddique, A., Barletta, B., Blake, N. J., Gartner, A., Khwaja, H., Meinardi, S., Zeb, J., and Blake, D. R.: Air quality in Mecca and surrounding holy places in Saudi Arabia during Hajj: Initial survey, Environ. Sci. Technol., 48, 15, 8529-8539, 2014.

Smirnov, A., et al., Maritime aerosol network as a component of AERONET – first results and comparison with global aerosol models and satellite retrievals, Atmos. Meas. Tech., 4, 583-597, doi:10.5194/amt-4-583-2011, 2011.

Suess, E.: Marine cold seeps and their manifestations: geological control, biogeochemical criteria and environmental conditions, Int. J. Earth Sci, 103, doi:10.1007/s00531-014-1010-0, 1889-1916, 2014.

Tian, B., Waliser, D. E., Kahn, R. A., Li, Q., Yung, Y. L., Tyranowski, T., Geogdzhayev, I. V., Mishchenko, M. I., Torres, O., Smirnov, A.: Does the Madden-Julian Oscillation influence aerosol variability?, J. Geophys. Res., 113, D12215, doi:10.1029/2007JD009372, 2008.

Virts, K., S., Wallace, J. M., Hutchins, M. L., and Holzworth, R. H.: Diurnal lightning variability over the Maritime Continent: Impact of low-level winds, cloudiness, and the MJO. *J. Atmos. Sci.*, **70**, 3128–3146, doi: http://dx.doi.org/10.1175/JAS-D-13-021.1, 2013.

Wang, J., Gei, C., Yang, Z., Hyer, E., Reid, J. S., Chew, B. N., and Mahmud, M.: Mesoscale modeling of smoke transport over the South Asian maritime continent: vertical distributions and topographic effect, Atmos. Res., 122, 486-503, 2013.

Xian, P., Reid, J. S., Atwood, S. A., Johnson, R., Hyer, E. J., Westphal, D. L., and Sessions, W.: Smoke transport patterns over the Maritime Continent, Atmos. Res., 122, 469-485, doi:10.1016/j.atmosres.2012.05.006, 2013.

Yu, F., G. Luo , T. Bates , B. Anderson , A. Clarke , V. Kapustin , R. Yantosca , Y. Wang , S. Wu, Spatial distributions of particle number concentrations in the global troposphere: Simulations, observations, and implications for nucleation mechanisms, J. Geophys. Res., 115, D17205, doi:10.1029/2009JD013473, 2010.

Yu, F., Wang, Z., Luo, G., and Turco, R.: Ion-mediated nucleation as an important global source of tropospheric aerosols, Atmos. Chem. Phys., 8, 2537-2554, doi:10.5194/acp-8-2537-2008, 2008.

Table 1. Aerosol and whole-air sample concentrations and associated particle data for key aerosol events during the study. Units are pptv unless otherwise noted. BDL=Below detectible limits. Local standard time is 8:00 ahead of UTC

Specie	Background Lowest quartile	Biomass Burning		Mixed	Apo Reef Nucleation Event			Puerto Princesa Local pollution and Nucleation			
		Sep 14 6:38Z	Sep 26 0:52Z	Sep 16 19:53Z	Pre-Event Sept 5 22:20Z	Early Event Sept 6 2:45Z	Late Event Sept 6 7:45Z	Inside Sep 13 2:47Z	Outside Sept 19 22:55Z	In plume Sep 19 23:52Z	Depart Sep 20 22:00 Z
CN (cm^{-3})	~500	2500	2100	1040	490	1100	1450	>10000	400	2230	317
~PM_1($\mu g\ m^{-3}$)	~1.5	30	21	14	1.2	1.8	1.9	10	1.5	8	2.5
CO (ppbv)	77+/-3	244	209	112	100	98	92	144	111	207	136
Exc. PM1:CO	N/A	0.17	0.15	0.36	-0.01	0.01	0.03	0.13	0.00	0.05	0.02
DRUM K:S	N/A	0.1	0.12	0.1	N/A	N/A	N/A	0.08	N/A	0.07	N/A
DRUM V:S	N/A	0.0015	0.002	0.003	N/A	N/A	N/A	0.003	N/A	0.03	N/A
CH_4 (ppmv)	1.77+/-0.01	1.77	1.76	1.77	1.768	1.81	1.77	1.77	1.94	1.82	1.82
DMS	24+/-12	27	31	24	7.3	19	9.1	8.6	13.2	9.8	11.1
CH_3I	0.7+/-0.7	1.38	1.48	5.47	0.95	0.55	2.9	0.42	1.25	0.43	0.48
Ethane	348+/-55	877	824	551	399	504	369	525	514	619	434
Ethene	47+/-32	376	490	106	101	212	69	274	381	880	235
Ethyne	68+/-18	561	501	195	107	131	102	315	116	953	123
Propane	67+/-33	137	166	105	86	90	68	140	111	374	78
Propene	24+/-12	76	148	114	49	80	76	62	249	236	62
i-Pentane	57+/-33	35	51	49	23	40	30	241	49	537	64
n-Pentane	40+/-23	26	43	28	18	24	19	106	50	258	56
Hexane	31+/-14	21	38	16	15	12	9	49	48	123	52
Benzene	32+/-27	140	162	58	36	40	23	96	42	198	40
Isoprene	22+/-36	4	BDL	3	6	3	BDL	3	18	59	14
i-$PrONO_2$	1.1+/-0.3	2.3	2.7	2.0	1.7	2.0	1.4	2.2	3.1	1.9	2.6
n-$PrONO_2$	0.3+/-0.2	0.4	0.4	0.5	0.3	0.2	0.5	0.5	0.2	0.3	0.6
$BuONO_2$	1+/-0.7	1.6	2.3	1.7	1.3	1.6	1.2	2.7	2.1	1.9	2.0
Ratio of i to n Pentane	~1.4	1.3	1.2	1.75	1.3	1.7	1.6	2.3	1	2.08	1.2

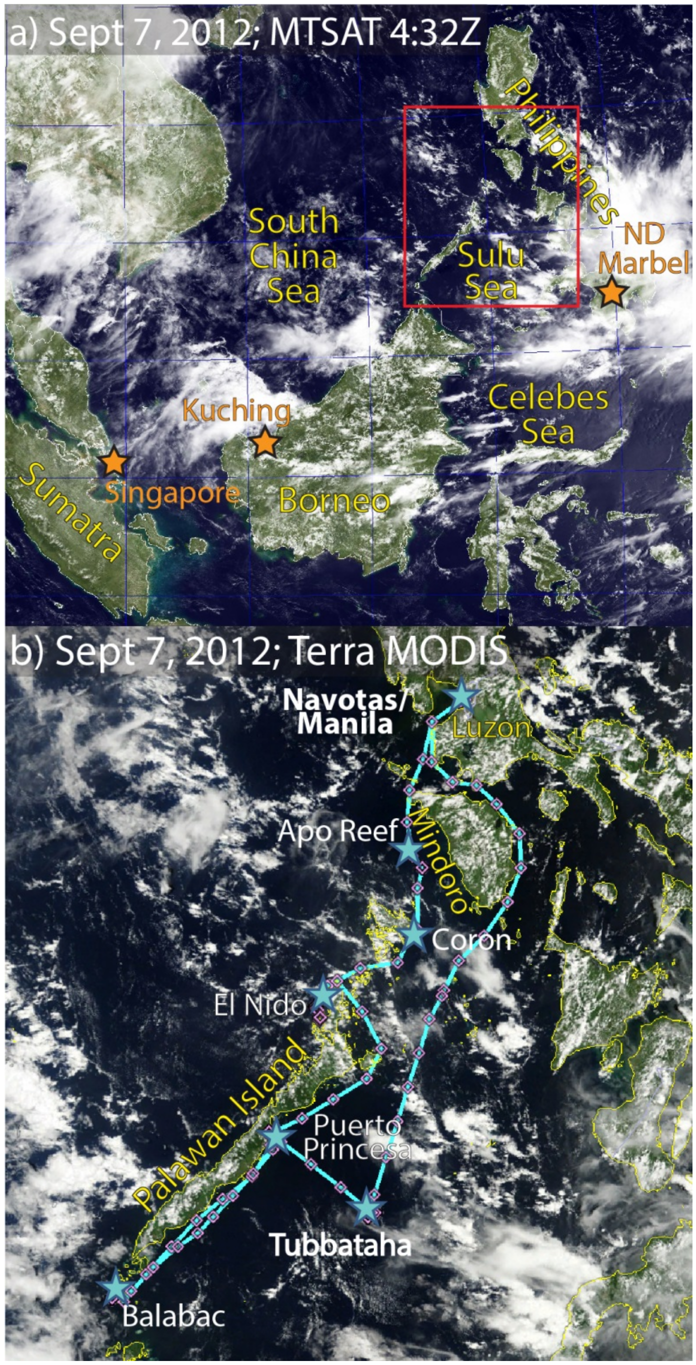

Figure 1. Overview of the study domain. (a) Regional MTSAT false color visible image of Sept. 7, 2012-the clearest day of the mission. AERONET sun photometer sites used in this analysis are also marked. (b) Cruise track with major sampling locations stared. Minor ticks during transits are three hours apart.

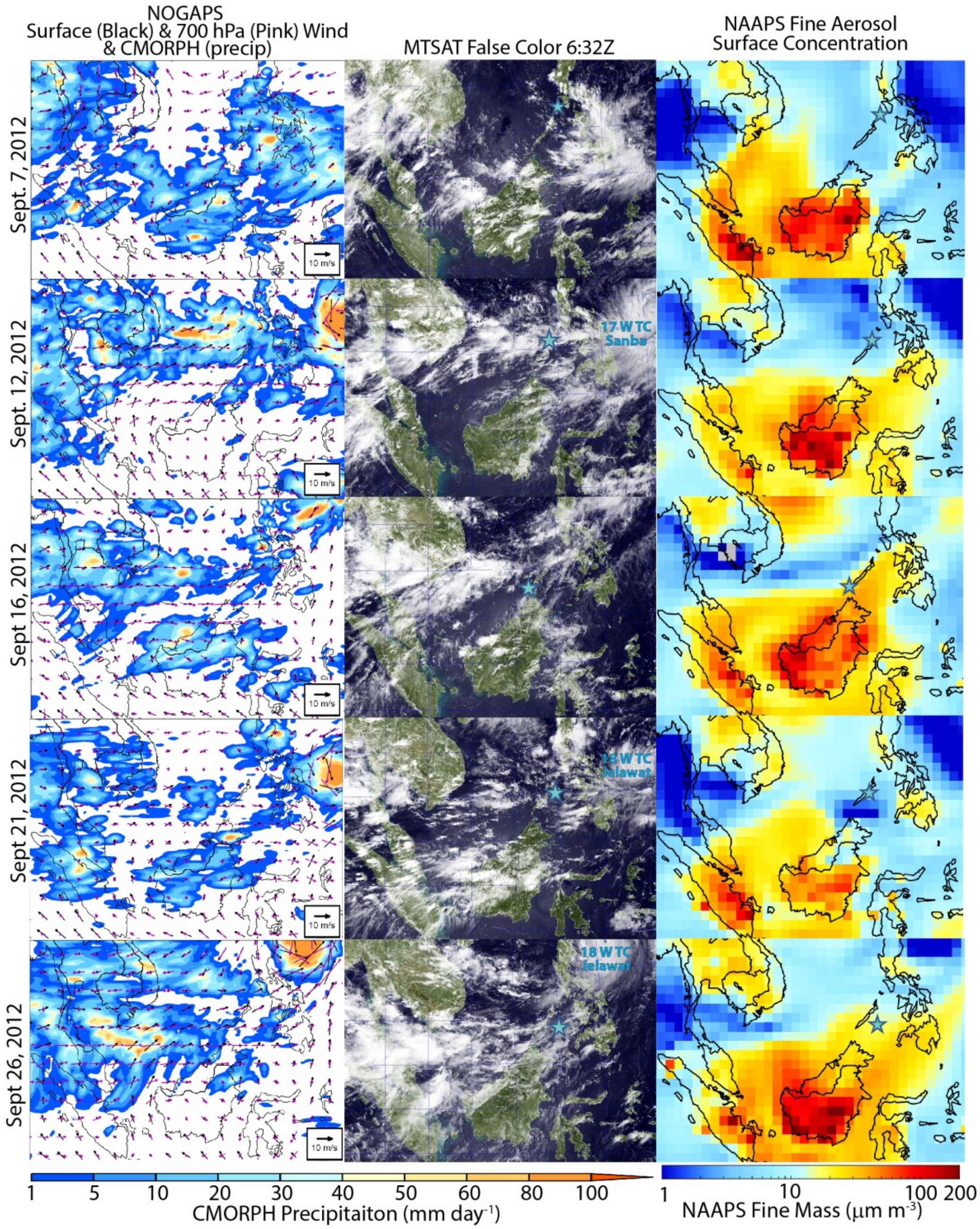

Figure 2. A matrix of NOGAPS wind (black surface, magenta 700 hPa) and CMORPH precipitation; MTSAT visible false color imagery, and NAAPS surface fine mode particle concentration (biomass burning plus anthropogenic and biogenic fine) for five representative days at major anchorages throughout the *Vasco* cruise. Selected dates are at major sampling moorings/anchorages Sept 7, at Apo Reef; Sept 12 at El Nido; Sept 16 at Balabac Island; Sept. 21st departing Puerto Princesa; and Sept. 24th at Tubbataha Reef.

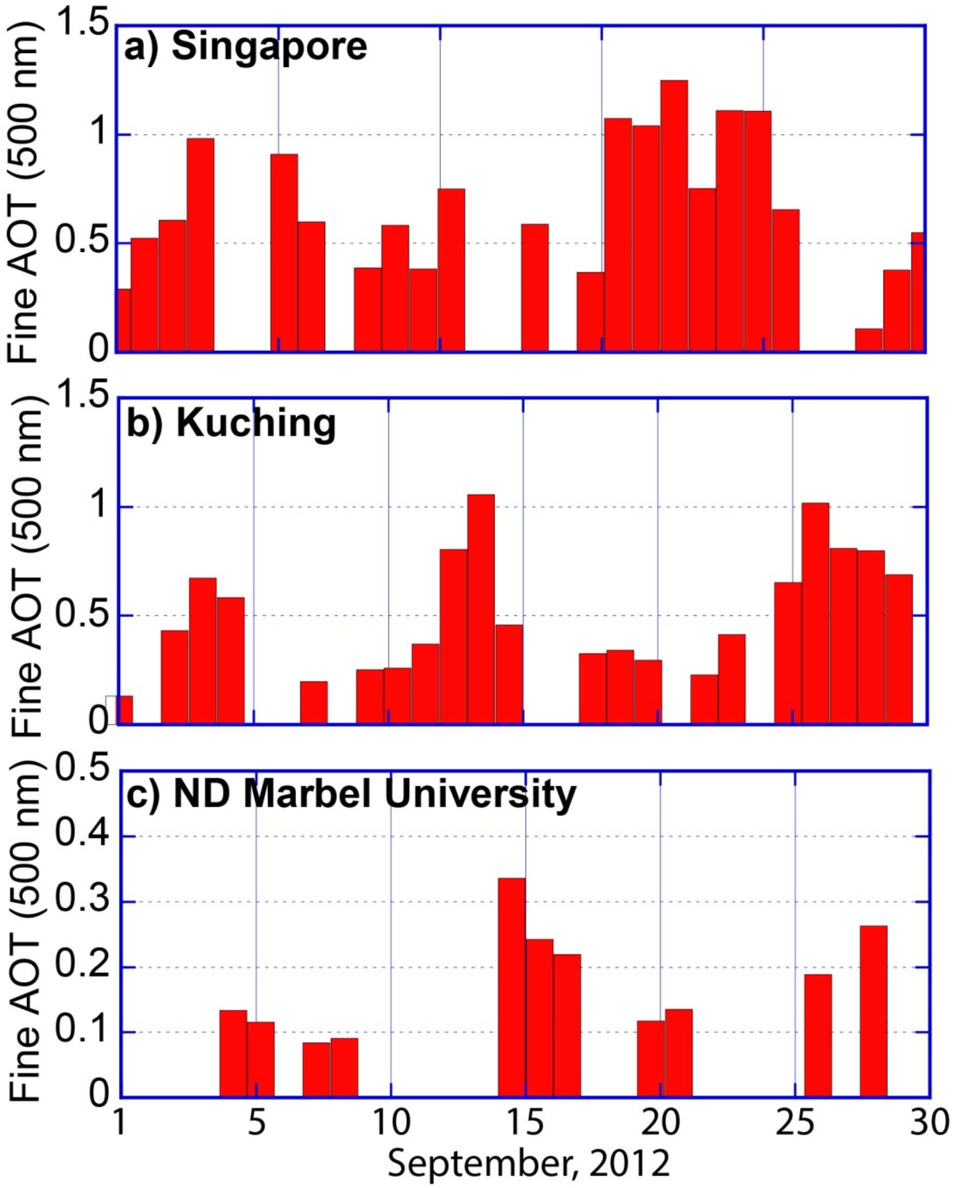

Figure 3. AERONET 500 nm fine mode aerosol optical thickness for three sites surrounding the study area.

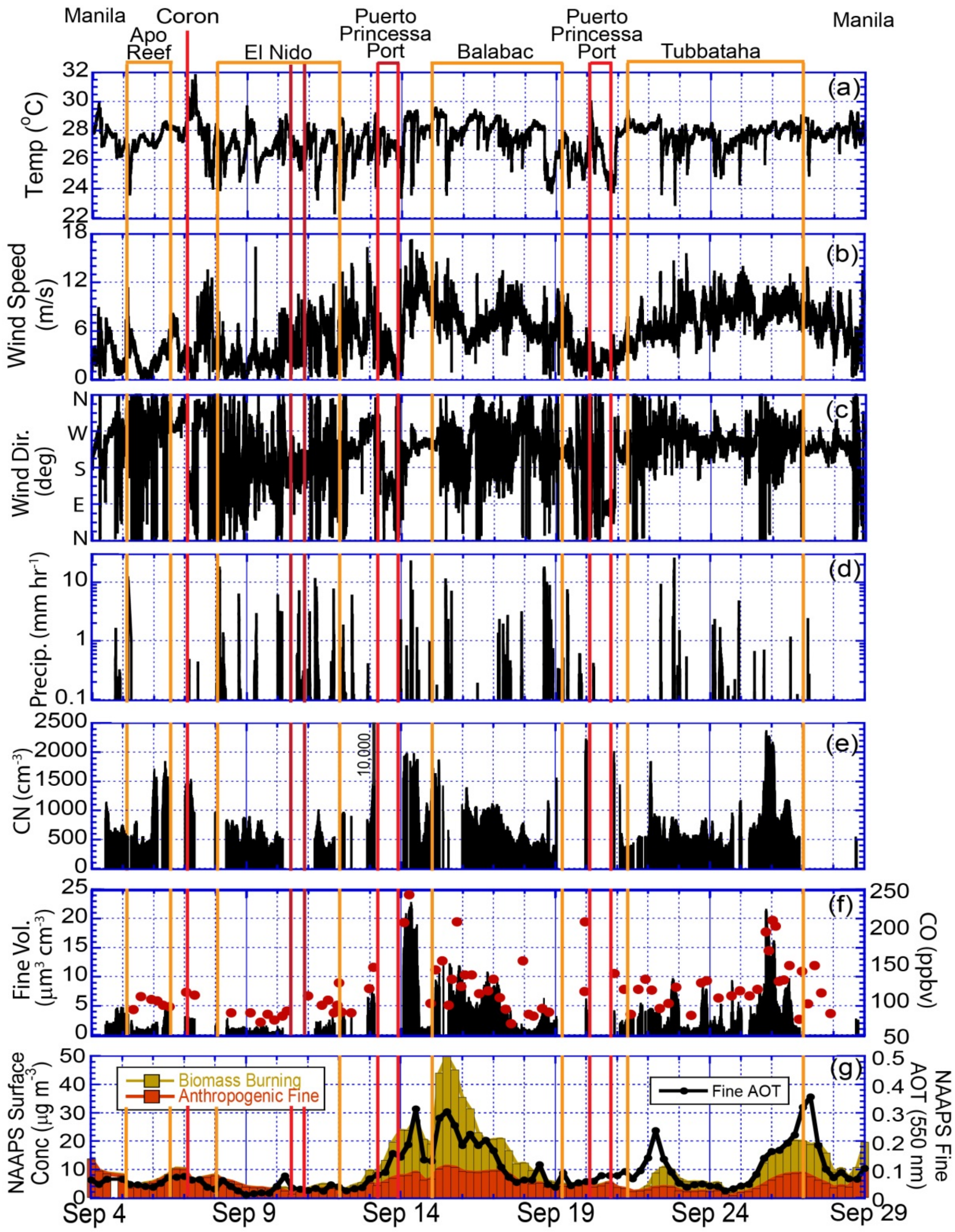

Figure 4. Time series of key meteorological and compositional data along the Vasco track (UTC Time). Locations of stationary sampling and in port periods are bound in orange and red brackets, respectively. Included are a) Temperature [^{o}C] ; b) Wind speed [m s^{-1}]; c) Wind direction; d) Precipitation rate [mm hr^{-1}]; e) Condensation nuclei count [cm^{-1}]; f) Fine mode volume as derived by the PCASP [black μm^{3} cm^{-3}] and the gas can CO [red dots ppbv]. Also shown is (g) Combined NAAPS model derived fine mode mass and AOT sampled along the *Vasco* track.

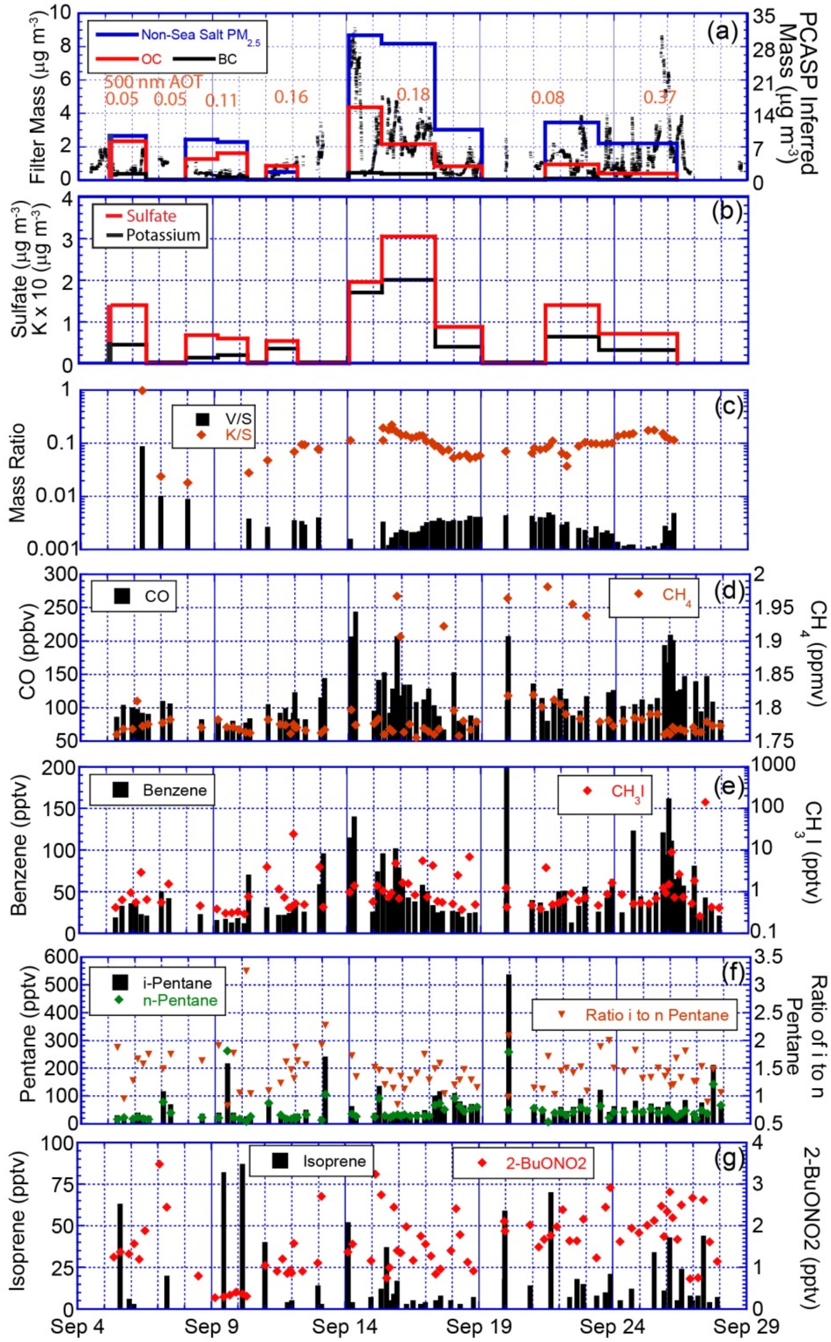

Figure 5. Time series of chemistry measurements including (a) filter based gravimetry and Organic-OC and Black-BC carbon. Also shown is 30 minute averaged fine mass inferred from the PCASP assuming a density of 1.35 g cm^{-3}. Labeled are 500 nm AOT from the MAN network MicroTops sun photometer; (b) Filter sulfate and potassium; (c) DRUM sampler elemental ratios of vanadium and potassium to sulfur; (d) Whole-air sampled CO and methane; (e) Whole-air sampled benzene and methy iodide; (f) Whole-air sampled i- and n-pentane with their ratio; (g) Whole-air sampled isoprene and 2-butanalkyl nitrate.

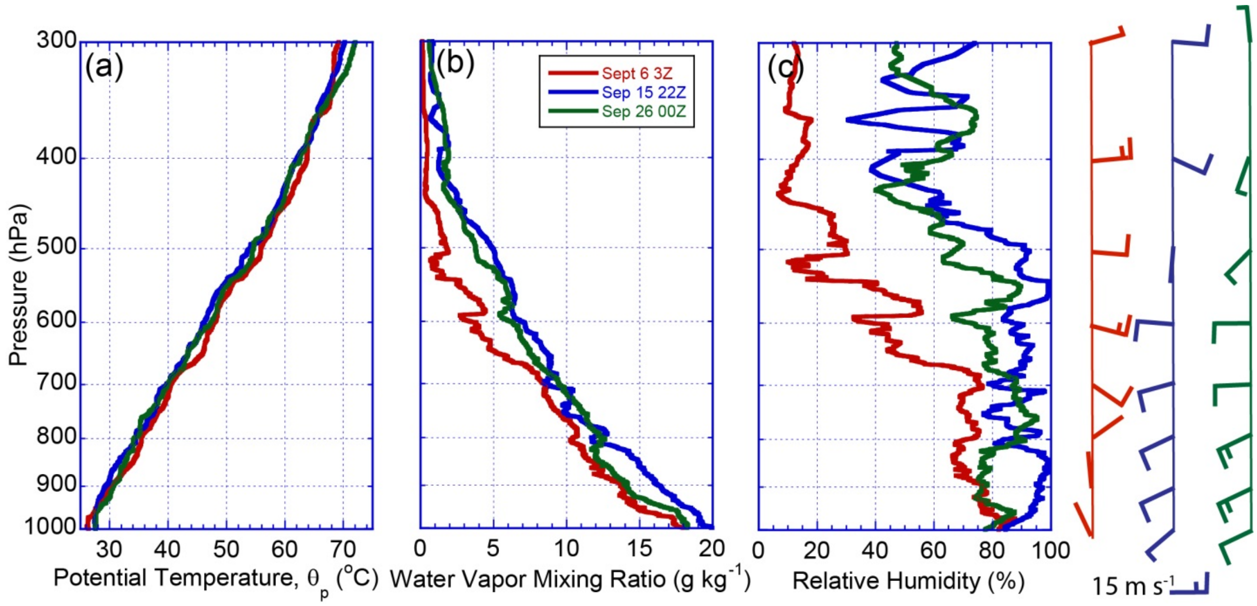

Figure 6. Sounding profiles of (a) Potential temperature; (b) Water vapor mixing ratio; and (c) Relative humidity for profiles corresponding to the nucleation event on Sept 6 at Apo reef, and the biomass burning cases of September 15 and 26th at Balabac Island and Tubbataha Reef, respectively. Wind flags for these cases are marked on the far right.

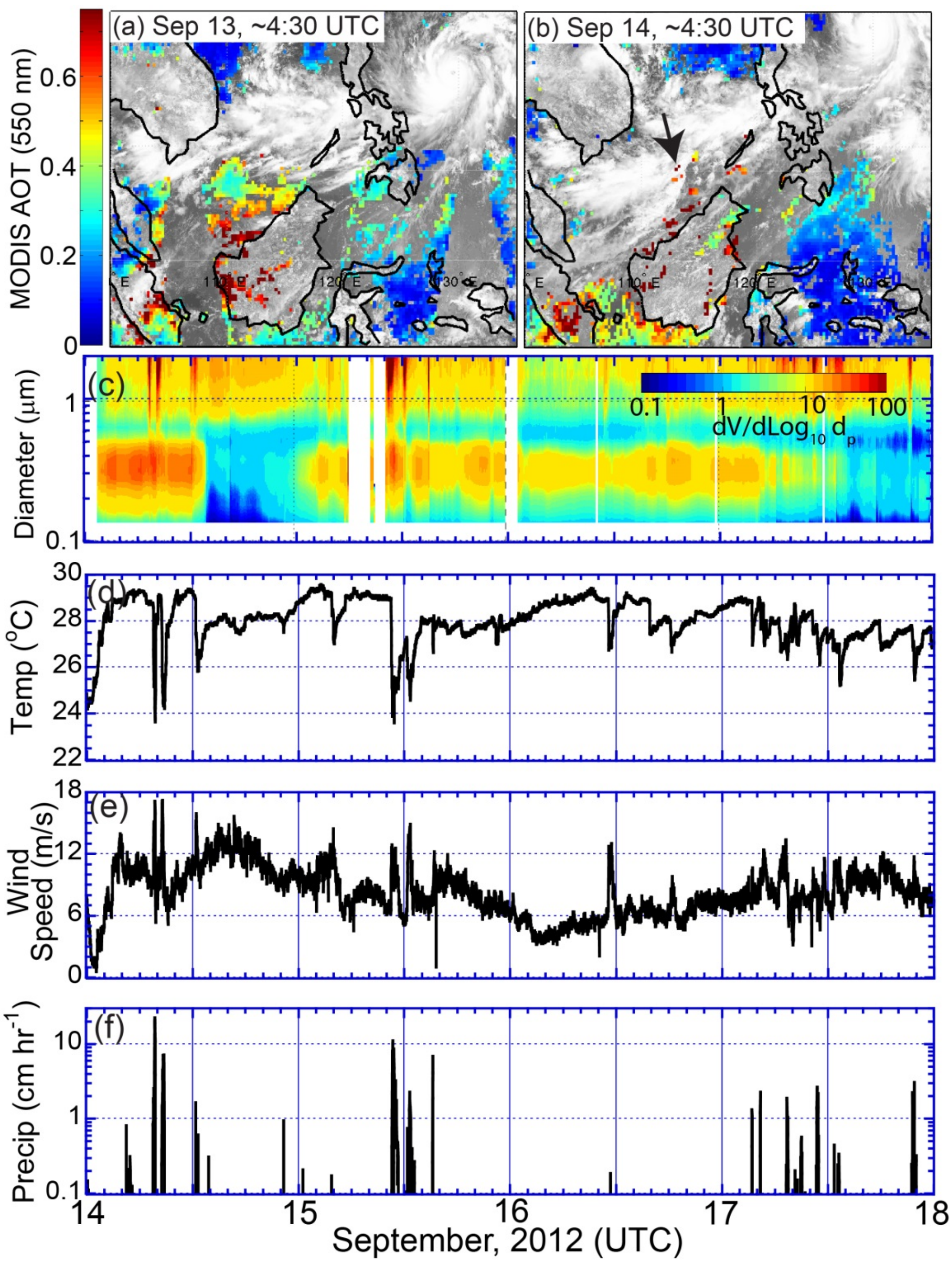

Figure 7. Satellite data and *Vasco* one-minute time series data describing the Sept. 14^{th} -17^{th} transport event. (a) and (b), combined Terra and Aqua MODIS C6 550 nm AOT overlaid on MTSAT visible channel for Sept. 13^{th} and 14^{th} , respectively; (c) PCASP volume distribution; (d) Temperature; (e) Wind speed; (f) Precipitation rate. The presence of a large squall line originating from a massive thunderstorm over the Malaya Peninsula that resulted in the Sept 14 12Z clean period as evident in (c) is marked with an arrow in (b).

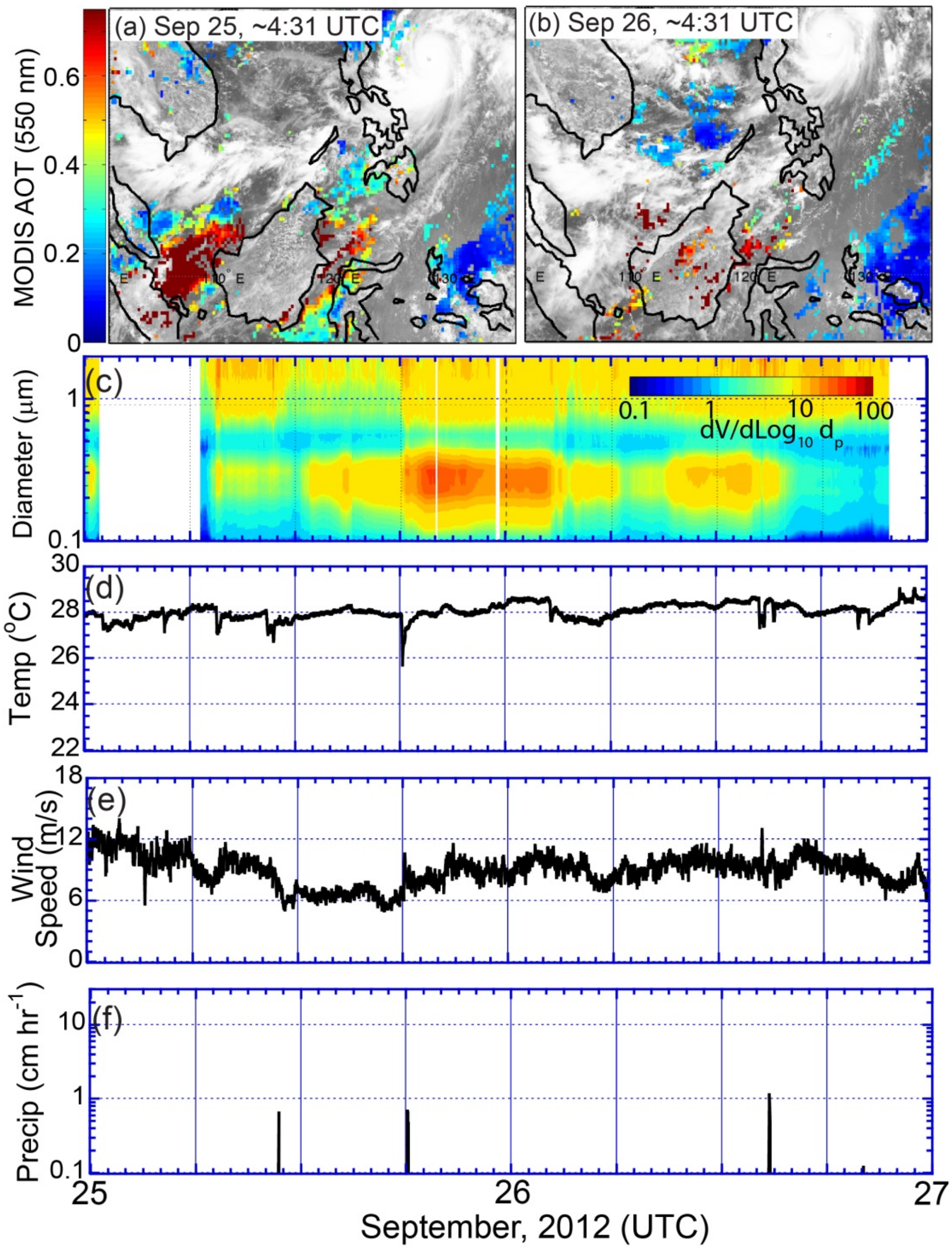

Figure 8. Same as Figure 7 but for the Sept 25-26, 2012 smoke event.

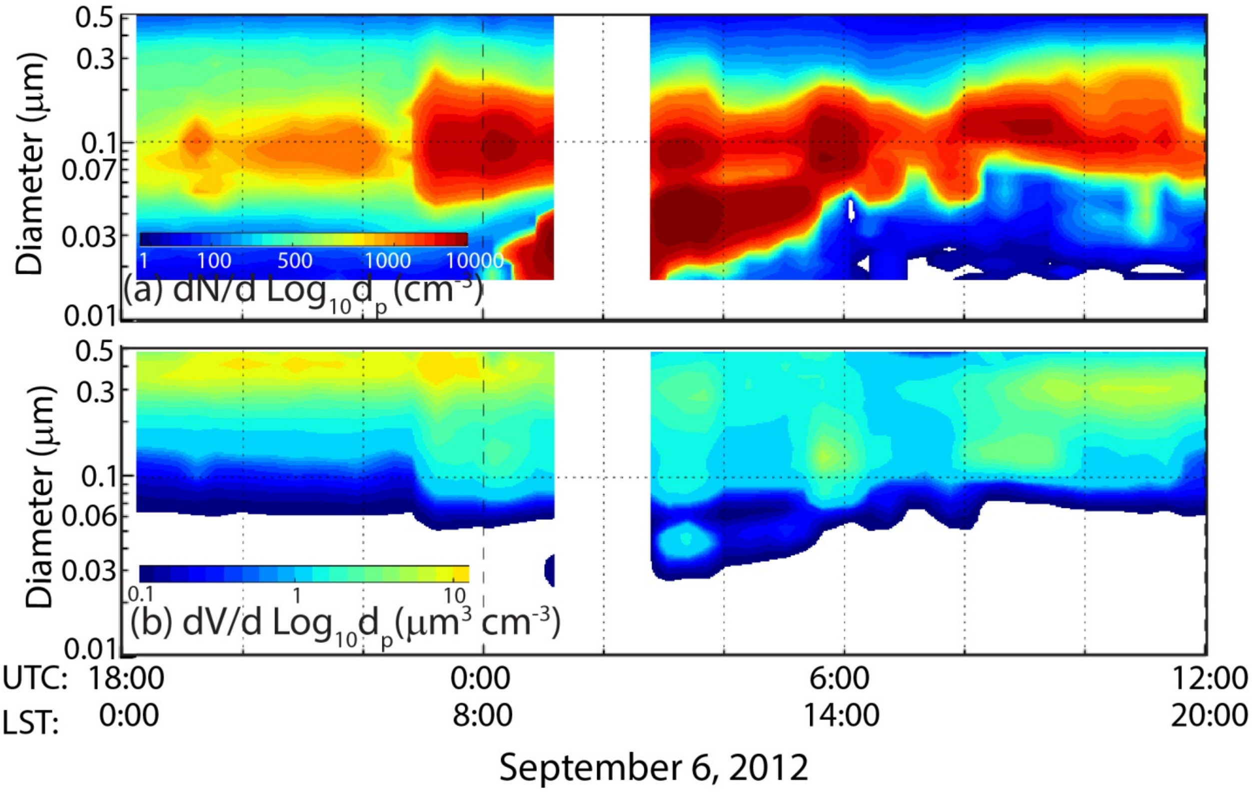

Figure 9. Electrostatic classifier particle number and volume distribution for the Sept 6th nucleation event at Apo reef. Corresponding whole-air samples are listed in Table 1 including 22:20Z Sept. 5th as a pre event can, 2:45Z Sept 6th in the middle of the event, and 7:30Z Sept 6, for post event.